

**A genetic screen for asymmetrically localized RNAs in
Drosophila tracheal cells**

Inaugural-Dissertation

zur

**Erlangung des Doktorgrades
der Mathematisch-Naturwissenschaftlichen Fakultät**

der Universität zu Köln

vorgelegt von

Jayan Nandan Nair

aus Kerala, Indien

Köln, Februar 2008

1. Berichterstatter:

Prof. Dr. Maria Leptin

2. Berichterstatter:

Prof. Dr. Siegfried Roth

Tag der mündlichen Prüfung: 28 April 2008

Table of Contents

1. INTRODUCTION	4
1.1 Tubulogenesis and branching morphogenesis - a general overview	4
1.2 Tracheal morphogenesis in <i>Drosophila</i>	4
1.3 Terminal branch development in <i>Drosophila</i> larvae	7
1.4 Unique aspects of terminal branch development.....	9
1.5 Localized translation as a means for targeting proteins and maintaining developmental plasticity	11
1.6 RNA localization in development	12
1.7 Mechanisms of RNA localization.....	13
1.7.1 Localized degradation.....	13
1.7.2 Diffusion and localized entrapment	13
1.7.3 Active transport along the cytoskeleton.....	14
1.8 Role of Untranslated Regions (UTRs) of mRNA in gene regulation.....	14
1.9 Techniques for visualizing mRNA.....	15
1.9.1 MS2-GFP labeling system	16
1.10 A genetic screen for localized RNAs in <i>Drosophila</i> tracheal cells	18
1.11 Aim of the project	18
2. MATERIALS AND METHODS.....	19
2.1 Materials	19
2.1.1 <i>Drosophila melanogaster</i> stocks.....	19
2.1.2 UAS Transgenes	19
2.1.3 Gal4 drive lines.....	19
2.1.4 EP-MS2 Transgenes	20
2.1.5 Mutants	20
2.1.6 Antibodies used	20
2.1.7 Primers.....	20
2.1.8 Sequencing primers for pUAST vector.....	20
2.1.9 Inverse PCR primers.....	20
2.1.10 Plasmids used for generating transgenes	21
2.1.11 Microscopes used.....	21
2.1.12 Imaging and data analysis software	21
2.1.13 Reagents.....	21
2.2 Methods.....	22
2.2.1 Fly maintenance and embryo collection	22
2.2.2 Antibody staining.....	22
2.2.3 Larval immuno-stainings	22

Table of Contents

2.2.4 Molecular biology.....	23
2.2.5 EP-MS2 construct.....	23
2.2.6 NLS-MS2-eGFP constructs.....	23
2.2.7 Inverse PCR protocol.....	24
2.2.8 Electron microscopic studies.....	24
Transmission electron microscopy.....	24
Scanning electron microscopy.....	25
3. RESULTS.....	26
3.1. Terminal branch development in larvae.....	26
3.1.1 Categorization of terminal branches based on lumen diameter.....	26
3.1.2 Lumen diameter decreases along the Proximal-Distal Axis from the nucleus.....	29
3.1.3 Cell diameter varies along the proximal-distal axis from the nucleus.....	30
3.2 Translational and co-translational machinery is present in terminal branches.....	31
3.2.1 Transmission Electron microscopic studies to analyze ribosome and ER.....	32
3.2.2 Immuno-histochemical studies to visualize ribosome, ER and Golgi bodies in terminal branches.....	33
3.2.3 Poly (A) binding protein localizes in terminal branches.....	35
3.3 A genetic screen for localized RNA in tracheal cells.....	36
3.3.1 Combining the MS2-GFP labeling system with the EP technique.....	37
3.3.2 Generating transgenes and fly reagents for the screen.....	38
3.3.2.1 Modifying the EP transposon and generating EP-MS2 transgene.....	38
3.3.2.2 Generating UAS-NLS-MS2-GFP transgenic flies.....	40
3.3.2.3 Recombining UAS-NLS-MS2-GFP with <i>btl</i> -Gal4.....	41
3.3.2.4 Hopping efficiency of the EP-MS2 insertion on the X chromosome.....	42
3.4 A pilot screen to evaluate the EP-MS2 technique.....	43
3.4.1 Phenotypic classification of the EP-MS2 lines based on pilot screen.....	44
3.4.2 Evaluating the EP-MS2 technique in the developing oocyte.....	47
3.4.3 Testing the EP-MS2 technique in dendritic arborization (da) neurons.....	48
3.4.4 MS2-GFP tagged candidate mRNA does not accumulate in stress granules.....	49
3.5 Molecular mapping of the EP-MS2 element insertion in candidate lines.....	51
3.6 Characterization of a candidate gene from the EP-MS2 screen.....	53
3.6.1 <i>bitesize</i> - a Synaptotagmin-like protein family gene in <i>Drosophila</i>	53
3.6.2 Functional characterization of <i>bitesize</i> in terminal tracheal branch development.....	56
3.6.3 Bitesize localizes at the apical membrane in terminal branches.....	58
3.6.4 C-terminal C2 in Bitesize is required for its membrane localization.....	59
3.6.5 Par3/Bazooka localization in terminal branches.....	61
3.6.6 Par6, aPKC and Crumbs localization in terminal branches.....	62
3.6.7 Phosphorylated Moesin localizes at the apical membrane facing the lumen in terminal branches.....	66
3.6.8 Function of Moesin in terminal branches.....	67
4. DISCUSSION.....	71

Table of Contents

1. Terminal branch patterning - a carefully orchestrated process.....	71
2. Localized translation and developmental plasticity of terminal branches.....	72
3. The EP-MS2 technique - a novel method of screening for localized RNAs.....	73
4. Candidate Characterization: <i>bitesize</i>, a determinant for lumen formation and stability in terminal branches?	75
5. Abnormal terminal branches in <i>bitesize</i> mutant larvae	76
5. BIBLIOGRAPHY	80
6. APPENDIX.....	92
6.1 List of genes involved in tracheal morphogenesis.....	92
6.2. Measurements from Type-A and Type-B branches: Data set 1 and data set 2.	93
6.3 Measurement along the proximal-distal axis of Type-A branch: Data set 3.	94
6.4 Lumen and cell diameter measurements from the same positions in Type-A branches: Data set 4.....	95
ABBREVIATIONS.....	97
ABSTRACT.....	98
ZUSAMMENFASSUNG	99
EIDESSTATTLICHE ERKLÄRUNG	101
LEBENS LAUF.....	102

1. Introduction

1.1 Tubulogenesis and branching morphogenesis - a general overview

Organogenesis is a complex process involving global changes in cell populations in terms of their proliferation, migration, differentiation and shape. Many vertebrate organs are tubular organs and consist of branched networks of interconnected tubes. The tubular organs in higher vertebrates include the lungs, vasculature, digestive and excretory systems, as well as secretory organs such as the pancreas, salivary, prostate, and mammary glands. Other tissues, including the embryonic heart and neural tube, have requisite stages of tubular organization early in development. The *Drosophila* tracheal system, equivalent to the vertebrate lung, has been extensively used as a model for investigating molecular and cellular bases of how cells are organized into tubular organs of various shapes and sizes. A particularly interesting aspect in *Drosophila* tracheal morphogenesis is the development of a subset of branches known as the terminal branches. The development of terminal branches is not pre-patterned, but is regulated by oxygen physiology, a phenomenon similar to angiogenesis in mammals. Events like the *de novo* tube formation in terminal branches and branch sprouting at positions distant from the nucleus, regulating the development of these dynamic branches have not been studied in great detail.

1.2 Tracheal morphogenesis in *Drosophila*

The *Drosophila* tracheal system is a complex network of branched and interconnected tubes that conducts oxygen from the exterior to the internal tissues. Tracheal branches are simple tubes: an epithelial monolayer wrapped into a tube surrounding a central lumen through which gases flow. It develops by sequential sprouting of primary, secondary and terminal branches from an epithelial sac of ~80 cells (known as tracheal placodes) in each body segment of the embryo and displays bilateral symmetry. Oxygen enters the network at the spiracular openings and passes through primary, secondary and terminal branches to reach the target tissues. Tracheal morphogenesis in *Drosophila* is biphasic. The first phase of development occurs in embryos. During this phase, cells of the tracheal placode migrate, reposition themselves,

Introduction

intercalate and fuse to form a network of interconnected tubes. This phase completes towards the end of embryonic development and results in larvae hatching with a fully functional respiratory system. During the five days of larval development, the size and length of embryonic tracheal tubes increases along with the increasing body size of the larva. A very significant aspect of tracheal development during the larval period is growth and ramification of new terminal tracheal branches in response to oxygen demands of individual targets. In the second phase, during the pupal metamorphosis, the tracheal branches undergo remodeling to meet the requirements of adult flies (Fig.1).

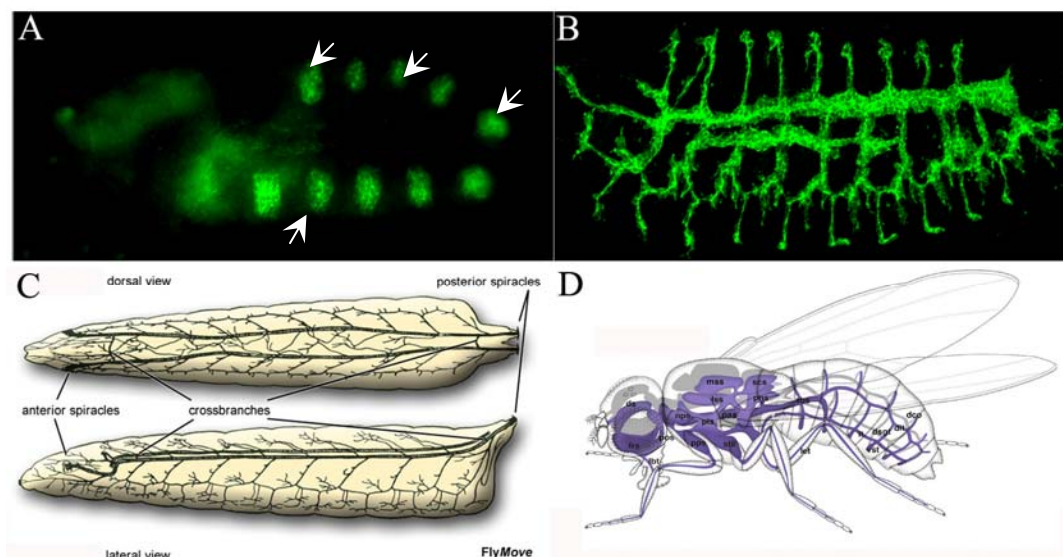


Figure 1. Tracheal morphogenesis from embryos to adult flies. A) The 10 tracheal placodes in a 6 hrs old embryo imaged laterally (white arrows mark four of these placodes). B) Fully developed tracheal branches in a stage 16 embryo. In A and B the tracheal cells are marked with Trachealess antibody. C and D are schematic representations of tracheal branches as seen in third instar larvae and adult flies respectively. C and D adapted from FlyMove.

The general tracheal branching program involves the Fibroblast Growth Factor (FGF) pathway that is used repeatedly from the embryo to the adult (Metzger and Krasnow, 1999; Sato and Kornberg, 2002; Skaer, 1997). The FGF pathway uses *branchless* (*bnl*, which is the ligand) and *breathless* (*btl*, which is the receptor) to activate downstream target genes required for tracheal morphogenesis. Studies have elucidated diverse pathways and events regulating the development of tracheal tubes. Moreover a different tubulogenesis mechanism is used at each level of branching; branching is thus

Introduction

not a strictly reiterative process. Fig. 2 highlights some of the major genetic aspects regulating tracheal development at different stages (adapted from Ghabrial et al., 2003).

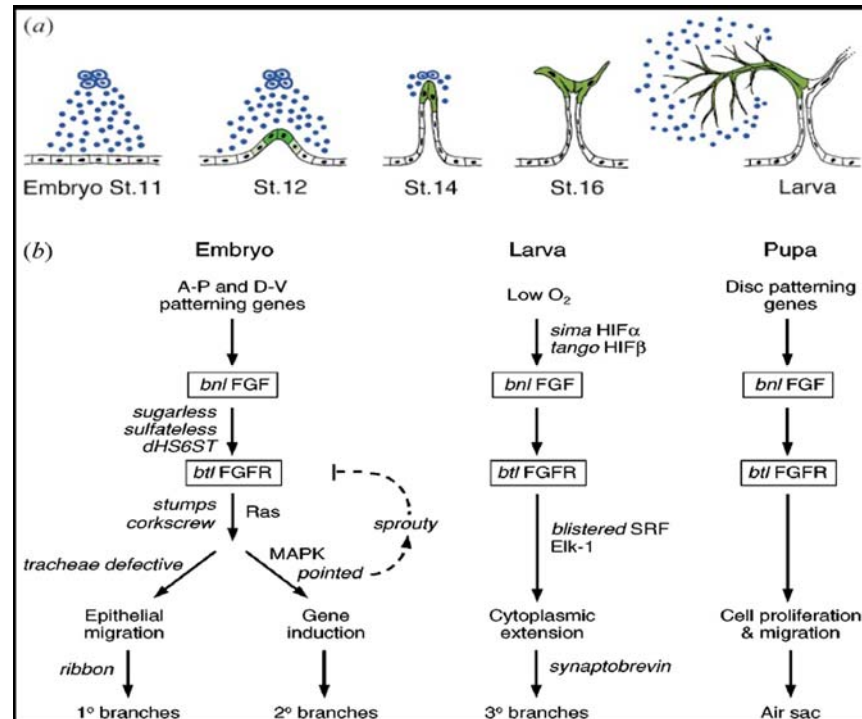


Figure 2. The FGF pathway controls each step of branching. (a) *branchless* FGF (blue) is expressed in clusters of cells surrounding the developing tracheal system, at each position where a primary branch will bud. The secreted growth factor activates the Breathless FGFR on nearby tracheal cells (black), and acts as a chemoattractant that guides outgrowth of primary branches. It also induces expression of secondary branch genes and triggers secondary branch sprouting at the ends of outgrowing primary branches (green; stages 12–16). *branchless* turns back on again, but in a completely different pattern, during larval life to control outgrowth of terminal branches. The gene is expressed yet again during pupal life where it controls budding of adult air sacs (not shown). (b) The genes that function upstream of Branchless and downstream of Breathless change during development, giving rise to different patterns and structures of branches at each step (figure adapted from Ghabrial et al., 2003).

Based on the sequence of migration and tube formation, the tracheal branches are divided into three types; the primary, secondary and tertiary (or terminal) branches. In each embryonic hemisegment six primary tracheal branches bud and migrate out first, followed several hours later by the sprouting of about two-dozen secondary branches. Most secondary branches sprout terminal branches (tracheoles) throughout the larval life, forming hundreds of fine terminal branches in each hemisegment. The pattern of primary and secondary branch budding is highly stereotyped and controlled by a hardwired

Introduction

developmental program, whereas terminal branch sprouting is variable and regulated by tissue oxygen need. Further, the process of lumen formation in each type of branch is distinct. Primary branches have multicellular tubes with two to four cells surrounding the central lumen connected by intercellular epithelial junctions. In the secondary branches lumen forms as a consequence of cell wrapping around its long axis until the edges of the cell meet and seal resulting in a tube with an autocellular junction. In comparison to the lumen in primary and secondary branches the terminal branches have a junctionless lumen. It is believed that the terminal branch lumen forms as result of vesicular fusion, in the cytoplasmic extensions of terminal tracheal cells, which subsequently is connected to the lumen of the secondary branch to form a continuous tube.

1.3 Terminal branch development in *Drosophila* larvae

Most of the studies on tracheal development in flies have concentrated on patterning and tube formation mechanisms in embryos, but the tracheal developmental events during the larval phase is relatively unexplored. Much of the terminal branch development, though they are specified in embryos, happens during the larval phase. Terminal branches arise as cytoplasmic extensions that grow along the surface of tracheal target tissues, much like axonal outgrowths. Subsequently an intracellular lumen forms within each extension, creating a fine junctionless tube continuous with the secondary branch from which it arises. This process of cytoplasmic extension and lumen formation repeats itself many times during the five days of larval life, generating individual terminal cells with complex branched structures and dozens of terminal branches. The branch points are regularly spaced and terminal branches do not cross over one another. Further, these branches attach tightly to internal tissues to facilitate gas exchange (Fig.3). The attachments are generally long lived, although under certain conditions, cellular projections from oxygen-starved cells can bind to and redistribute nearby terminal branches to satisfy their oxygen need (Ghabrial et al., 2003; Uv et al., 2003). Studies have shown that each terminal cell can sprout up to 20 branches (on an average) and have

Introduction

an average lumen diameter of approximately 1 μ m or less (Guillemin et al., 1996; Lubarsky and Krasnow, 2003).

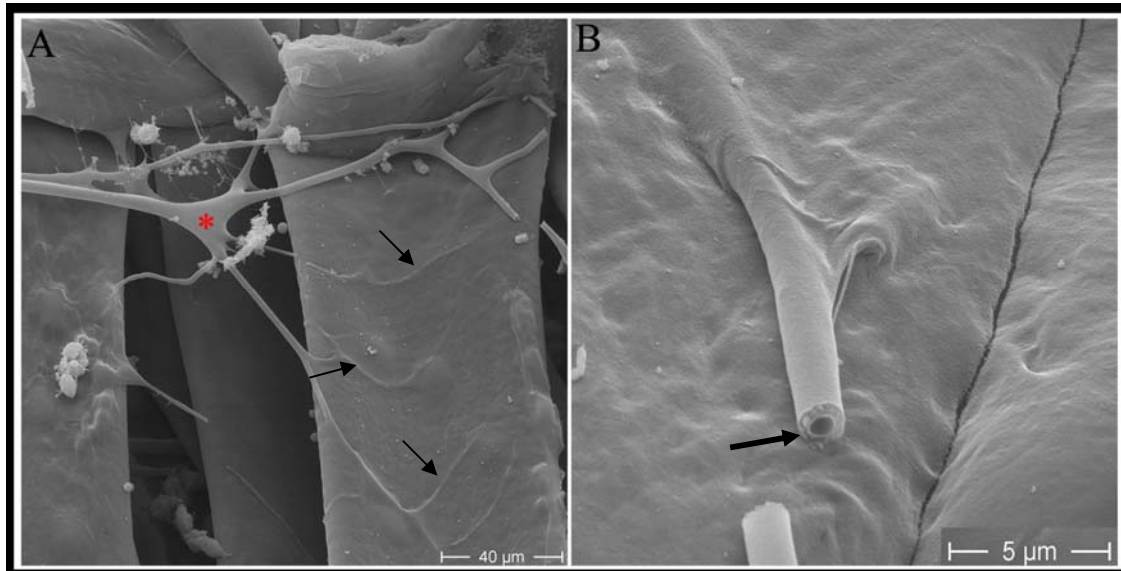


Figure 3. Scanning Electron micrographs of terminal branches in third instar larvae. A) Terminal cell with terminal branches innervating the body wall muscle. The nucleus of the cell is marked with a red asterisk and the branches are marked with arrow. B) Cut end of a terminal branch, innervating the body wall muscle, showing the lumen (arrow).

The complex pattern of terminal branching is regulated by the oxygen physiology of the target tissue. Oxygen-starved cells secrete a tracheogenic signal that can attract new terminal branches from as far as one segment away. The tracheogenic signal generated by oxygen-starved cells was identified as Branchless FGF. *Drosophila* cognates of hypoxia-inducible factors (HIF pathway components) including the HIF α (*sim*) and β (*tango*) subunits have been identified (Nagao, et al., 1996; Adryan, et al., 2000; Lavista-Llanos, et al., 2002) and they are activated by hypoxia as in the mammalian pathway. Further, genomic analysis of HIF-responsive targets in *Drosophila* larval tissues and cell culture RNAi experiments have identified *branchless* as one of the targets. The effects of Branchless on terminal branching are mediated by Breathless FGFR (Reichman-Fried & Shilo, 1995; Jarecki, et al., 1999). Studies have also revealed an important transcription factor *blistered* that acts downstream of the Bnl/Btl FGF pathway in specification and development of terminal branches. *blistered* encodes the *Drosophila* homologue of mammalian serum response factor (SRF, a MADS domain

Introduction

transcription factor). *Blistered/DSRF* together with the ETS domain protein Elk-1 forms part of a transcription complex whose activity is regulated by RTK signaling and the Ras/MAPK cascade. *blistered/DSRF* is specifically expressed in tracheal terminal cells. In *blistered/DSRF* loss-of-function mutants, cytoplasmic outgrowth and terminal branching is severely reduced, whereas constitutively active forms of SRF and Elk-1 cause excessive branch outgrowth (Affolter et al., 1994; Guillemin, et al., 1996, Montagne, et al., 1996; Treisman, R., 1994). Recent studies have implicated *rhea* (gene encoding *Drosophila* Talin), *myospheroid*, (β *mys*, the major *Drosophila* β -integrin) and *IKK ϵ* , a member of the IKK protein kinases having a significant role in development and maintenance of the lumen in terminal branches. *rhea*, β *mys* and *IKK ϵ* were shown to be essential for proper lumen development, probably by regulating the organization of the actin cytoskeleton in the terminal branches (Oshima, et al., 2006; Levi, et al., 2006). Excluding the above mentioned few details, the genetic regulation, cell biological, physiological and morphological changes regulating terminal branch development during the larval phase is largely unresolved.

1.4 Unique aspects of terminal branch development

Two aspects of terminal branching are of special interest and distinguish it from the earlier stages of branching. One is that terminal branches have a distinct cellular structure: they are extremely fine (<1 μ m diameter), lack junctional structures along the length of the branch and are formed by individual cells that undergo a remarkable process of cellular morphogenesis. Equivalent terminal cells in different larvae can form different numbers of branches and display different patterns of branching (Fig.4). The other distinguishing feature is that terminal branching is not stereotyped nor under fixed developmental control. Terminal branching is highly variable and is regulated by oxygen physiology; although variable, the pattern is not unorganized. Sprouting and outgrowth of terminal branches is carefully regulated to meet the oxygen needs of target tissues, much like angiogenesis in mammals. Low oxygen (hypoxia) stimulates terminal branch

Introduction

formation and high oxygen (hyperoxia) suppresses it (Wigglesworth, 1954; Locke, 1958; Jarecki et al., 1999).

These two unique aspects of the terminal branches i.e., the cellular morphology and their development in response to oxygen physiology of target tissues distinguish them from other tracheal branches, conferring a high degree of developmental plasticity. The terminal cells have to develop branches, efficiently and quickly, to meet the oxygen demands and a delay in this response would be critical for the target tissues. In response to hypoxic signals terminal branches are formed at distances as far as 100 μ m or more from the nucleus. These special attributes of terminal branch development raise a few important questions, for example, how does the terminal cell, efficiently and quickly, sprout branches away from the nucleus? How does the terminal cell make available the proteins required at the sites of outgrowth as and when required? Does localized translation contribute to supply of proteins required at the site of out growth? If so, do specific mRNAs localize in the terminal branches and are translated onsite when required?

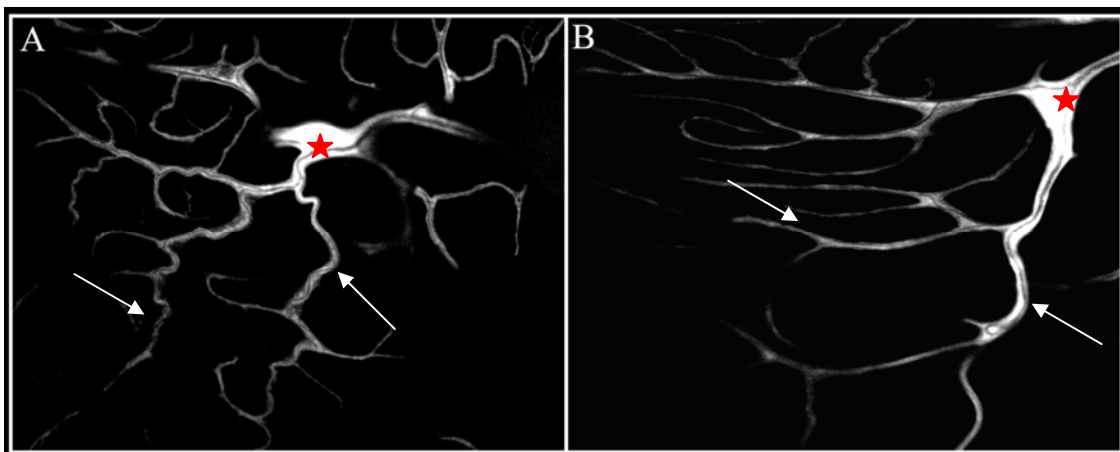


Figure 4. Two equivalent terminal branches from two different larvae. A and B demonstrate that equivalent terminal branches can have completely different morphology. White arrows mark the branches and the position of nucleus is marked with red star.

1.5 Localized translation as a means for targeting proteins and maintaining developmental plasticity

The extreme polarity and developmental plasticity exhibited by many cells, for example tracheal terminal cells or neurons, imposes a number of unique constraints with respect to development, growth and survival. The axon, for example, must navigate through a complex environment during its development and must form and maintain specific synaptic connections at its targets, often at a significant distance from the cell body. This raises a very important question: what is the source of axonal proteins required for its local morphological differentiation at sites far away from the cell body? Does the cell transport proteins from the cell body to axonal growth cones or is there an alternate method of providing proteins to developing regions? Studies in the past decade have revealed that localized translation of mRNAs transported to specific subcellular locations is an alternative way of targeting proteins to micro-domains within a cell (Fig. 5). Substantiating this possibility, a number of mRNAs have been reported in axons, growth cones and in dendrites of mammalian neurons, a few examples are *β actin*, BC1, *FMR1*, *α CaMKII* and *GluR1* (Gottlieb, 1990; Job and Eberwine, 2001; Martin, 2004). There is a growing body of evidence that such localized protein synthesis provides a means for developmental plasticity. Localized protein synthesis provides a polarized cell with the capacity to regulate its structure and function, by spatially restricting gene expression within cells. The mechanism underlying both the localization of these RNAs and the regulation of their translation are beginning to be delineated in a variety of systems.

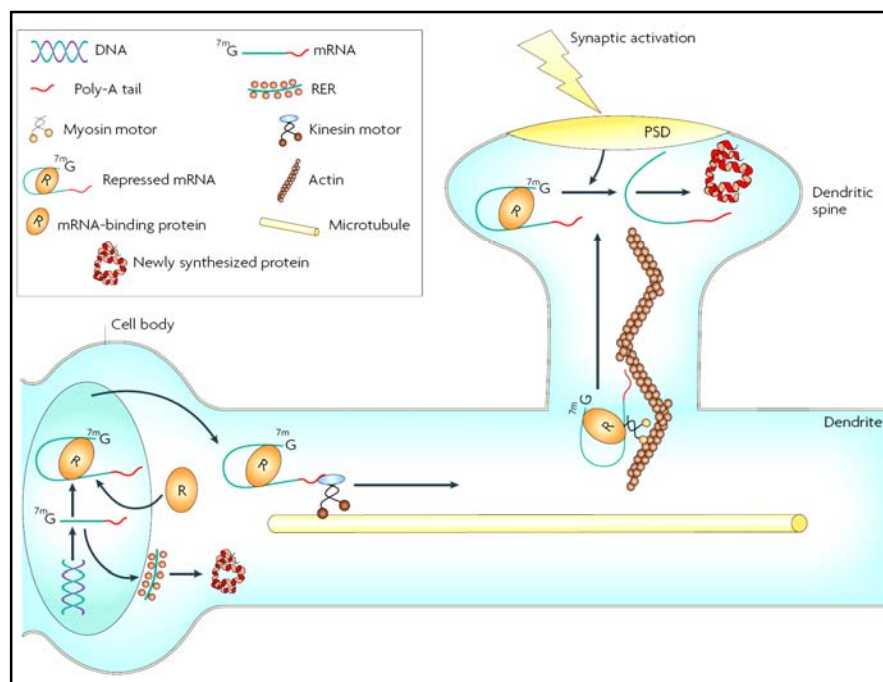


Figure 5. mRNA localization and subsequent translation in dendritic spines. Image adapted from Bramham and Wells, 2007.

1.6 RNA localization in development

Eukaryotic cells regulate gene expression at multiple levels including transcriptional, post-transcriptional and translational levels. Studies in the past few years have elucidated an essential step in gene regulation involving RNA localization and the translational activation of the localized RNA. This allows cells to spatially control protein function by determining their sites of synthesis. The localization of RNAs occurs in a wide range of organisms, including fungi (e.g. *Ustilago maydis*), plants (*Arabidopsis*), and various animal species (e.g. ascidians, echinoderms, *Drosophila*, zebrafish, *Xenopus*, and mammals). Further, studies suggest that RNA localization occurs in many cell types and regulates distinct functions ranging from the control of body axis formation to learning and memory. The targeting of RNAs to specific microdomains within a cell begins with the nascent mRNA being co-transcriptionally packed with *trans*-acting proteins into messenger ribonucleoprotein particles (mRNPs). Subsequently they are exported from the nucleus through nuclear pores. In the cytoplasm the mRNP is then delivered to its target cytoplasmic destination (St Johnston, 2005; Jansen and Kiebler,

Introduction

2005). At the target site, the mRNP is anchored and upon receiving the appropriate signal, the complex is remodeled to relieve translational repression and the mRNA is locally translated (Czaplinski and Singer, 2006).

1.7 Mechanisms of RNA localization

mRNAs can be localized by a variety of mechanisms such as diffusion and localized anchoring, local protection from degradation or active transport by motor proteins along the cytoskeleton.

1.7.1 Localized degradation

In *Drosophila*, several RNAs localize to the precursors of the germ cells (pole cells) in the embryo, for example *hsp83* mRNA. In the fertilized egg, *hsp83* mRNA is uniformly distributed but as the nuclear divisions advance, *hsp83* mRNA is degraded except in the pole plasm where the RNA is protected (Ding et al., 1993). Not much is known about the machinery required for stabilizing *hsp83* RNA in the pole plasm, although in some mutants (e.g. *smaug*) degradation of *hsp83* RNA is not triggered and consequently localization does not occur.

1.7.2 Diffusion and localized entrapment

Diffusion and entrapment allows for the localization of *Xcat2* and *Xdazl* mRNAs to the vegetal pole during early stages of oogenesis in *Xenopus* (King et al., 2005). At stage one of oogenesis, the RNAs localize to a structure called the mitochondrial cloud (MC), which lies next to the nucleus. This RNA localization seems not to involve active transport, since microtubule depolymerization has no effect on mRNA localization. Further, studies have shown that *Xcat2* and *Xdazl* transcripts localize to the MC through diffusion and association with the ER within the cloud and do not involve active transport (Chang et al., 2004). Localization of mRNA through a similar mechanism has been reported for *nanos* mRNA (*Xcat2* and *Xdazl* related *Drosophila* gene) localization at the posterior pole in the developing oocyte (Santos and Lehmann, 2004; Forrest and Gavis, 2003).

Introduction

1.7.3 Active transport along the cytoskeleton

Active transport is the most commonly used mechanism for RNA localization. Molecular motors which move directionally along the cytoskeleton and are widely used to traffic organelles and other cargoes, are used by RNAs to reach their destination within the cytoplasm. Localized transcripts are selected from the general population of RNAs because of the presence of specific localization sequences in them (Fusco et al., 2003). These specific signal sequences (*cis*-acting elements) in localizing RNA are recognized by *trans*-acting factors that recruit motor proteins that move along the cytoskeleton towards the final destination. A few examples for actively transported RNAs are *Ash1* mRNA in yeast, *wingless*, *bicoid*, *oskar* in *Drosophila* and *Vg1* mRNA in *Xenopus* (Wilkie and Davis, 2001; St Johnston, 2005; Deshler et al., 1997; Czaplinski, K and Mattaj, 2006).

1.8 Role of Untranslated Regions (UTRs) of mRNA in gene regulation

The untranslated regions (UTRs) of mRNAs play crucial roles in the post-transcriptional regulation of gene expression, including modulation of the transport of mRNAs out of the nucleus and in translation efficiency, subcellular localization and stability. Motifs contained within the UTRs of many mRNAs serve as information for the specific placement of that transcript within the cytoplasm and for the timing of its translation. Such localization signals contain discrete stem loops structures that associate with a particular combination of RNA binding *trans-acting* factors, determining the composition of the RNP complexes and site of localization of the transcripts. This can be achieved by recruiting specific molecular motors, influencing the activity of motors, dictating a mode of anchoring as well as promoting or preventing degradation (Fig. 6). Generally, such *cis*-acting localization signals are placed in the 3'UTRs of localizing transcripts, although in a few exceptions, signals are also found in the 5'UTR or in the exons (Gottlieb, 1990 and 1992; Mignone et al., 2002; Wickens et al., 1997; Hamilton, and Davis, 2007).

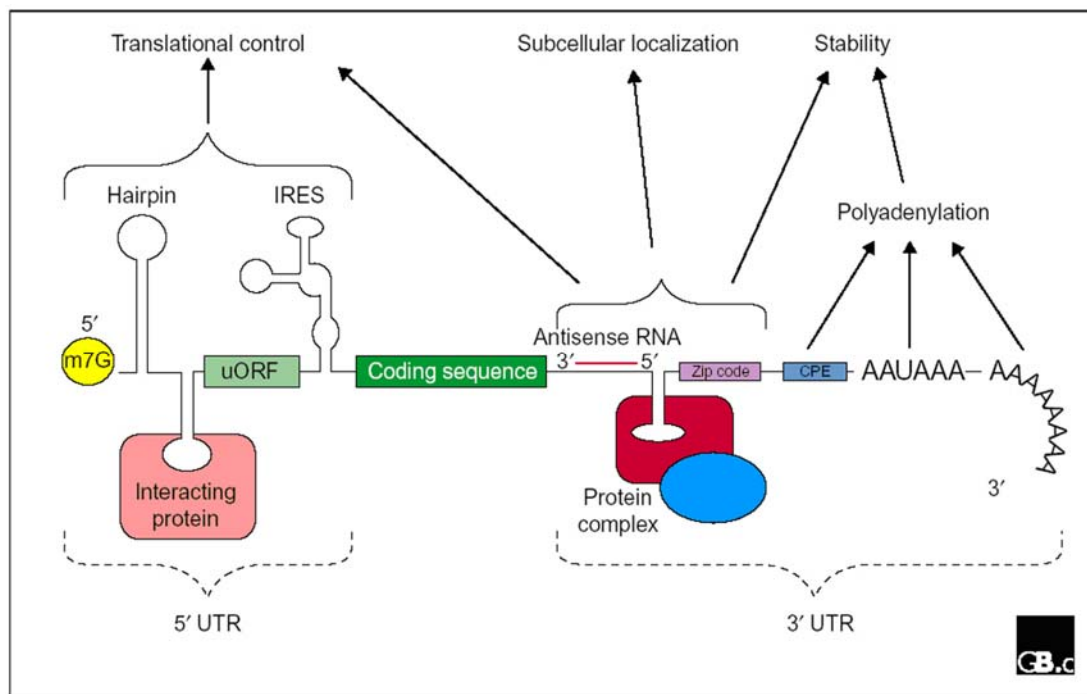


Figure 6. A schematic describing the functional relevance of untranslated regions of mRNA in post-transcriptional gene regulation. Schematic adapted from Mignone et al., 2002

1.9 Techniques for visualizing mRNA

Two approaches are widely used to detect localized RNA. The earliest and most used method is *in situ* hybridization, predominantly with labeled RNA probes. One glaring limitation of *in situ* hybridization as an experimental approach is that the material is fixed and hence dynamic processes cannot be followed directly. Secondly, the signal-to-noise ratio can be high, affecting the sensitivity of the assays. These limitations could be alleviated by the injection of fluorescently labeled RNA. The RNA can be tagged using fluorescent nucleotides during *in vitro* transcription. Live cell imaging has provided the ability to track the movements of such fluorescently tagged RNA. As endogenous RNA cannot be visualized using this method, the labeled non-functional RNA serves as a surrogate marker for the *bona fide* localization pathway. While this approach provides a good approximation for the various steps in the localization pathway, it may well miss out on certain fronts. The first is that the RNA destined for localization may actually be recognized by the cellular machinery in the nucleus, where the RNA is first synthesized

Introduction

and the injected RNA bypasses this process of biogenesis. The pre-mRNA or mature transcripts may bind to a protein required, for instance, for translational repression or assembly with a motor. Naked RNAs microinjected into the cell form complexes with proteins, but these may not be identical to those forming under endogenous conditions. Second, RNAs may be structurally modified when they are tagged with a fluorochrome. Specific proteins that identify 'zipcodes' in the RNA may not bind properly to such modified RNAs, possibly allowing binding by non-specific proteins. A third problem is that microinjection of RNA may not recapitulate either the timing or the level of its endogenous expression (Bratu, 2003; Singer, 2003).

1.9.1 MS2-GFP labeling system

To investigate the dynamics of mRNA movement a new technique, the MS2-GFP labeling system, was developed a few years ago, which allows tracking specific mRNAs in real time in live cells. The MS2-GFP labeling system utilizes the high affinity interaction between sequence-specific RNA stem-loops (MS2 protein binding sites) and the bacteriophage capsid protein MS2. Incorporation of multiple repeats of the MS2 stem-loops into an RNA sequence of interest creates an interaction platform capable of binding to multiple MS2 proteins. When coupled to GFP (MS2-GFP fusion protein), MS2 protein that binds to the MS2 stem loops carrying RNA tags the RNA with GFP, thus enabling visualization of the RNA *in vivo*. The simultaneous expression of a MS2 stem-loop containing mRNA and the MS2-GFP in cells provides a powerful method for detecting specific mRNP complexes (Fig. 7, modified from Bertrand et al., 1998). A solution to the signal to noise problem, while tracking specific mRNAs within the cytoplasm, is provided by a Nuclear Localization Signal contained within the MS2-GFP protein. The Nuclear Localization Signal sequesters MS2-GFP within the nucleus when not bound to an MS2-containing RNA target. The high affinity interaction between the stem-loop sites and the MS2 protein ensures that most reporter mRNAs are bound by a number of MS2-GFP fusion proteins and that the majority of GFP signal emanates from bona fide target transcripts. Importantly, the mRNAs generated from this reporter are

Introduction

transcribed in the nucleus and are properly packaged, exported, targeted, and translated, making MS2-GFP a good system to track mRNAs from their sites of synthesis to translation.

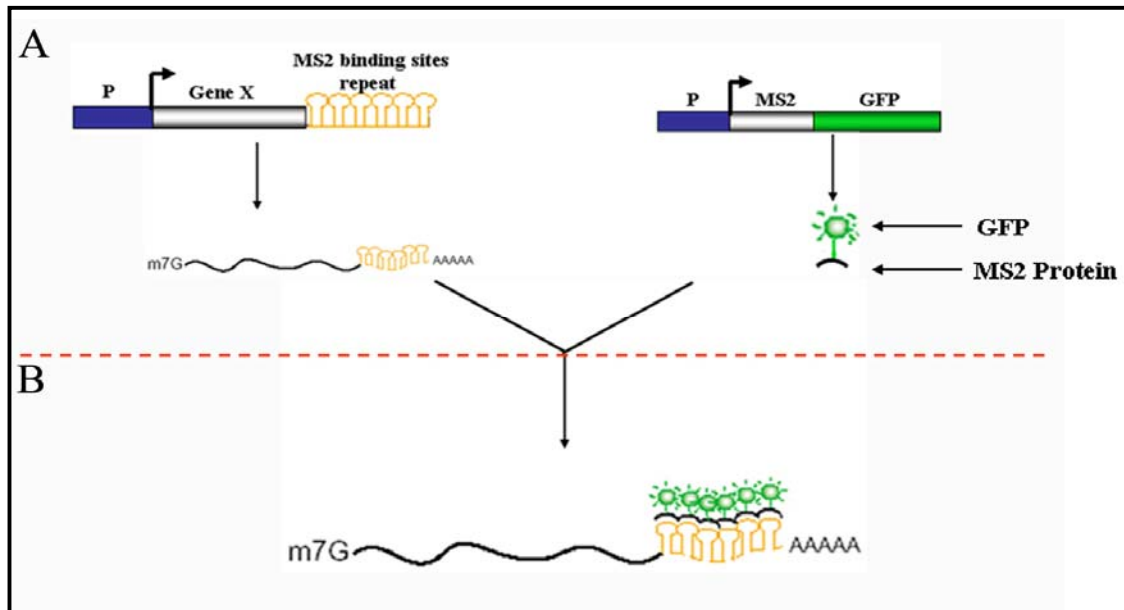


Figure 7. Schematic describing the MS2-GFP labeling system. A) MS2-GFP labeling is a two component system. The gene of interest is tagged with MS2 protein binding site stem loop sequence. The second component is the MS2 protein fused to GFP. B) When both the components are expressed in a cell, the MS2-GFP fusion protein binds to the stem loop (MS2 binding sites) and consequently the GFP tagged mRNA can be visualized and tracked in the cell. Image modified from Bertrand et al., 1998.

The MS2-GFP labeling technique was initially used in yeast (Bertrand et al., 1998) and in cultured mammalian cells and later adapted in *Drosophila* for tracking RNA localization in tissues. To visualize localization of *nanos* mRNA *in vivo* in the *Drosophila* oocyte, Forrest and Gavis used the MS2-GFP labeling system (Forrest and Gavis, 2003). In this study the RNA of interest, *nanos*, was synthesized from a transgene into which binding sites for the fusion protein had been inserted. The MS2-GFP fusion protein, the second component of the reporter system, was provided from another transgenic fly. The modified and MS2-GFP tagged *nanos* RNA behaved similar to normal endogenous RNA, at least in the localization studies. The authors, using the MS2-GFP labeling system, show features of *nanos* mRNA localization previously unseen.

1.10 A genetic screen for localized RNAs in *Drosophila* tracheal cells

The high degree of developmental plasticity exhibited by terminal branches raise the interesting question whether their development is regulated by localized translation at the site of branch growth. If so, a prerequisite is localization of specific RNAs to sites of branch outgrowth. To study if RNAs localize asymmetrically in terminal tracheal cells we decided to perform a genetic screen. In this screen the localizing RNAs will be visualized by making use of the MS2-GFP labeling system, which provides an efficient means for visualizing RNAs *in vivo*. To visualize transcripts of randomly tagged genes in the *Drosophila* genome, we decided to combine the MS2-GFP labeling system with the modular miss-expression system, the EP technique. The existing EP transposon element will be modified by introducing MS2 binding sites downstream of the promoter that initiates expression of the neighboring gene. The transgenic lines generated from the modified EP insertion would then be screened using a tracheal specific Gal4 Driver (*breathless*-Gal4) in conjunction with a second transgene encoding the NLS-MS2-GFP. This screen would essentially combine the advantages of a conventional EP screen, including analysis of over expression phenotypes, cloning of the gene by plasmid rescue and mutagenesis by P element excision, with visualization of mRNA localization.

1.11 Aim of the project

The aim of my thesis project is to develop a genetic technique that can be used for screening RNAs exhibiting specific subcellular localization in *Drosophila*. Using this technique, I sought to identify asymmetrically localizing RNAs in terminal tracheal cells and to study the functional relevance of RNA localization in the regulation of terminal branch development.

2. Materials and Methods

2.1 Materials

2.1.1 *Drosophila melanogaster* stocks

Wild type flies used were Oregon R.

2.1.2 UAS Transgenes

From Bloomington stock centre

w[1118]; P{w[+mC]=UAS-Btsz2-Poly}2;+/+

w[1118]; P{w[+mC]=UAS-Moe.IR.327-775}3

w[1118]; P{w[+mC]=UAS-Moe.TD.MYC}2

w[1118]; P{w[+mC]=UAS-Moe-GFP.K}2

w[1118]; P{w[+mC]=UAS-GFP.KDEL}11.1/Cyo

w[1118]; P{w[+mC]=UAS-GFP.KDEL}15.2/TM6B, Tb[1]

From other sources

w[1118]; ;P{w[+mC]=UAS-RpS2^{L315}-TAP} (From Stefan Luschnig)

w[1118]; P{w[+mC]=UAS-PABP^{L423}-TAP}; +/+ (From Stefan Luschnig)

w[1118]; P{w[+mC]=UAS-Fng.DXD^{M917}-MYC}; +/+ (From Mathew Freeman)

w[1118]; P{w[+mC]=UAS-Btsz2-ΔC2-HA}2;+/+ (From Thomas Lecuit)

w[1118]; P{w[+mC]=UAS-NLS-MS2-eGFP⁶⁷};+/+ (Generated for this work)

2.1.3 Gal4 drive lines

w[1118]; P{w[+mC]=*btl*-Gal4}; +/+

w[1118]; +/+; P{w[+mC]=*btl*-Gal4}

w[1118]; If/Cyo; P{w[+mC]=*btl*-Gal4}

w[1118]; If/Cyo; P{w[+mC]=*btl*-Gal4, UAS-GFP}

w[1118]; If/Cyo; P{w[+mC]=*btl*-Gal4, UAS-DsRed}

w[1118]; P{w[+mC]=*btl*-Gal4, UAS-MS2-e GFP⁶⁷}; +/+

w[1118]; +/+; P{w[+mC] vp16:*nanos*-Gal4, UAS-MS2-GFP}/TM3 Ubx-LacZ

w[1118]; P{w[+mC]=*krupple*-Gal4}/CyO; +/+

Materials and Methods

2.1.4 EP-MS2 Transgenes

w[1118], P{w[+mC]=EP-MS2 (6X binding sites)};; (Generated for this work)

w[1118] ;P{w[+mC]=EP-MS2 (12X binding sites)} (Generated for this work)

w[1118], P{w[+mC]=EP-MS2 (24X binding sites)};; (Generated for this work)

2.1.5 Mutants

w;;*btsz*^{K13-4}/TM3Sb *KrGal4-UAS-GFP*

w;;FRT82B *btsz*^{J5-2}/TM3Sb *KrGal4-UAS-GFP*

2.1.6 Antibodies used

Following primary antibodies were used; rat anti-HA (1:100, Boehringer Mannheim), rabbit anti-Dof (1:20, Vincent *et al.*, 1998), rabbit anti-P Moe (1:50, Cell Signaling), rabbit anti-Pac (1:500, Gift from S. F. Newbury), rabbit anti-DCP-1 (1:10, Ming-Der Lin, 2006), rabbit anti-DCP-2 (1:200, Ming-Der Lin, 2006), rabbit anti-Baz (1:200, Kuchinke U. *et al.*, 1998), rabbit anti-Par6 (1:100, Petronczki, M. & Knoblich, J. A., 2001), rabbit anti-aPKC (1:200, Santa Cruz), rabbit anti-PolyG (1:50, Cell Signaling) and rabbit anti-GFP (1:500, Torrey Pines Biolabs Inc). Fluorochrome conjugated secondary antibodies; Alexa468 and Alexa568 and Alexa647 (Molecular Probes) were used at a dilution of 1:500.

2.1.7 Primers

GCAGCGGCCGAGTGAGCAAGGGCGAGGAGC eGFP 5 prime

CGTCTAGATTACTTGTACAGCTCGTCCATGCC eGFP 3 prime

2.1.8 Sequencing primers for pUAST vector

GAAGAGAACTCTGAATAGGGAATTGG pUAST 5 prime

GGTAGTTTGTCCAATTATGTCAC pUAST 3 prime

2.1.9 Inverse PCR primers

GTAACGCTAATCACTCCGAACAGGTCACA Pwht1

Materials and Methods

CACCCAAGGCTCTGCTCCCACAAT	Plac1
CCTTAGCATGTCCGTGGGGTTTGAAT	Pry1
CTTGCCGACGGGACCACCTTATGTTATT	Pry2
CAATCATATCGCTGTCTCACTCA	Pry4
ACACAACCTTTCCTCTCAACAA	Sp1
GACACTCAGAATACTATTC	Spep1

2.1.10 Plasmids used for generating transgenes

pUAST (Brand A. and Perrimon N., 1993), EP vector (Rorth P., 1996),

2.1.11 Microscopes used

Leica TCS SP2, Zeiss Axioplan 2-imaging, Zeiss Apotome and Leica M2 16FA were used for microscopy. Quantix (Photometrix) and AxioCam HRm (Zeiss) cameras were used for imaging.

2.1.12 Imaging and data analysis software

Images acquiring software Leica Confocal Software LCS, Axiovision Rel 4.6 (Zeiss) and Axiovision 1 (Zeiss) were used. Images were edited using Adobe Photoshop (Adobe Systems) and ImageJ software. DNA sequence alignments, analysis and oligonucleotide designing were done using the VectorNTI.

2.1.13 Reagents

TritonX 100, Tween20 and BSA were purchased from Sigma. Vectashield mounting media for fluorescent samples were from Vector Laboratories. Restriction enzymes used were from New England Biolabs. Expand High Fidelity PCR system was supplied by Roche Diagnostics GmbH. Agarose electrophoresis grade was from Gibco BRL. Unless otherwise mentioned, all the other chemicals were purchased from Merck, Sigma or Roth.

*Materials and Methods***2.2 Methods****2.2.1 Fly maintenance and embryo collection**

The flies were maintained under standard conditions (Ashburner, 1989; Wieschaus and Nüsslein-Volhard, 1986)

To fix the embryos, properly staged embryos were collected on an apple juice – agar plate, dechorionated using 50% bleach and washed in tap water. Embryos were fixed in 4% Formaldehyde in PBS:heptane (1:1) solution at room temperature for 20 minutes, with vigorous shaking followed by devitellinization with methanol:heptane (1:1) solution by vortexing for half a minute. Embryos were washed several times in methanol and stored in methanol at -20°C if not used immediately.

2.2.2 Antibody staining

The fixed embryos were rehydrated in PBST, followed by one hour blocking at room temperature using 1% BSA in PBST. The liquid phase was taken off and the primary antibody was added. The reaction was left at 4°C overnight. Embryos were washed with PBST several times, at room temperature followed by incubation in secondary antibody (biotin labeled or Alexa fluoro-chrome conjugates) at room temperature for 90 minutes. The secondary antibody was washed away by PBST. After incubation in Alexa secondary antibodies the embryos were washed thoroughly in PBST. The embryos were mounted in Vectashield (Vector Laboratories) and taken for microscopy.

2.2.3 Larval immuno-stainings

3rd instar larvae were filleted and fixed with 4% paraformaldehyde for 20 minutes. Post fixation fillets were washed with 0.1% PTX (1XPBS+ 0.1 % TritonX 100) three times for 10 min each followed by 1 hour incubation in blocking reagent (1XPBS+ 0.1 % TritonX 100 + 1% BSA). After blocking the fillets were incubated overnight in antibody solution at 4°C. Fillets were washed 4 times (15 minutes each) in 0.1% PTX after overnight incubation. Fillets were incubated in Alexa fluoro-chrome conjugated secondary

Materials and Methods

antibodies for 2 hours at room temperature. Next, the fillets were washed for two hours at room temperature, mounted in Vectashield (and taken for microscopy).

2.2.4 Molecular biology

Standard molecular biology techniques were used for cloning (Sambrook et al., 1989).

2.2.5 EP-MS2 construct

The EP-MS2 constructs were generated by modifying the EP vector (Rorth, 1996). Three EP-MS2 constructs were cloned (EP-MS2 6X, EP-MS2 12X and EP-MS2 24X). MS2-BS (6 BS and 24 BS) fragments were digested from pSL-MS2 plasmid (Singer, 1999) using BamH1 and Nsi1 enzymes. The protruding BamH1 and Nsi1 overhangs were blunted using T4 DNA polymerase. The EP vector was digested with Pst1 enzyme and was blunted using T4 DNA polymerase and the MS2 BS fragment was blunt-end ligated into the Pst1 site in the EP Vector. The EP-MS2 constructs were transformed into DH5 α cells and subsequently the colonies were screened for positive clones. The positive EP-MS2 clones were digested with Not1 enzyme and the Kanamycin resistance gene was cloned into the Not1 (the EP vector has an Ampiciline resistance gene). The addition of Kan Res gene is the plasmid rescue feature of the vector. The construct was transformed and colonies that were both Kan and Amp positive were selected. The positive clones were confirmed by restriction digestion using Not1 and Bgl2 enzymes prior to injection to generate transgenes.

2.2.6 NLS-MS2-eGFP constructs

The NLS-MS2 coding sequence was digested, using BamH1 and Not1 enzymes, from NLS-MS2-GFP construct (NLS-MS2-GFP cloned in pUASp, Filardo, P., unpublished construct). The eGFP coding sequence was PCR amplified from pBI eGFP plasmid using the following primers; 5' GCAGCGGCCGCAGTGAGCAAGGGCGAGGAGC 3' (with Not1 overhang and does not include the initiation codon ATG) and 3' CGTCTAGATTACTTGTACAGCTCGTCCATGCC 5' (with Xba1 overhang). The pUAST vector was digested with Bgl2 and Xba1 enzymes and the NLS-MS2 fragment

Materials and Methods

along with the PCR amplified eGFP fragment was ligated into Bgl2/Xba1 site in the pUAST vector. The cloned constructs were transformed into DH5 α and colonies were screened for positive clones. The positive clones were confirmed by sequencing and the transgenic constructs were injected.

2.2.7 Inverse PCR protocol

Inverse PCR protocol from BDGP (<http://www.fruitfly.org/about/methods/inverse.pcr.>) was used for molecular mapping of EP-MS2 insertions. From each line genomic DNA was isolated from adult flies and they were digested with either HnPI or MspI were used. The digested DNA was allowed to self ligate to circular plasmid. Self ligated plasmids would have fragments from the either the 5prime or 3prime of EP-MS2 element together with the flanking genomic sequences. The self ligated plasmid were then used as the template for a PCR reaction with specifically designed primers (Pry1, Pry2, Pry4, PLac1 and Pwht1) that would amplify the region including the inverted repeat of the transposon insertion along with the immediate flanking genomic region. The amplified PCR product was then sequenced with specific sequencing primers (Sp1 and Sp1) and the sequences were subjected to Blastn analysis to locate them in the genome.

2.2.8 Electron microscopic studies

Transmission electron microscopy

Third instar larvae were dissected in PBS, and immediately fixed for 20 minutes at room temperature in 4% paraformaldehyde/PBS. Fillets were postfixed for 1 hour in 0.5% glutaraldehyde followed by 1 hour in 1% osmium tetroxide and stained overnight in 0.5% uranyl acetate at room temperature. Samples were kept in 2% osmium tetroxide, 0.5% uranyl acetate (prepared from a 20% stock solution in methanol) and 0.5% glutaraldehyde. After washing with acetone the samples were transferred into an acetone-Epon mixture (1:1 for 4 h, 1:2 for 12 h), at room temperature followed by incubation in Epon (3 changes 10 min each) and polymerised at 60 C for 48 h. Fillets were sectioned using microtome and the sections (100nm) were stained with 2% uranyl

Materials and Methods

acetate in 70% methanol for 10 min and in 0.4% lead citrate in 0.1 N NaOH for 2 min were viewed in a Philips CM10 electron microscope at 60 kV.

Scanning electron microscopy

For scanning electron microscopy fillets were fixed for 20 minutes in 4% paraformaldehyde followed by 1 hour fixation in 0.5% glutaraldehyde at 4°C. The fillets were incubated in osmium treated (1% osmium tetroxide in 100 mM phosphate buffer, pH 7.2), dehydrated through an ethanol series, subjected to critical point drying from CO₂ and sputter coated with 10 nm Au-Pd. Samples were examined at 20 kV accelerating voltage in a Hitachi S800 field emission scanning electron microscope.

3. Results

3.1. Terminal branch development in larvae

Most of the studies carried out in tracheal development in flies have concentrated on patterning and tube formation mechanisms in embryos. The tracheal developmental events during the larval phase, when most of the terminal branching occurs, are almost entirely unexplored. I started by analyzing the morphological characteristics of terminal branches in third instar larvae.

3.1.1 Categorization of terminal branches based on lumen diameter

Terminal branches undergo extensive ramification during larval development, resulting in widespread coverage of target tissues with oxygen supplying blind-ended tubes. Studies in *Rhodnius prolixus* have illustrated that the terminal branch lumen has a diameter of 0.7 to 1 μ m or less at its origin and tapers over its length to a blunt end of 0.1 to 0.3 μ m (Wigglesworth, 1954). Lumen diameters of *Drosophila* terminal branches were also described to be similar (Wigglesworth and Lee, 1982). While this description holds good, a closer look at the terminal branches reveals that lumen diameter varies not only along its length (from proximal to distal positions from the nucleus) but also in different branches.

The terminal tracheal cells exhibit different terminal branching patterns; nevertheless one does see a general pattern of terminal branching vaguely resembling the pattern of veins in a feather. In general, terminal cells have branches, usually one or two, growing to a length of approximately 200 μ m and have an average lumen diameter of approximately 1 μ m or less. Along the length of these branches, new branches that have thinner lumen diameter develop. In addition to these extensions, one can also observe fine filopodial extensions devoid of lumen, arising from random positions along the branches (Fig. 8). In order to evaluate the differences in lumen diameter in different branches and along the proximal-distal axis, I have categorized branches into Type-A and Type-B. Type-A category consists of branches with the widest lumen diameter and Type-B branches have a thinner lumen diameter. Figure 9 is a schematic explaining this categorization of terminal branches based on lumen diameter.

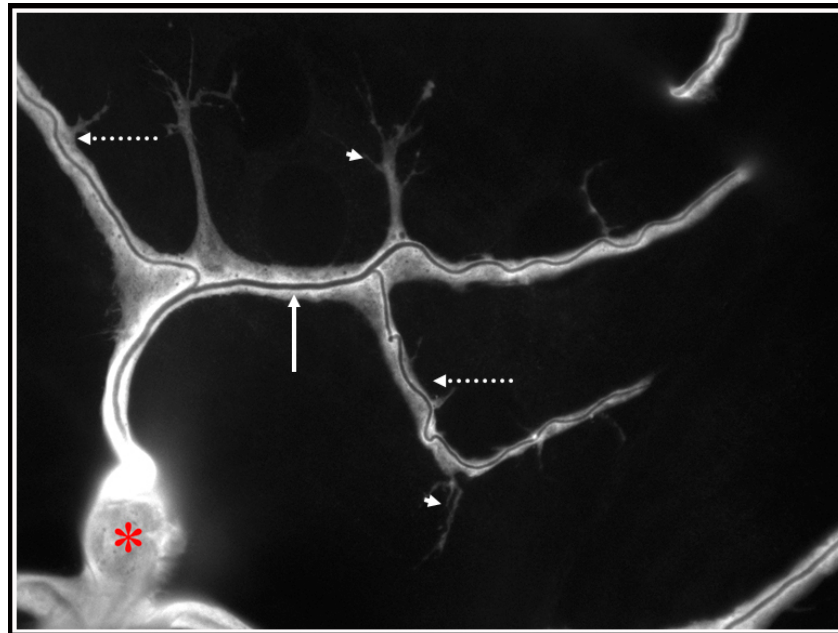


Figure 8. Terminal branches from a third instar larva. The Red asterisk marks the nucleus of the terminal cell. White arrows mark different types of branches. The continuous arrow shows a branch with bigger lumen diameter than the ones marked with dotted arrows. The arrowheads mark filopodial extensions.

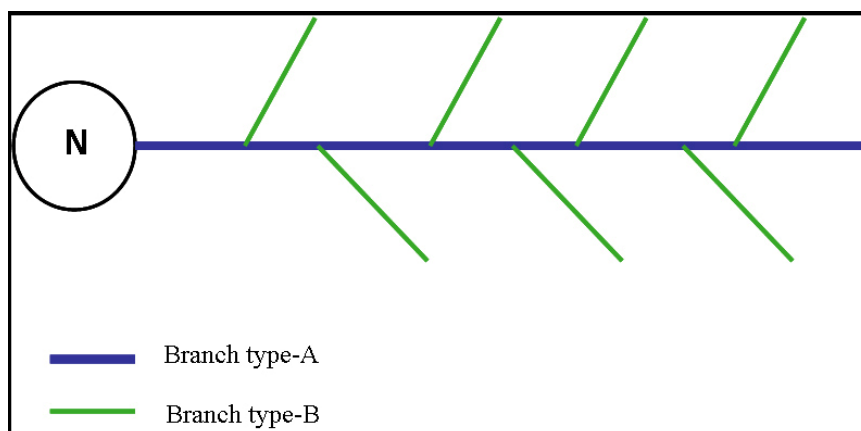


Figure 9. Schematic representation of terminal branches categorized based on lumen diameter. The circle with 'N' represents the nucleus. The thick blue line represents the Type-A branch with widest lumen (axial stem). The green line represents bifurcated Type-B branches, with thinner lumen diameter.

To evaluate the lumen diameters of Type-A and Type-B branches, measurements were taken from six different terminal cells. Two data sets were made with lumen diameters measured at random positions along the Type-A and Type-B branches. From each terminal tracheal cell at least four measurement points on the Type-A branches along the Proximal-Distal axis and six measurement points from three different Type-B branches were taken (Fig. 10). A total of 33 measurements for

Results

Type-A branches and 37 measurements for Type-B branches were gathered and sorted as data set-1 and data set-2 (data sets in appendix) respectively.

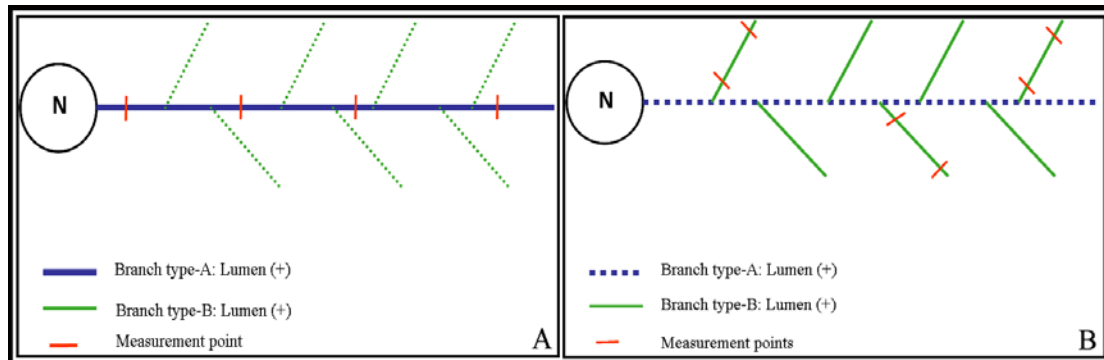


Figure 10. Schematic depicting the positions along the Type-A and Type-B branches from a single terminal cell, where measurements were taken for statistical analysis. A) Measurement points along the Type-A branch. B) Measurement points on the Type-B branches.

The data sets were subjected to statistical analysis and the median values and standard deviation, for the measurements of each of the data set were calculated. Data set-1 and data set-2 had the median values of $1.17\mu\text{m}$ and $0.74\mu\text{m}$ respectively (Appendix). The standard deviation for measurements within each data set was 0.17 for data set-1 and 0.07 for data set-2; both values were within the permissible range. The standard deviations suggest that although the lumen diameter varies within each type of branch, the variation is not very high. Further, the difference in lumen diameter between Type-A and Type-B branches was about 37%; in other words the Type-B branches had lumen diameter 37% thinner than the Type-A (Fig. 11).

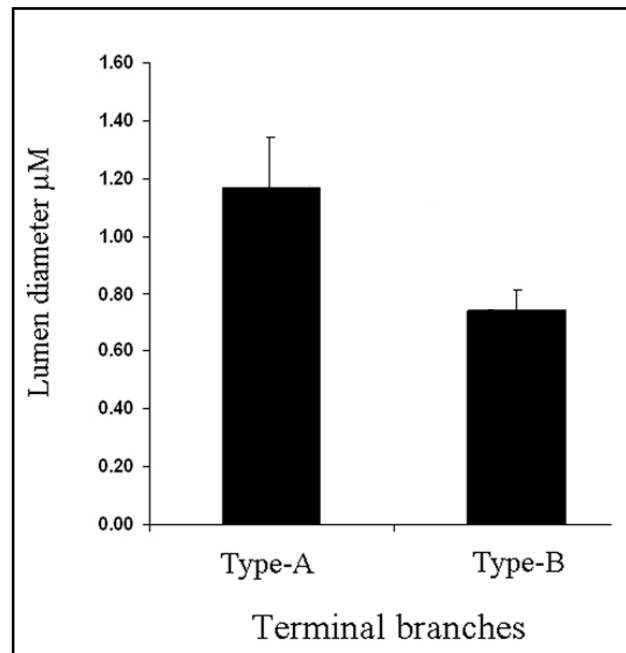


Figure 11. Difference in lumen diameter of terminal branches. The graph illustrates the difference in lumen diameter between Type-A and Type-B branches. There is significant difference in lumen diameter between the two types of branches. The diameter of Type-B branches is 37% thinner than Type-A.

3.1.2 Lumen diameter decreases along the Proximal-Distal Axis from the nucleus

Analyses were also done to study if the lumen diameter is constant along the proximal-distal axis of Type-A branches. For this experiment, six groups of measurements taken along the proximal-distal axis of Type-A branches from six different cells, were used (data set-3 Appendix). Data set-3 was analyzed to study whether the variation in lumen diameter within the Type-A branches occurred randomly or exhibited a pattern along the proximal-distal axis. In the first set of analyses measurements ($P_1 \dots P_n$) from each of the six groups were plotted in a graph (Fig. 12A). The data showed that the lumen diameter decreases from the proximal to the distal end. Further, the data also shows that though the diameter decreases from the proximal end to distal end it does not always occur in a progressive manner. The percentage fall (percentage decrease) in lumen diameter between the proximal end and the distal end was also determined (Fig. 12B). The percentage fall was determined by comparing the difference in lumen diameter in percentages, between the most proximal and distal measurements (P_1 and P_n) from each group. The results

Results

clearly showed that the lumen diameter is not constant along the length and decreases progressively in Type-A branches, with the difference being 38%.

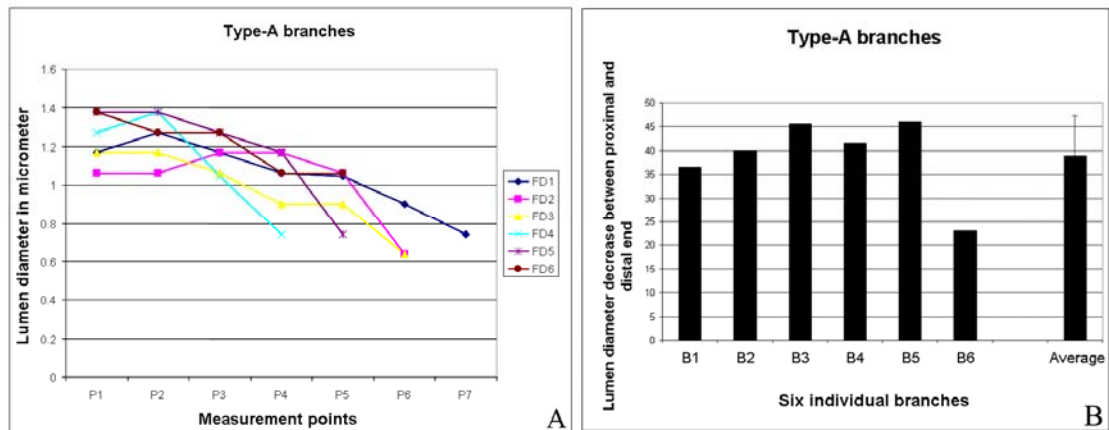


Figure 12. Lumen diameter decreases along the proximal-distal axis of Type-A branches. A, Plot diagram representing the lumen diameter along the proximal-distal axis of 6 different branches. B, The bar diagram shows the difference (in percentage) in lumen diameter between the most proximal and most distal end from the six groups of data. B1-B6 represents 6 Type-A branches. The average percentage fall in lumen diameter between the two ends in Type-A branches is about 38%.

3.1.3 Cell diameter varies along the proximal-distal axis from the nucleus

Experiments done to analyze the lumen diameter in terminal branches had revealed that the diameter varies between Type-A and Type-B branches and also along the proximal-distal axis in Type-A branches. To study whether there is any correlation between the cell diameter and the lumen diameter in terminal branches, I have analyzed the cell diameters in the terminal branches. For this analysis, measurements of lumen diameter and the cell diameter (from the same positions) along the proximal-distal axis of Type-A branches from six different terminal cells were used (data set-4 appendix). Altogether, 33 measurements of lumen diameter and corresponding cell diameter from six branches were included in data-set 4. The median value of the lumen diameters measured was $1.17\mu\text{m}$ and the standard deviation between the individual measurements was within the permissible range (SD: 0.213). The cell diameter measurements, 33 measurements corresponding to 33 lumen diameters, had a median value of $3.71\mu\text{m}$, but in this case the standard deviation was significant with a value of 1.11. The data suggests that there is a considerable degree of variation in the cell diameter when compared with the lumen diameter in Type-A branches (Fig. 13A). Further, when the cell diameter measurements are plotted in a

graph it was clear that there is no apparent pattern in the cell diameter variation and it is random along the proximal-distal axis of the branches (Fig. 13B).

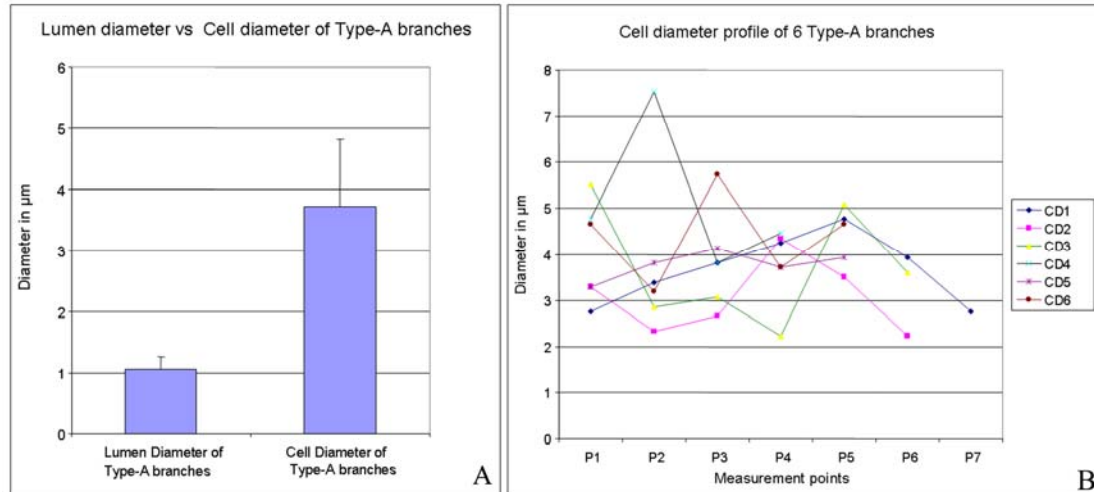


Figure 13. Comparison of lumen diameter versus cell diameter of terminal branches. A, Median values of lumen and cell diameters measured at the same positions in six Type-A branches. The lumen diameter has a median value of about $1.17\mu\text{m}$. The cell diameter had a median value of $3.71\mu\text{m}$. The standard deviation in this case was significant, indicating considerable variation within the set of measured cell diameters. B, Cell diameter measurements from six branches (CD1-CD6). P₁...P_n measurements form six points along the proximal-distal axis from six branches. The graph demonstrates that the cell diameter along the proximal-distal axis in the branches has no apparent pattern and the variation is random.

3.2 Translational and co-translational machinery is present in terminal branches

The main objective of my thesis project was to identify RNAs that asymmetrically localize in the terminal tracheal cells. The screen was based on the assumption that some of the proteins required at the site of outgrowth are synthesized locally rather than near the nucleus. For translation to occur in sites of outgrowth, at significant distances from the nucleus, these sites would have to contain components of the translational and co-translational machinery. Subcellular organelles such as ribosomes, polysomes, endoplasmic reticulum (ER) and Golgi bodies are present in axonal growth cones and pre and/or post synaptic regions in dendrites, where localized translation occurs (Black and Lasek, 1977; Giuditta et al. 1977; Giustetto et al. 2003; Martin et al. 1998; Steward and Levy, 1982). I have characterized the subcellular distribution of the above mentioned cellular organelles in terminal branches in third instar larvae.

Results

3.2.1 Transmission Electron microscopic studies to analyze ribosome and ER

Transmission electron microscopic (TEM) studies were carried out to analyze the distribution of subcellular organelles in the terminal branches. Fillets of third instar larvae were sectioned at random positions and selected cross-sections containing terminal branches were imaged and analyzed. Based on the diameter of the lumen in the electron micrograph, it was possible to assess whether the sections were from Type-A or Type-B branches. Micrographs with sections of Type-B branches were analyzed, since Type-B branches are more distant from the terminal cell nucleus. The TEM studies revealed that ribosomes are present in the cytoplasm of the terminal branches. Further, both cytosolic and ER associated polysomes were observed in these micrographs (Fig. 14A and B). Analysis of EM micrographs also showed that both smooth and rough ER is present in the terminal branches (Fig. 15A and A’). A few, small, “swollen” rough ER was also observed in some of the sections. Such swollen rough ER is usually a consequence of the ER lumen being filled with freshly translated protein (Fig. 15A’). The presence of free cytoplasmic ribosomes, the polysomes and the ER is an indication that the conditions for translation to occur exists in the terminal branches, away from nucleus.

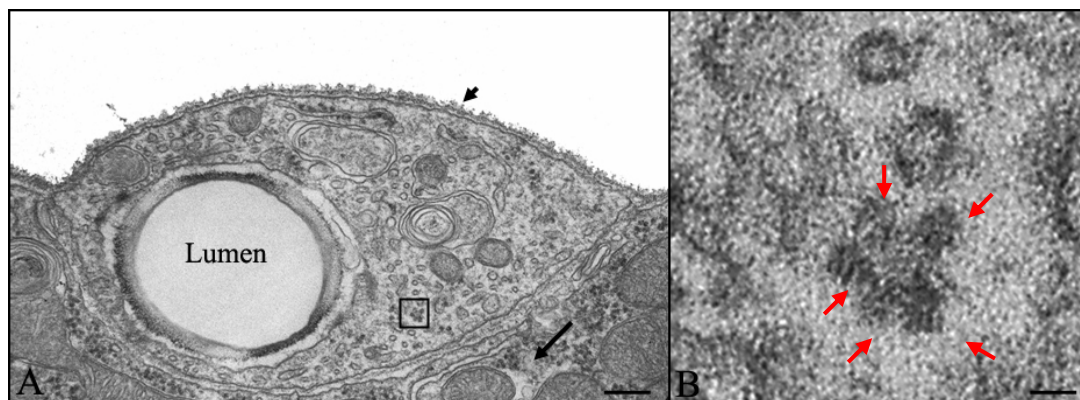


Figure 14. Electron micrograph of a section through Type-B terminal branch. A, Cross-section of Type-B terminal branch. The lumen in the section is a hollow cavity (marked as Lumen) towards a side of the section. The small black arrow shows the basal lamina encapsulating the branch. The long black arrow marks the underlying muscle in which the branch is embedded. The black box encloses a cytosolic polysome. B) The area within the black box is enlarged in B. The five red arrows mark the ribosomes that are part of polysomes. Scale bars: 1.19 μ m in A and 60nm in B

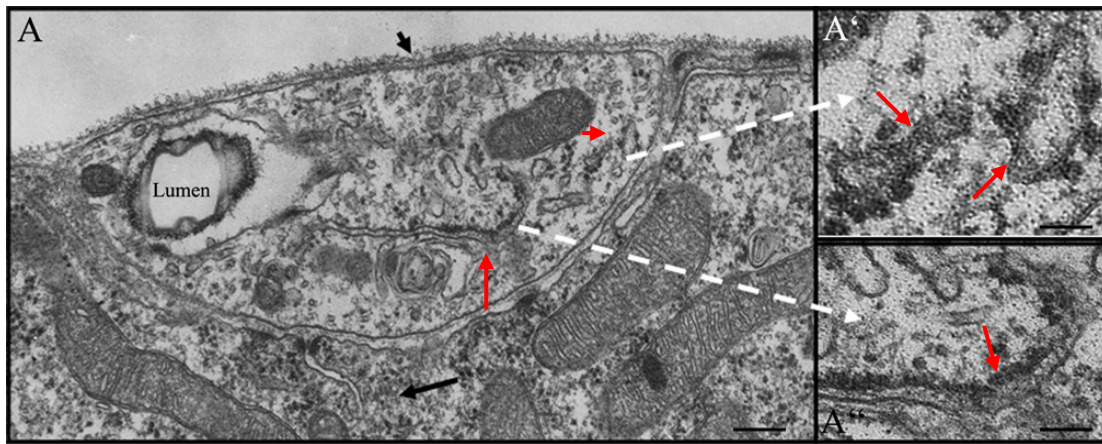


Figure 15. Electron micrograph of a section through Type-B terminal branch. A, The lumen in the section is hollow cavity towards a side of the section. The small black arrow shows the basal lamina encapsulating the branch. The long black arrow marks the underlying muscle on which the branch is juxtaposed. The black box encloses a cytosolic polysome. The red arrows mark the rough ER. A', Blow up shows two small blotted rough ER, marked with red arrows. A'', is a blow up of the rough ER (marked with red arrow) visible in A. Scale bars: 1.19 μ m in A and 230nm in A' and A''.

3.2.2 Immuno-histochemical studies to visualize ribosome, ER and Golgi bodies in terminal branches

In addition to the TEM studies, I analyzed the distribution of the translational and co-translational machinery by immuno-staining experiments. To analyze ribosome distribution in the terminal branches, a TAP tagged UAS-RpS2 transgene was expressed in the tracheal cells using the tracheal specific *btl*-Gal4. *Drosophila* RpS2 codes for a protein which is a constituent of the small ribosomal subunit. The over-expressed TAP tagged RpS2 protein was visualized by immuno-stainings using Rabbit (IgG)-anti-goat Alexa antibodies (Fig. 16). The TAP-RpS2 protein was seen in the terminal branches at positions distant from the nucleus, substantiating the findings of from the TEM studies.

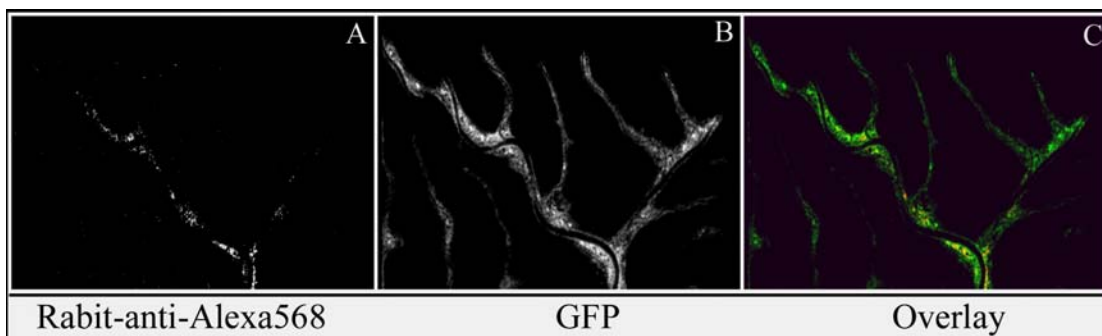


Figure 16. Ribosomes localize in terminal branches away from the nucleus. A, TAP-RpS2 localization in terminal branches. B, Cytosolic GFP labeling the terminal branches. C, Overlay

Results

Next, I looked at the distribution of ER and Golgi bodies in terminal branches. The ER distribution was studied by analyzing the distribution of KDEL-GFP fusion protein (GFP fused to the KDEL peptide sequence) expressed in tracheal cells. The KDEL motif functions as an ER retention signal in many ER resident proteins and GFP fused to the KDEL peptide sequence is a reliable marker for visualizing ER. The results show that the over-expressed GFP-KDEL protein is present throughout the terminal cell cytoplasm and did indeed extend into the terminal branches (Fig. 17). The Golgi localization in terminal branches was assessed next. To visualize the Golgi, the distribution of a Myc tagged Fringe protein (Munro and Freeman, 2000) was expressed in tracheal cells together with cytosolic GFP. *Drosophila* Fringe is a Golgi-localized glycosyltransferase. A single amino acid substitution in the Fringe protein abolishes its function but does not affect its localization in Golgi bodies and this modified form of Fringe can be used as a Golgi marker. The modified Fringe-Myc protein, expressed in the terminal cells, was visualized by immuno staining against Myc. Golgi bodies, like ER, are seen distributed throughout the terminal cell, well into the terminal branches (Fig. 18). The results from these immuno-histochemical experiments substantiate the findings from the TEM studies and confirm the presence of translational and co-translational machinery in terminal branches.

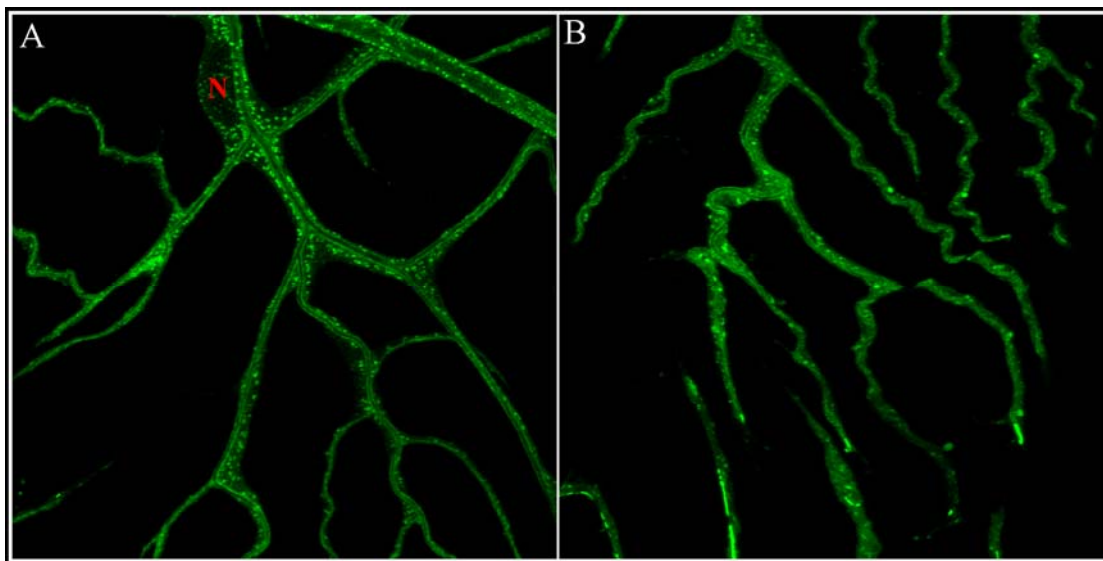


Figure 17. ER distribution in terminal branches was visualized by expressing KDEL-GFP fusion protein in tracheal cells. A shows the distribution of ER in terminal tracheal cells and terminal branches. The nucleus of the cell is marked with N (in red). B, a few terminal branches showing the distribution of ER.

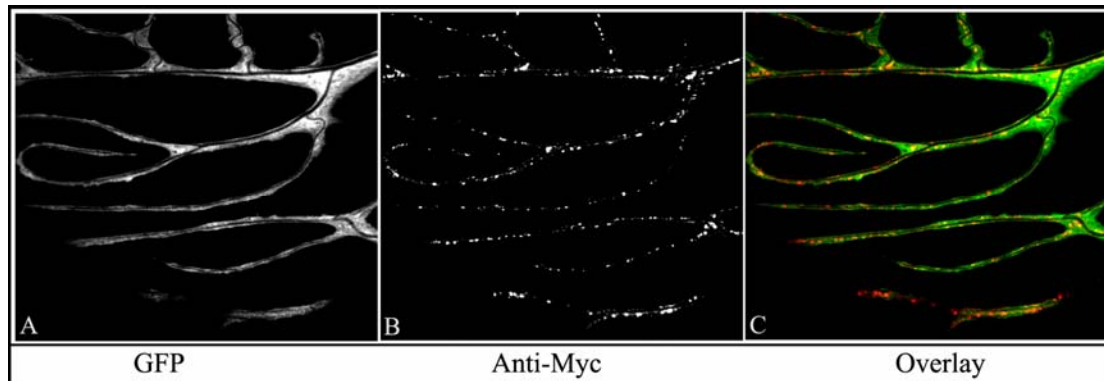


Figure 18. Golgi body distribution in terminal branches in third instar larva. UAS-Fng-Myc was expressed in tracheal cells together with cytosolic GFP. A, cytosolic GFP. B, Myc tagged Fringe protein labeling the Golgi. C, Overlay of GFP and Myc-Fringe in the terminal branches.

3.2.3 Poly (A) binding protein localizes in terminal branches

If localized translation regulates the development of terminal branches, then one would expect specific RNAs to localize in these branches. RNA binding proteins should therefore be present in the terminal branches along with the RNA that they are bound to or interact with. Hence, the presence of RNA binding protein in these branches could be taken as an indirect evidence for the presence of localized RNA. I have looked at the distribution of the Poly(A) binding protein (PABP) in the terminal branches. PABP is a general RNA binding protein that binds to the poly-A-tail of mRNAs and regulates different aspects of mRNA biogenesis (David et al., 2003). To visualize PABP in terminal branches, a TAP tagged cytoplasmic PABP was expressed together with a cytosolic GFP. Over-expression of PABP in tracheal cells resulted in an abnormal phenotype. In the PABP over-expressed larvae, the terminal branches were present but the distribution of cytoplasmic GFP was abnormal and in aggregates (Fig. 19). Nevertheless, it was possible to look at the distribution of TAP-PABP in this condition. The over-expressed PABP was present in the terminal branches. Compared to GFP, the PABP distribution appeared to be less diffused and more in granules or small aggregates. Such a distribution, i.e. in granules or small aggregates, very likely reflects the RNA bound PABP, since mRNAs that are actively transported are also clustered into granules. Figure. 20A illustrates the distribution of over-expressed TAP-PABP in terminal branches and Figure. 20B shows the growing tip of a terminal branch with PABP in granules.

Results

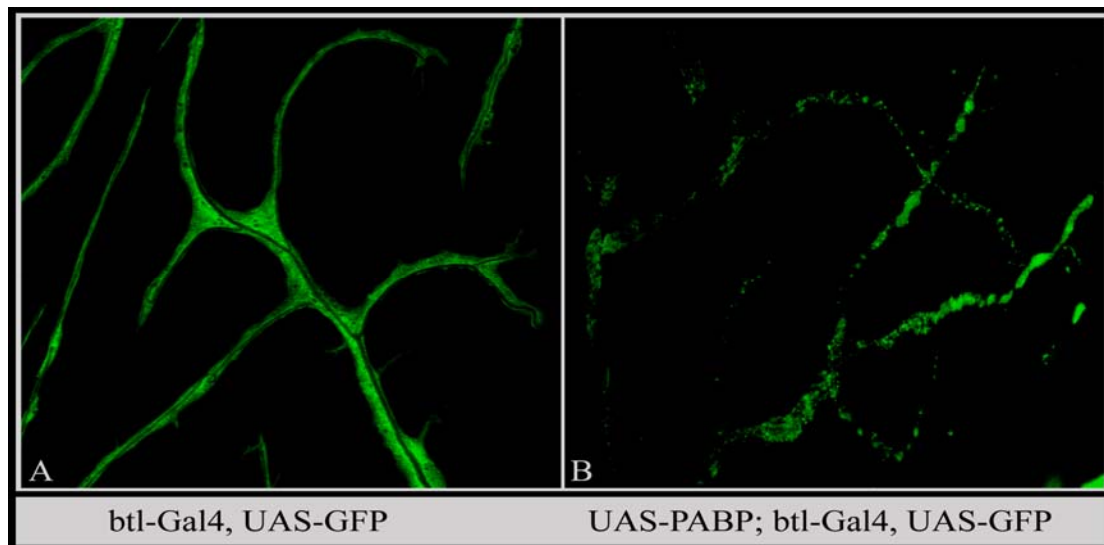


Figure 19. TAP tagged PABP over-expression in tracheal cells. UAS-PABP-TAP and UAS-GFP were expressed in tracheal cells using *btl-Gal4*. A, GFP (cytosolic) marking the terminal branches. GFP is diffused throughout the cytoplasm of terminal branches. B, Expression of PABP-TAP results in abnormal aggregates of cytosolic GFP.

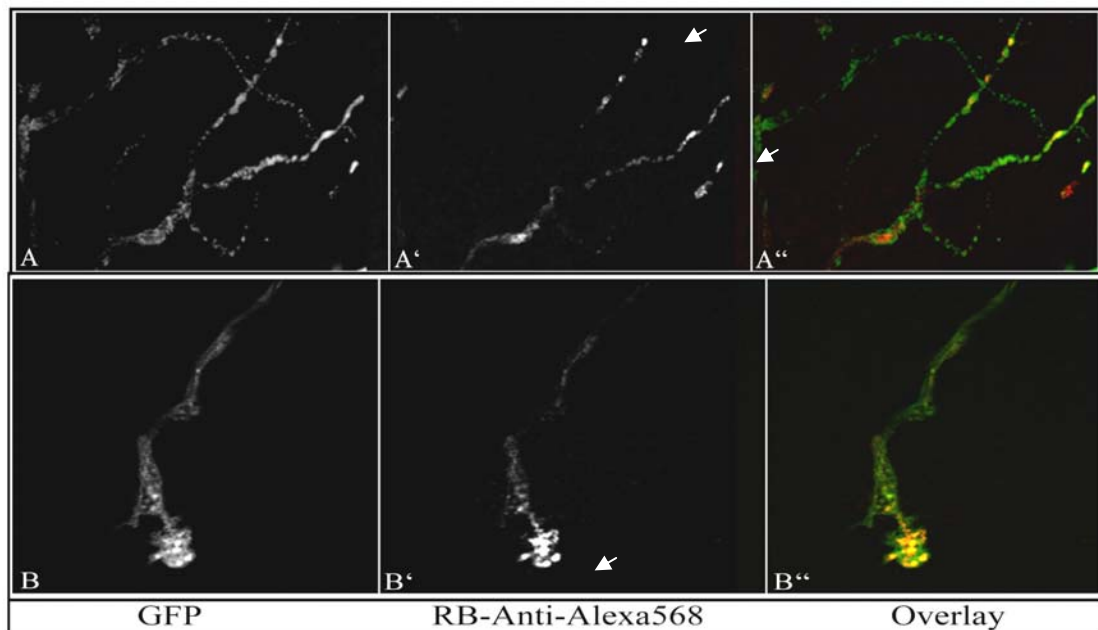


Figure 20. TAP tagged PABP over-expression in tracheal cells. A and B shows the GFP distribution in terminal branches where PABP is expressed. A' and B' shows PABP-TAP localization in the same branch as A and B. A & B, GFP is not uniformly distributed in the cytoplasm. A' & B', PABP-TAP is seen in granules (white arrows). A'' and B'' are overlay.

3.3 A genetic screen for localized RNA in tracheal cells

On the assumption that some of the proteins required at the site of growth in the terminal branches are synthesized locally rather than near the nucleus, we decided

Results

to perform a screen for localized RNAs in the tracheal cells. To investigate if specific RNAs localize in terminal branches, we have developed a new technique, the EP-MS2 technique. The strategy was to tag RNAs with GFP *in vivo* and to track the localization of such tagged RNA in the *Drosophila* terminal tracheal cells. For the screen, three transgenic fly reagents namely EP-MS2 transgenes, UAS-NLS-MS2-eGFP transgenes and *breathless*-Gal4 driver were necessary, and were generated.

3.3.1 Combining the MS2-GFP labeling system with the EP technique

In order to screen for asymmetrically localizing RNAs, we have combined the MS2-GFP labeling system with the EP technique. The EP technique (modular mis-expression system) is based on the inducible expression of genes tagged by insertion of a P-element vector carrying a GAL4 regulated promoter. In such screens, a transgene encoding the transcriptional activator GAL4 is expressed in specific tissues (“GAL4 driven lines”) to induce the expression of “target lines” harboring P-elements in random positions. These “target lines” carry an EP-element (Fig. 21), which has GAL4 binding sites that activate a promoter close to the 3prime inverted repeat of the P element in the vector. Binding of GAL4 induces the promoter within the EP element and leads to the expression of the gene downstream to the insertion site. The GAL4 dependent transcription begins within the P-element and extends out in to the genomic region that happens to lie next to the insertion (Rorth, 1996). This EP technique takes advantage of the fact that the P-element preferentially integrates into 5prime ends of genes and thus allows the expression of essentially full-length transcripts.

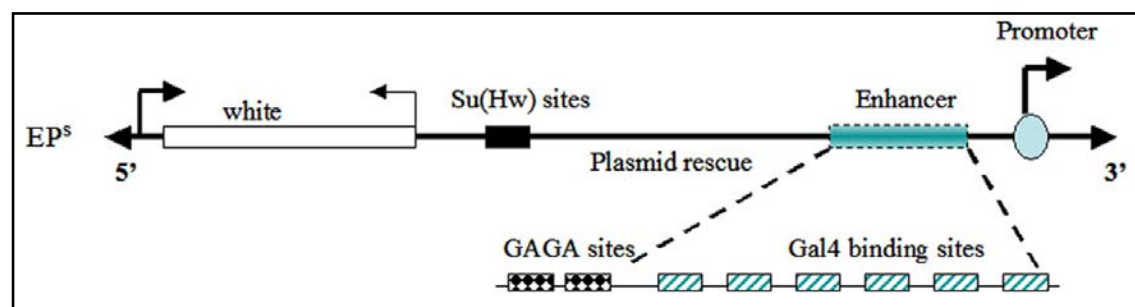


Figure 21. Schematic of the EP transposon Vector. The schematic represents the essential features of the EP transposon vector within the three and five prime inverted repeats of the P element. In addition the vector also has an ampicillin resistance cassette in the vector backbone, outside the P element inverted repeats. Within the P element inverted repeats a Gal4 inducible promoter (Gal4 binding sites and a basal promoter) is positioned close to the three prime inverted repeat. A

Results

transcriptionally independent white gene (the selectable marker) is positioned towards the five prime inverted repeat. In addition the EP element has Su(Hw) sites and GAGA sites as insulator sequences and a plasmid rescue site within the inverted repeats. Image adapted from Rorth, 1996.

I have modified the existing EP transposon vector by introducing MS2 binding sites three prime to the promoter that initiates the expression of the neighboring gene. The GAL4 induced transcript would therefore contain MS2 binding sites provided by the modified EP element along with the sequences of the tagged gene. In most cases, the resulting mRNA hybrid will include all the sequences sufficient for mRNA localization, as these sequences usually reside in the 3'UTR and P elements preferentially integrate at the 5prime ends of genes.

3.3.2 Generating transgenes and fly reagents for the screen

To perform the screen three important reagents were required; a tracheal specific Gal driver, UAS-MS2-GFP transgenes and EP-MS2 transgenes. Transgenic *btl*-Gal4 stocks were already available and were tested for their spatio-temporal expression patterns. UAS-MS2-GFP and EP-MS2 transgenes were generated for the screen

3.3.2.1 Modifying the EP transposon and generating EP-MS2 transgene

The EP transposon vector (described earlier) was modified by incorporating MS2 binding sites. Studies have shown that six binding sites, tagged with six molecule of MS2-GFP, are sensitive enough to visualize a single transcript. Hence, six tandem repeats of MS2 binding sites were cloned into the EP vector, making use of a restriction site downstream of the basal promoter and upstream of the 3prime inverted repeat of the P-element. In addition, a plasmid rescue feature was added by cloning a Kanamycin resistance gene in the plasmid rescue site of the EP transposon vector. This modified version of the EP transposon vector will be referred to as EP-MS2 vector henceforth (Fig. 22). Transgenes carrying the EP-MS2 element when induced using Gal4 driver would transcribe RNA which would contain the MS2 binding sites and the sequence of the tagged endogenous gene. The choice of P-element based vector for tagging genes were based on two important reasons; P-elements preferentially integrates at the five prime of genes and generally the *cis*-

Results

acting signals, essential for subcellular localization, in RNAs reside in the three prime UTR. Therefore, we expect that in most cases the MS2 binding site tags would be at five prime of the transcript and it is unlikely that the endogenous localization signals will be affected. Before injecting the EP-MS2 vector to generate transgenes it was sequenced, to check for erroneous mutations while cloning. Seven EP-MS2 transgenic insertions in the X chromosome were tested for hopping efficiency and one among them, EP-MS2⁶⁶, was used in the screen.

The number of MS2 binding sites that are usually used for tagging RNA range from 6 to 24 binding sites, as it was observed that in some cases more than 6 binding sites resulted in better resolution than with 6 binding sites. Therefore I had cloned two additional combinations of MS2 binding sites, 12 and 24 binding sites, in EP transposon vector. Nevertheless, transgenic flies carrying these EP-MS2 transposon vectors (with 12 and 24 MS2 binding sites) have not been generated yet.

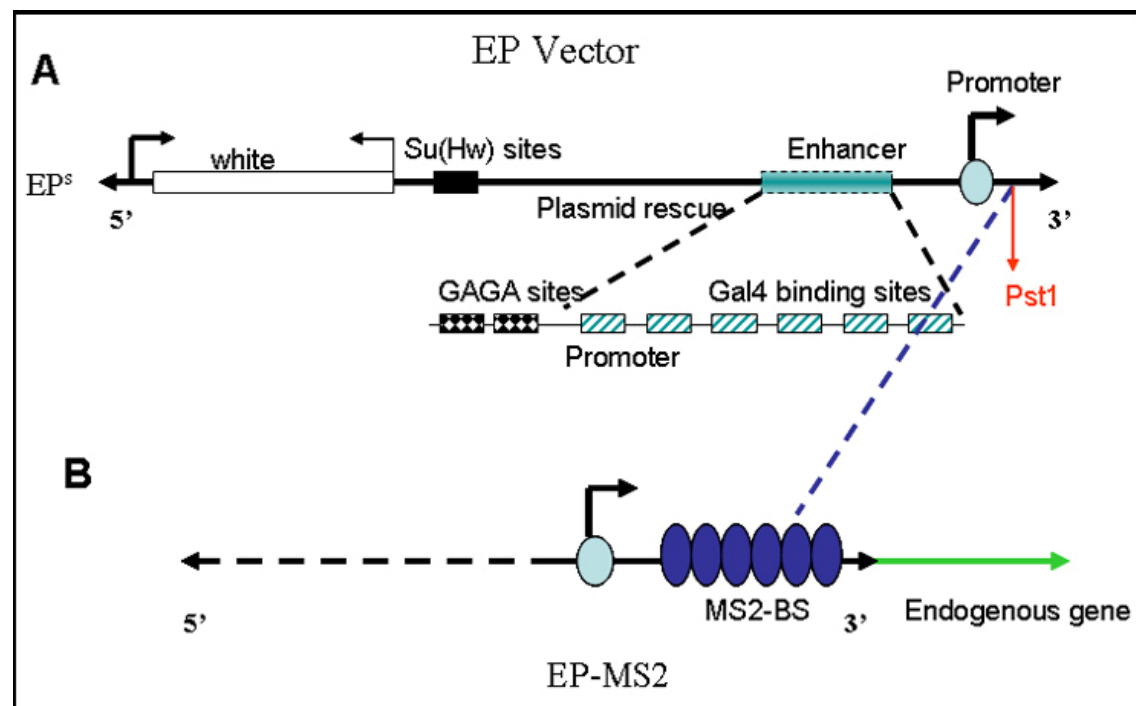


Figure 22. Schematic describing the modified EP-MS2 transposon vector. The EP transposon vector (A) was modified by cloning six tandem repeats of MS2 binding sites. The MS2 binding sites were cloned in Pst1 restriction site downstream of the basal promoter and upstream of the 3 prime inverted repeat of P-element. The resultant modified EP vector was named EP-MS2 (B).

3.3.2.2 Generating UAS-NLS-MS2-GFP transgenic flies

The MS2-GFP labeling system utilizes the high affinity interaction between sequence-specific RNA stem-loops and the bacteriophage capsid protein MS2 (Bertrand et al., 1998). To generate UAS-NLS-MS2-GFP transgenes, I have cloned the NLS-MS2-GFP translational fusion construct in the pUAST vector (Brand and Perrimon, 1993). Before generating the UAS-NLS-MS2-eGFP transgenes, the construct was sequenced to check for erroneous mutations while cloning. Henceforth, the UAS-NLS-MS2-eGFP construct and transgene will be referred to as MS2-GFP construct and MS2-GFP transgene respectively. Two features of this MS2-GFP fusion construct are worth mentioning. First, the NLS signal is incorporated to avoid background signal from the unbound cytoplasmic MS2-GFP. Presence of the NLS signal would target the unbound MS2-GFP protein into the nucleus and the cytoplasmic MS2-GFP signal would reflect only the RNA bound MS2-GFP. Second, the wild type MS2 coat protein oligomerizes and this is dependent on a small stretch of amino acids at the C-terminus end of the protein. This property of the MS2 coat protein could act as a hindrance in controlling the number of MS2-GFP protein tags on a target RNA. Hence, a mutant form of the MS2 protein lacking 10 amino acids that are essential for oligomerizing was used for generating the MS2-GFP fusion. Figure 23 explains the details of the fusion construct that was used for generating the MS2-GFP transgene.

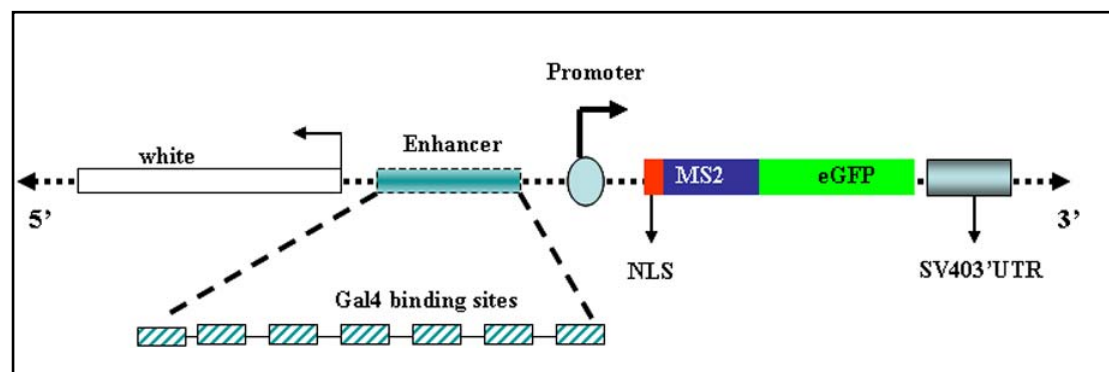


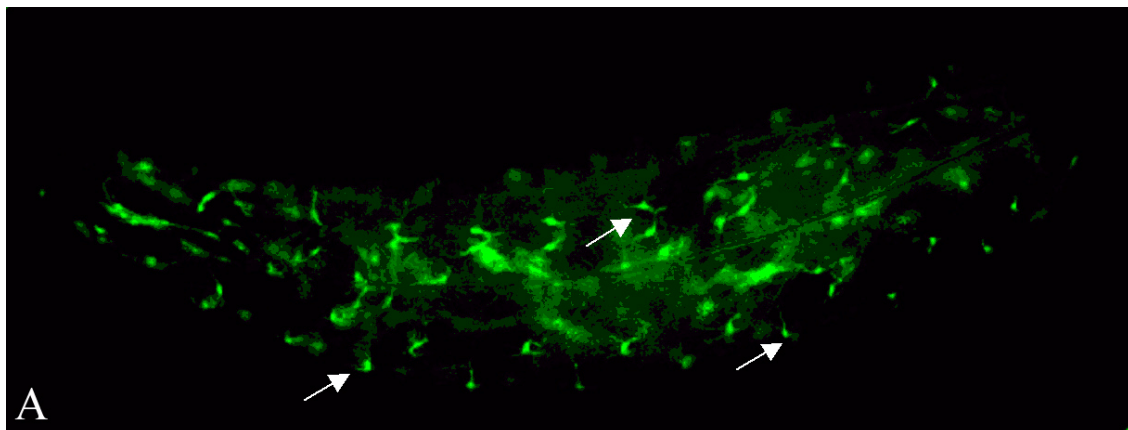
Figure 23. Schematic describing the NLS-MS2-eGFP fusion construct. The NLS-MS2-eGFP cassette, translational fusion construct, was cloned into the MCS of pUAST transposon vector. The essential features of the vector are represented in the schematic above. The pUAST transposon vector has five prime and three prime inverted repeats from the P element transposon and placed within these inverted repeats is the transcriptionally independent white gene (selectable marker), Gal4 binding sites, hsp70 basal promoter, the multiple cloning site and three prime UTR sequence from SV40.

Results

The MS2-GFP transgenes, balanced and mapped to 2nd and 3rd chromosomes, were tested for their efficiency. Seven transgenes, three on the 2nd and four on the 3rd chromosome, were crossed to two different Gal4 driver lines, viz., *kruppel*-Gal4 and *btl*-Gal4. Out of the seven lines tested, three (MS2-GFP¹² and MS2-GFP⁶⁷ on the 2nd chromosome, MS2-GFP³⁸ on the 3rd chromosome) showed the brightest GFP signal and were subsequently used for recombination with *btl*-Gal4.

3.3.2.3 Recombining UAS-NLS-MS2-GFP with *btl*-Gal4

MS2-GFP transgenes were recombined with *btl*-Gal4. A *btl*-Gal4 insertion on the 2nd chromosome was recombined separately with two different MS2-GFP insertions on the 2nd (MS2-GFP¹² and MS2-GFP⁶⁷). Recombination was done by standard genetic crosses and the recombinants were identified by GFP expression in tracheal cells. One of the recombinants *btl*-Gal4, MS2-GFP¹² was partially homozygous whereas the second recombinant *btl*-Gal4, MS2-GFP⁶⁷ was a homozygous viable line and this recombinant was used in the screen. Figure 24A shows a representative larva from the *btl*-Gal4, MS2-GFP⁶⁷ recombinant and Figure 24B shows the expression pattern of NLS-MS2-GFP in a single terminal cell in a 3rd instar larva from the same line.



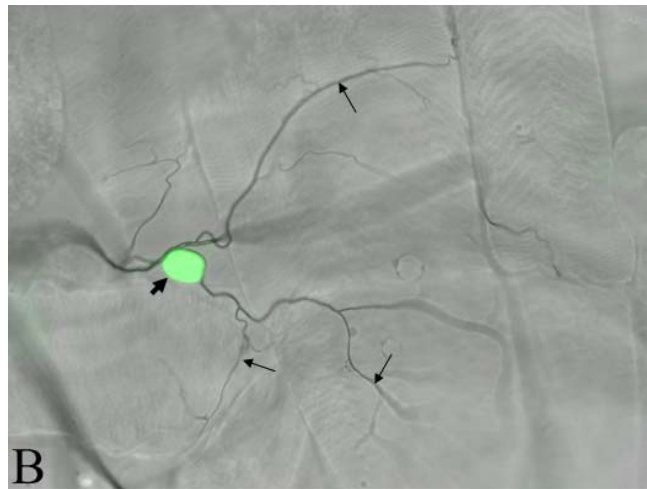


Figure 24. Images showing NLS-MS2-GFP expression in a *btl-Gal4*, MS2-GFP⁶⁷. A, MS2-GFP expression in a 3rd instar *btl-Gal4*, MS2-GFP⁶⁷ larvae. Few tracheal cells with nuclear MS2-GFP are marked by white arrows. Image B shows a single terminal cell with MS2-GFP (green) localized in the nucleus (thick black arrow). The terminal branches of the cell, imaged using Normaski optics, are marked by regular arrows.

3.3.2.4 Hopping efficiency of the EP-MS2 insertion on the X chromosome

To tag genes in the fly genome with the EP-MS2 element, we decided to mobilize the EP-MS2 element and establish new lines. Each of the lines carrying an independent new EP-MS2 element insertion could then be tested in the screen. For the same we chose insertions on the X chromosome as the starting material (ammunition for mobilization) that could be transposed to new locations within the genome. Hence, I tested the hopping efficiency of the seven EP-MS2 insertions on the first chromosome.

To test the hopping efficiency, virgin females from EP-MS2 insertions on X chromosome were crossed to males from the transposase providing flies *y,w;+/+; Δ 2-3, Ki/Δ 2-3, Ki (Δ 2-3)*. F1 males, carrying both the EP-MS2 element and Δ2-3, were crossed to white eyed virgin females (flies with mutated white locus but otherwise wild type). Transposition would occur in the germline of F1 male. F2 males do not inherit their X chromosome from the paternal side (F1 male); hence red eye color in F2 male would mean a new insertion event (on the 2nd, 3rd or 4th chromosomes) independent of the paternal EP-MS2 insertion on the X chromosome. Accordingly, in the F2 generation 300 males from each of the seven experiments were screened for red eye color to evaluate the hopping efficiency. Out the seven lines tested, one line

Results

EP-MS2⁶⁶, showed the maximum hopping efficiency of approximately 58% (Fig. 25). The line EP-MS2⁶⁶ was subsequently used in the pilot screen.

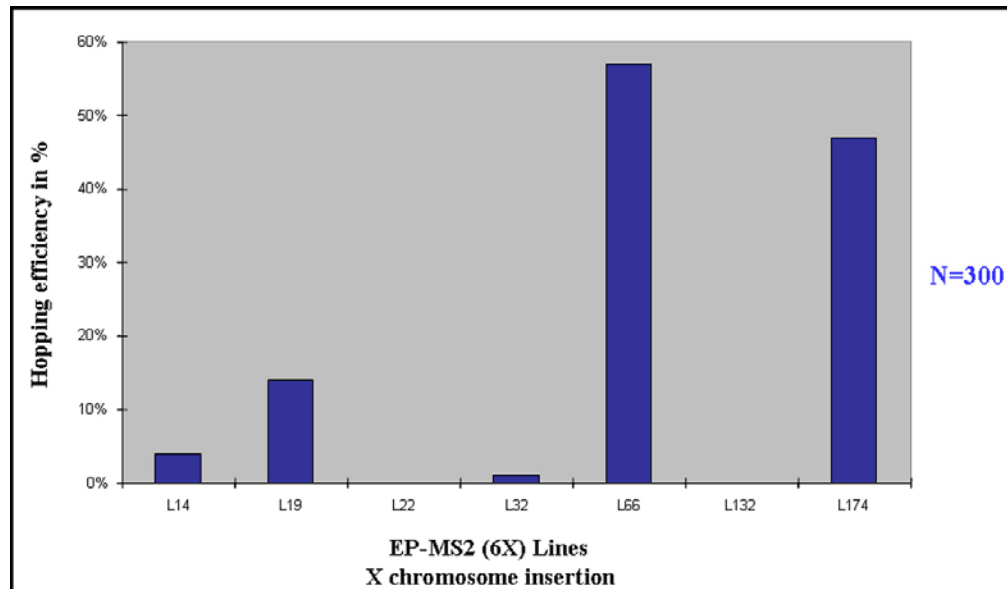


Figure 25. Graph illustrating the hopping efficiency of 7 independent EP-MS2 insertions on the X chromosome. The EP-MS2 insertions were mobilized from the X chromosome by providing transposase. 300 F2 males were screened for assessing the hopping efficiency of each line. The seven insertions tested showed a range of hopping efficiency, with EP-MS⁶⁶ exhibiting the maximum efficiency, approximately 58%. The hopping efficiency is plotted on the Y axis and the lines tested are plotted on the X axis.

3.4 A pilot screen to evaluate the EP-MS2 technique

The EP-MS2 technique that we have developed was evaluated by performing a pilot screen. The pilot screen was done as an F3 screen. For the screen, the EP-MS2⁶⁶ insertion was mobilized from the X chromosome and 250 lines, each carrying an independent insertion, were established. For the screen, males from the new insertion lines were crossed to flies carrying the recombinant *btl*-Gal4, MS2-GFP⁶⁷ on the second chromosome. Third instar larvae (F3 generation) were then screened for mRNAs that showed specific subcellular localization in terminal tracheal cells (Fig. 26).

Results

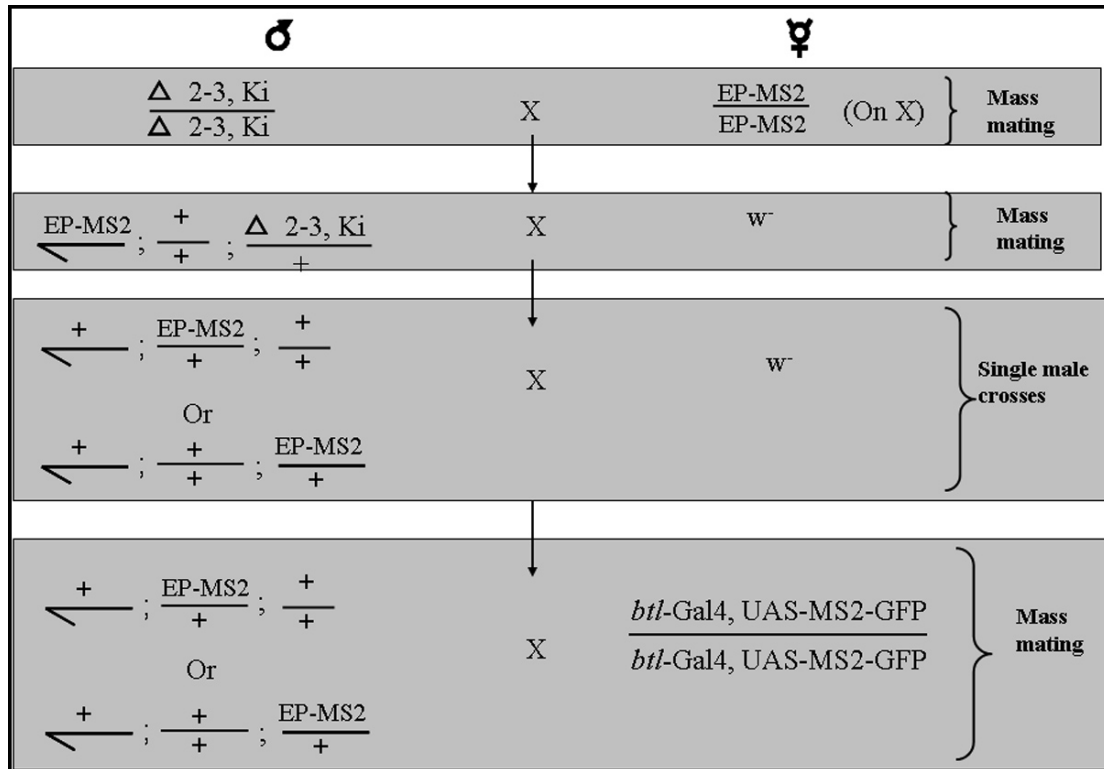


Figure 26. A schematic of the genetic crosses of the pilot screen. The EP-MS2 insertion on the X chromosome was mobilized and new independent insertion lines were established. These lines were screened for localizing mRNA in tracheal cells.

3.4.1 Phenotypic classification of the EP-MS2 lines based on pilot screen

250 EP-MS2 lines were generated and tested in the pilot screen. Males from these EP-MS2 independent insertion lines were crossed to virgin *btl-Gal4*, MS2-GFP⁶⁷ females. 250 individual crosses were set, out of which 27 lines died out during the course of the experiment. The larvae from the remaining 223 lines were screened and the results documented. An average of 16 larvae from each cross was analyzed. The third instar larvae from each cross were observed under the stereomicroscope with fluorescent attachment. For observations, the larvae were first immobilized by drowning them in 50% methanol for half hour. After the methanol treatment, the immobilized larvae were mounted on a slide and were taken to the stereomicroscope for observation.

Based on the expression pattern of MS2-GFP (which represents MS2-GFP tagged RNA) in the terminal tracheal cells, the 223 lines tested were classified into Class 1 and Class 2 phenotypic groups. In a control terminal cell, i.e., a terminal cell

Results

from *btl*-Gal4, MS2-GFP⁶⁷, the MS2-GFP tightly localizes in the nucleus. When compared to MS2-GFP expression pattern in a control cell, both Class 1 and Class 2 phenotypic groups showed distinctly different MS2-GFP distribution. In Class 1 phenotypic group, the MS2-GFP localized either in the cytoplasm immediately around the nucleus or in the region of terminal branches proximal to the nucleus. In Class 2 phenotypic group, MS2-GFP localized into the terminal branches away from the nucleus. Out of the 223 lines tested, 211 were grouped in to phenotypic group Class 1 and the remaining 12 lines were placed in phenotypic Class 2. Figure 27 shows the phenotypic classification, based on the MS2-GFP expression pattern of the lines tested in the pilot screen. The 12 lines of phenotypic Class 2 (about 5% of the total number of lines screened) showed MS2-GFP expression pattern that was both interesting and promising. Hence all the 12 lines of this group and a few representative lines of phenotypic group Class 1 were taken for further thorough analysis.

In the second round of analysis, larvae were filleted and fixed in 4% paraformaldehyde. Post fixation, the larvae were mounted on a slide and were observed under a high resolution microscope. At least six larvae from each line were processed and analyzed in this manner. This analysis revealed a clear difference in the expression pattern of the MS2-GFP between representatives of Class 1 and Class 2 phenotypic groups. In the terminal cells of larvae from phenotypic group Class 2, MS2-GFP appeared in a punctate manner extending far into the terminal branches (Fig. 28A). RNAs that are actively transported are usually packed into small clusters and transported to specific locations in the cell. Such localizing RNAs when visualized appear as tiny dots or punctas. The MS2-GFP tagged transcripts, from candidate lines of phenotypic group Class 2 appear in a punctate manner resembling the known pattern of localized RNAs. In comparison, the MS2-GFP expression pattern in terminal cells of phenotypic group Class 1 was substantially different and did not appear in a punctate manner. Instead the MS2-GFP signal was diffused and was restricted to the cytoplasm around the nucleus or extended a little into the terminal branch proximal to the nucleus (Fig. 28B and C). Based on the results of this second round of analysis, the 12 lines of phenotypic group Class 2 were taken as putative candidates and the rest were considered negatives. Further, the integration

Results

sites of the EP-MS2 elements of the positive candidates, were molecularly mapped to find the genes affected (Table.1).

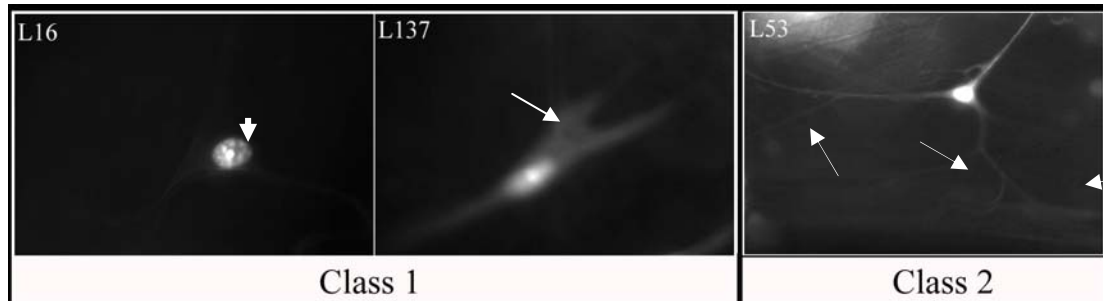


Figure 27. Phenotypic classification of EP-MS2. Phenotypic classification was done based on the MS2-GFP expression pattern in terminal cells. Class 1, MS2-GFP expression pattern in terminal cells of most of the lines (223 out 250) was restricted to the nucleus (Line16 arrowhead) or in the cytoplasm immediately next to the nucleus (arrow). Class 2, MS2-GFP expression in the terminal cells from 12 lines extended well into the terminal branches (arrows). Line 53 is a representative line from the Class 2 phenotypic group.

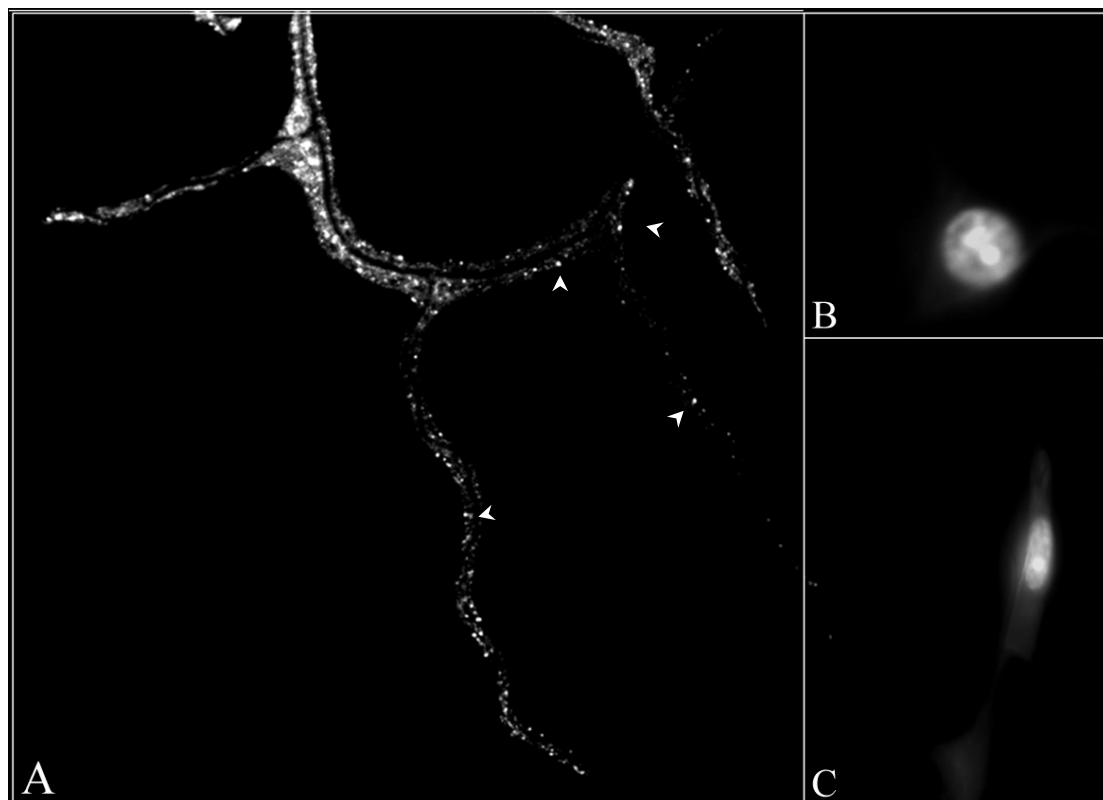


Figure 28. Examples of a positive candidate and negative from the pilot screen. A, MS2-GFP tagged mRNA localizing in the terminal branches in a candidate line. The GFP tagged mRNA appears as dots (arrowhead) in the terminal branches. Two examples showing MS2-GFP either localized in the nucleus of the terminal cell (B) or diffused in the cytoplasm around the nucleus (C), both were negative lines.

3.4.2 Evaluating the EP-MS2 technique in the developing oocyte

Until now tracheal system in *Drosophila* has not been used as a system to study mRNA localization and our studies are the first in this direction. In comparison, the developing oocyte in *Drosophila* is an extensively used system for studying how mRNAs are differentially sorted within a cell. In oocytes, a number of examples have been studied both in the context of mechanistic and functional relevance of mRNA localization. Hence, to evaluate the EP-MS2 technique, I decided to test it in the developing oocyte, a tried and tested system for mRNA localization studies.

75 EP-MS2 lines were expressed in the oocyte, which included the 12 putative candidate lines from the tracheal screen, using *nos*-Gal4, MS2-GFP. *nos*-Gal4 is an oocyte specific Gal4 driver. Males from the 75 EP-MS2 lines were crossed to *nos*-Gal4, MS2-GFP virgin females. F1 females (15 from each cross) were collected separately and the oocytes were dissected. The dissected oocytes were fixed and immuno-stained with an antibody against GFP before analyzing them under the microscope. Immuno-staining against GFP in oocytes was a deviation from the strategy that was used to visualize MS2-GFP in tracheal cells. In tracheal cells either endogenous MS2-GFP in live (immobilized) larvae or endogenous MS2-GFP in fixed filleted larvae were analyzed without any immuno-staining against GFP. Although it is possible to visualize endogenous MS2-GFP RNA bound in oocyte, I decided to immuno-stain against GFP to amplify the specific MS2-GFP signal, thereby improving the signal to noise ratio (background signal from yolk in the oocyte). Out of the 75 EP-MS2 lines tested in the oocyte, one showed an interesting pattern of MS2-GFP localization. In oocytes (stage 10a-10b) from this line, MS2-GFP localized tightly at the anterior part of the oocyte suggesting anterior localization of the MS2-GFP tagged mRNA of the affected gene (Fig. 29). There are examples of anteriorly localizing mRNAs in the *Drosophila* oocyte, viz., *bicoid* mRNA and *gurken* mRNA (Cha et al., 2001 and MacDougall et al., 2003), but the localization pattern of the MS2-GFP tagged candidate mRNA was not similar to that of the known examples. The MS2-GFP tagged mRNA seemed to localize in the region where the microtubule organizing center (MTOC) is positioned. This EP-MS2 line with the anteriorly localizing MS2-GFP tagged transcript, was one among the 12 putative candidate lines

Results

from the tracheal screen (Table.1). Details of the molecular mapping of the EP-MS2 insertion, the putative candidate line from the oocyte screen will be discussed later.

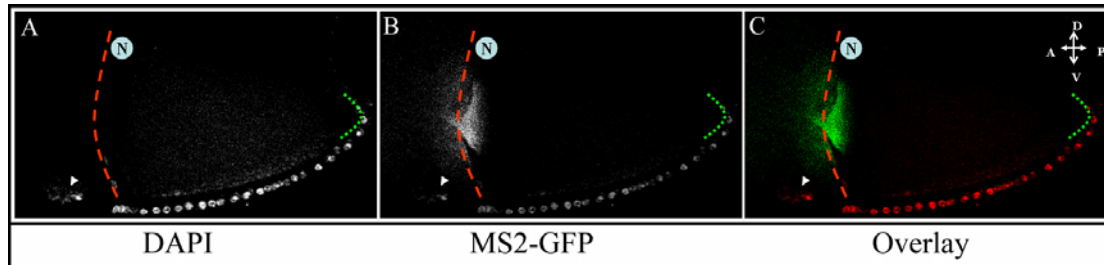


Figure 29. Localization of MS2-GFP tagged mRNA of the putative candidate from the oocyte screen. For the oocyte screen, 75 EP-MS2 lines were crossed to *nos*-Gal4, MS2-GFP. The image represents the putative candidate line from the oocyte EP-MS2 pilot screen. A, Nuclei are marked with DAPI and pseudo-colored in Red. B, MS2-GFP bound candidate mRNA localized tightly at the anterior region in the oocyte (Green). In A, B and C the arrowhead marks the nurse cell nucleus, the Red and Green broken lines mark the anterior and posterior regions of the oocyte respectively and the position of the oocyte nucleus is marked with a circle (shaded in light blue). The orientation of the oocyte is indicated in C with the arrows.

3.4.3 Testing the EP-MS2 technique in dendritic arborization (da) neurons

Neurons are extensively used for studying mRNA localization and dendritic arborization (da2) neurons in *Drosophila* have also been used in a similar context. Therefore, we thought of testing the EP-MS2 technique in da2 neurons as an additional system for evaluating the technique (experiments done in collaboration with Elizabeth R. Gavis, Princeton University). Five EP-MS2 lines have been tested so far in the da2 neurons, out of which two were putative candidates and the rest three were negative lines from tracheal screen. In these experiments, the EP-MS2 lines were expressed in the da neurons using Gal4⁴⁻⁷⁷, UAS-mCD8-GFP driver line (Ye et al., 2004) recombined with UAS-NLS-MS2-RFP (Gavis, E.R., unpublished transgene). The F1 third instar larvae from the crosses were observed live and the MS2-RFP distribution in the da2 neurons was analyzed. As a positive control for these experiments *nanos* mRNA (known to localize in the dendrites of da2 neurons, Gavis, E.R., personal communication) tagged with MS2-RFP was used. Out the five EP-MS2 lines tested, one showed a MS2-RFP localization pattern similar to *nanos* mRNA tagged with MS2-RFP, suggesting that the mRNAs from this EP-MS2 line does localize in the dendrites of the da2 neurons (Fig. 30) and the remaining four lines did not show any specific MS2-RFP localization in the dendrites. The putative candidate from the da2 neuron screen does not overlap with the candidates from the

tracheal screen and the EP-MS2 element insertion in this candidate line is yet to be mapped.

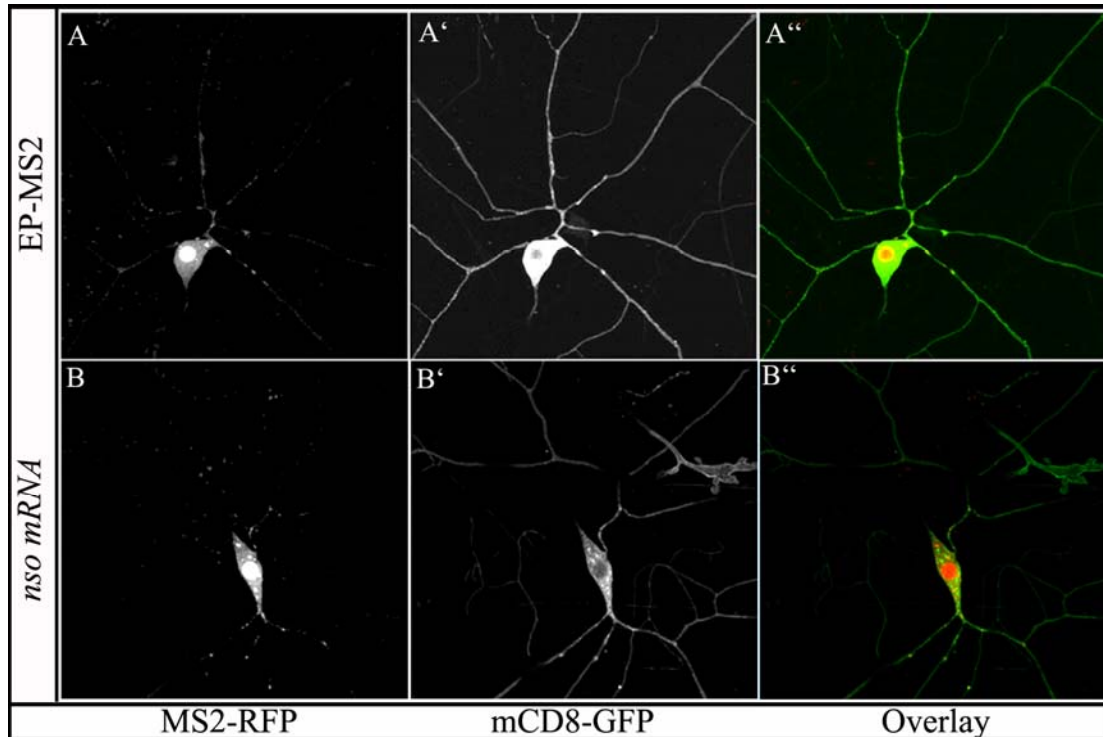


Figure 30. MS2-RFP bound candidate mRNA in da neurons. 5 EP-MS2 lines were tested in larval da2 neurons by crossing them to Gal4⁴⁻⁷⁷, mCD8-GFP, MS2-RFP. One out of 2 putative candidates, is shown in the image. A, A' and A'' are images of putative candidate and B, B' and B'' are images of *nos* mRNA (control), both tagged with MS2-RFP. In A and B MS2-RFP tagged mRNAs (arrowheads) of putative candidates and *nos* respectively are shown. In A' and B' the da neurons are marked with mCD8-GFP. A'' and B'' are overlays.

3.4.4 MS2-GFP tagged candidate mRNA does not accumulate in stress granules

RNAs that are actively transported along the cytoskeleton are usually transported in clusters. But this is not the only scenario when mRNAs aggregate and form clusters. Under physical stress, RNAs in the cytosol form aggregates and can be subsequently targeted for degradation. Such mRNA aggregates formed under stress are known as stress granules (Kedersha et al., 2005). A few other mRNA clustering events which leads to post translation degradation of RNAs have been described in the past few years, P-bodies are an example for this type of RNA aggregates (Anderson and Kedersha, 2006).

The EP-MS2 technique is an over-expression technique and could possibly lead to the accumulation of MS2-GFP tagged mRNA in stress granules. To assess

Results

whether this is the case, I did immuno-stainings using a marker that labels stress granules. The logic was to assess whether the stress granule marker colocalizes with the MS2-GFP tagged mRNAs of putative candidates in the terminal branches. The marker that I have used is an antibody against Pacman (Pac, *Drosophila* Ribonuclease1 - XRN1) ((Chernukhin et al., 2001; Kedersha et al., 2005). Pacman degrades 5 prime uncapped mRNA from the 5prime to the 3prime. It has been reported in stress granules as well as in other mRNA degradation mechanisms, such as in P-bodies (Anderson and Kedersha, 2006).

Firstly, the distribution of the stress granule (and P-body) marker Pac (Chernukhin et al., 2001) was assessed in wild type terminal branches. For this, 3rd instar larvae (*btl-Gal4*, *UAS-GFP*, wild type) were filleted, fixed and immuno-stained with an antibody against Pac. The experiment showed anti-Pac antibody labeled bodies that appeared in granules in terminal branches (Fig. 31A). This result was not surprising for two reasons; firstly, the terminal branches grow in response to hypoxic signals from the surrounding tissues and tracheal cells themselves are very sensitive to hypoxia. Hypoxia is a stressful cell physiological condition and could lead to stress granule formation even in the wild type tracheal cells. Secondly, the anti-Pac labeled bodies could also be P-bodies since Pac has been reported in P-bodies also. The terminal branches do have the required conditions to carry out translation. Hence, one could expect the presence of post translational RNA degradation machinery, such as P-bodies, in the terminal branches.

Using the anti-Pac immuno-staining pattern in wild type terminal branches as a control, I analyzed anti-Pac staining in terminal branches where MS2-GFP tagged putative candidate RNAs was over-expressed. Three of the twelve putative candidate lines (from the tracheal screen) were used for analysis. In all the three lines tested the anti-Pac labeling did not colocalize with the majority of the over-expressed MS2-GFP tagged candidate mRNAs (Fig. 31B). Owing to technical limitations in imaging and analysis, it was difficult to judge whether there was absolutely no colocalization of MS2-GFP and Pac labeling. Nevertheless, the results clearly showed that most of the MS2-GFP did not colocalize with Pac, suggesting that the MS2-GFP tagged mRNA aggregates were independent of stress granules and/or P-bodies.

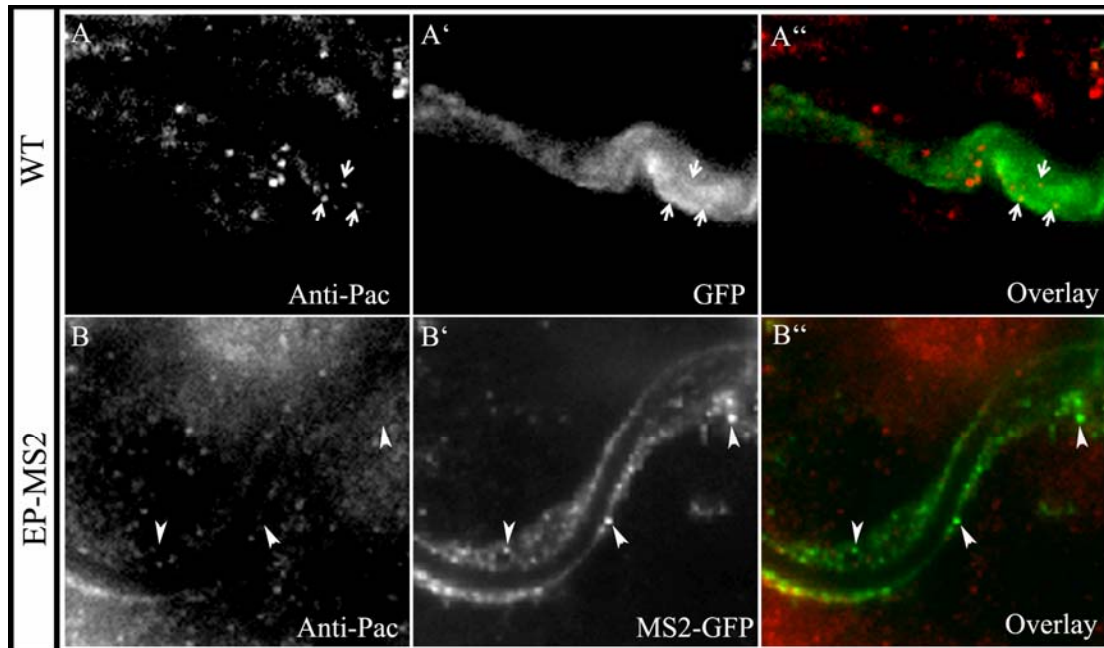


Figure 31. MS2-GFP tagged candidate mRNA does not localize in stress granules. A, A' and A'' shows stress granules in wild type terminal branches (*btl-Gal4*, UAS-GFP). A represents Pac distribution, A' shows a terminal branch marked with GFP and A'' is an overlay. B, B' and B'' shows Pac distribution in a putative candidate EP-MS2 line from the tracheal screen, expressed together with MS2-GFP. B shows the Pac distribution, B' shows MS2-GFP tagged putative candidate mRNA and B'' is an overlay. Most of the MS2-GFP tagged mRNA granules do not colocalize with Pac.

3.5 Molecular mapping of the EP-MS2 element insertion in candidate lines

The EP-MS2 element insertions in the putative candidate lines were molecularly mapped to find out which gene (or genes) is affected in each candidate lines. To map the EP-MS2 element insertions, I used the inverse PCR method (from BDGP). The EP-MS2 insertions in the 12 putative candidate lines from the tracheal and oocyte screens were mapped by inverse PCR. Out of the 12 candidate lines, 10 were successfully mapped to genomic positions whereas two mapping results were not conclusive. Out of the ten successfully mapped insertions six were in independent genes, three mapped to the same gene. In one line, there were two independent EP-MS2 insertions in two different genes. Table.1 describes the list of putative candidate EP-MS2 lines, the molecular mapping results and the genes affected in the candidate lines.

Results

Putative candidate	Insertion mapped to chromosome	Gene affected	Tissue screened
EP-MS2 ¹²	X, 2 nd , 3 rd and 4 th	Transposon docking sites	Terminal branches
EP-MS2 ¹⁸	2R	<i>lola</i>	Terminal branches
EP-MS2 ⁴⁷	3R	<i>HsP70Aa</i>	Terminal branches
EP-MS2 ⁵³	2L	<i>Hr39</i>	Terminal branches
EP-MS2 ⁶⁷	3R	<i>btsz</i>	Terminal branches
EP-MS2 ⁹⁴	3R	<i>btsz</i>	
EP-MS2 ¹²⁸	3R	CG9924	
EP-MS2 ¹³¹	3R	<i>ATPalpha</i>	
EP-MS2 ¹⁵²	2L	<i>cenG1A</i>	Oocyte
	3R	<i>btsz</i>	Terminal branches
EP-MS2 ¹⁵⁴	ND	ND	Terminal branches
EP-MS2 ¹⁹³	2R	CG30403	Terminal branches
EP-MS2 ²⁰⁷	3R	<i>btsz</i>	Terminal branches

Table 1. Summary of the list of putative candidate genes from the pilot screen. EP-MS2 element insertion was mapped by Inverse PCR. Out of the 12 candidates 10 were successfully mapped, whereas in two cases (rows shaded in red) the mapping results were not conclusive. One of the lines EP-MS2¹⁵² carried two EP-MS2 element insertions, one on 2L (in *cenG1A*, positive in oocyte) and the second insertion on 3R (in *btsz*), row shaded in green. Three lines EP-MS2⁶⁷, EP-MS2⁹⁴ and EP-MS2²⁰⁷ were clones as revealed by exactly matching genomic coordinates in blast results.

Subsequent to molecular mapping, the initial list of 12 putative candidates narrowed down to 8 candidate genes, (two being clones and two could not be mapped precisely). In this list of 8 genes, at least three genes namely, *ATPalpha*, *Hsp70Aa* and *longitudinal lacking (lola)* are known to be expressed in tracheal cells and have functions in tracheal morphogenesis. Three of the lines (EP-MS2⁶⁷, EP-MS2⁹⁴ and EP-MS2²⁰⁷) were clones since the genomic coordinates in the blast results mapped to exactly the same position in the genome. In these three lines, the EP-MS2 elements were mapped to the *bitesize (btsz)* gene, which has a P element insertion hotspot. In two of the putative candidate lines, the EP-MS2 element insertion mapped to CG9924, CG30403 and in one line the insertion was in *Hormone receptor39 (Hr39)* gene. The line that was positive in the oocyte, EP-MS2¹⁵², carried two insertions, one in the gene *bitesize (btsz)* and the other in the gene *centurion Gamma1A (CenG1A)*. In the oocyte screen, two other independent EP-MS2 lines carrying insertion in *btsz* were also tested. These two lines did not show any specific MS2-GFP localization

Results

pattern suggesting that the localization pattern of EP-MS2¹⁵² is due to the insertion in *cenG1A*.

Literature survey revealed that among the 8 candidate genes, at least three are known to transcribe mRNAs that localize to specific subcellular domains within a cell. These three genes are *btsz*, CG9924 and *lola*, but none of them has been extensively studied to understand the localization properties of their mRNAs. *btsz* encodes the only known member of Synaptotagmin family of proteins (SLP) in *Drosophila*. Studies have shown that the *btsz* mRNA localizes apically in follicular epithelial cells, early embryonic epithelial cells and in eye imaginal disc cells. Further, the *cis*-acting mRNA signal required for apical localization has been narrowed down to a 2.1kb long sequence in the 8th exon of the gene (Serano and Rubin, 2000). The minimal essential localization signal, the secondary structure of the sequence responsible for localization, the trans-acting protein interacting with the sequence etc., has not been studied yet. In a recent genome wide RNA *in situ* screen in *Drosophila* embryos CG9924 and *lola* were reported to transcribe mRNAs that localize apically in embryonic cells (Lecuyer et al., 2007). Details of the attributes regulating localization of these two mRNAs are yet unknown.

3.6 Characterization of a candidate gene from the EP-MS2 screen

I have started characterizing the functional requirement of one of the candidates from the screen, in terminal branch development. The candidate that I chose to characterize was *bitesize* (*btsz*). *Btsz*, together with Moesin, is known to regulate the organization of the actin cytoskeleton in epithelial cells (Pilot et al., 2006). A recent study had speculated on the possible role of the actin cytoskeleton in terminal branch development (Levi et al., 2006). Putting these findings together, *Btsz* seemed to be a good candidate gene to analyze further.

3.6.1 *bitesize* - a Synaptotagmin-like protein family gene in *Drosophila*

Btsz, the only *Drosophila* member of the Synaptotagmin-like protein family (SLP family) identified so far, is characterized by the presence of tandem carboxy-terminal C2 domains. The *btsz* transcription unit covers approximately 50 kb and is predicted to have at least 15 exons. To date four *bona fide* *btsz* protein coding

Results

transcript isoforms have been described. cDNA library screens identified three alternatively spliced forms of *btsz* which differ in their transcription start sites and exon usage. All three isoforms share the same C-terminal region of 423 amino acids. Two of these isoforms, *btsz-1* and *btsz-2*, encode proteins that are 1099 and 2645 amino acids respectively and do not share any amino acids outside of the C-terminal region. A third transcript, *btsz-3*, is similar to *btsz-2* except that its transcription start site occurs 3013 nt further downstream, in the middle of exon 8 (Fig. 32, modified from Serano and Rubin, 2003). In a subsequent study, *btsz0* transcript isoform was identified in RT PCR analysis (Pilot et al., 2006).

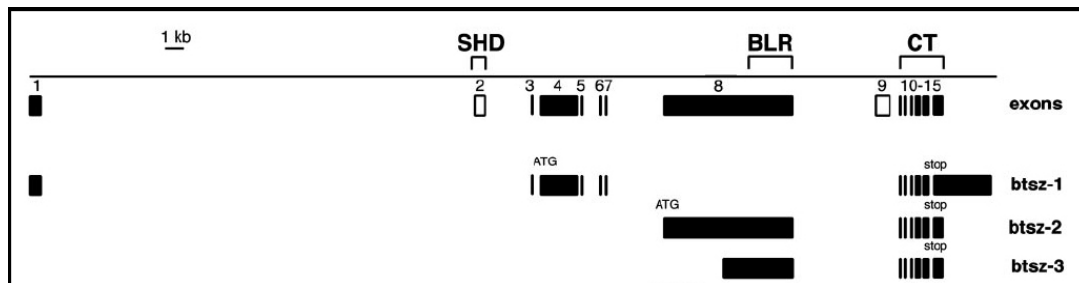


Figure 32. Diagram of the *btsz* transcription unit. The line represents approximately 50kb genomic region, below which are boxes (numbered 1–15) representing *btsz* exons. The solid boxes represent exons used in cDNAs and the open boxes (numbers 2 and 9) represent computationally predicted exons (release 3 of the *Drosophila* genome on www.flybase.org). Also shown are structures of three different *btsz* transcripts (*btsz-1*, *btsz-2*, and *btsz-3*). The *btsz* SHD is encoded by exon 2, the *btsz* BLR is located in exon 8, and the *btsz* C-terminal region is encoded by exons 10–15. Image modified from Serano and Rubin, 2003.

The amino-terminal regions of Btsz protein isoforms show no homology to any known or predicted proteins, whereas the C-terminal region contains two C2 domains (calcium binding domains from protein kinase C) and is most homologous (41% identity, 57% similarity) to the corresponding region of a mammalian SLP, Granuphilin. As with the other SLPs, neither of the Btsz C2 domains contain the five conserved aspartate residues required for Ca^{2+} -binding. *btsz* exon 2 encodes a typical Synaptotagmin like protein family Homology Domain (SHD), including the Zn^{2+} -binding motif and conserved Rab-binding site (SGEWF). The Btsz SHD is most homologous to the Granuphilin SHD (44% identity, 58% similarity). Although exon 2 is not present in *btsz-1*, *-2*, or *-3*, it is present in the partial *btsz* cDNA GH06647 (Serano and Rubin, 2003). Because of the complexity of the *btsz* transcription unit, it is likely that additional *btsz* isoforms exist.

Results

Two *btsz* transcript isoforms were reported to localize at the apical plasma membrane. A 2.2-kb region known as the *btsz* localization region (BLR), that is necessary and sufficient to mediate apical mRNA localization has been identified in the 8th exon of the *btsz* transcription unit. BLR is the first example of a fully functional mRNA localization sequence contained entirely within the protein-coding region of a gene. The BLR shares a number of sequence stretches that show extensive nucleotide-level homology with the *Anopheles gambiae btsz* gene. In particular, one 59-nt region of the BLR is 92% conserved between flies and mosquito. Such conserved sequences may represent functionally conserved mRNA localization elements. On examination of the BLR to identify RNA secondary structures, one predicted stable stem-loop structure (*btsz-2*; nucleotides 5311–5405) was discovered. The functional relevance of this predicted stem loop structure is not clear yet and it is not conserved in *Anopheles* (Serano, J. and Rubin, G., 2003).

Granuphilin, a mammalian SLP family protein and the closest homologue of *Drosophila* Btsz, has been implicated in exocytosis and vesicular trafficking (Yi Z, *et al.*, 2002). But so far it is not clear whether Btsz shares a similar function. Two studies have reported on functions of *btsz* in *Drosophila*. In one of the studies, *btsz* was implicated in the regulation of cell growth and proliferation. Further, it was suggested that *btsz* acts cell-nonautonomously and that it might have a role in the vesicular transport of growth regulators like its closest homologue in mammals, Granuphilin (Serano and Rubin, 2003).

Pilot *et al.*, described *btsz* as an important regulator of actin organization in the apical junctional region, where adherens junctions form in *Drosophila* embryonic epithelia. In this report it was shown that the Btsz protein localizes apically in epithelial cells and is required for recruiting Moesin (*Drosophila* Ezrin–Radixin–Moesin protein) to the adherens junction. This interaction regulates the actin organization at adherens junctions, which in turn is essential for the stability of *Drosophila* E-Cadherin in adherens junctions (Pilot *et al.*, 2006). Further, the study showed that the C2 domains of Btsz interact with phosphatidylinositol mono and bisphosphate in a Ca²⁺ dependent manner. In *baz* RNAi knockdown mutants, Btsz does not localize at the adherens junction and is cytoplasmic. Based on these findings, Pilot *et al.*, conclude that PtdIns(4,5)P₂ together with Baz act as the polarized spatial

cue for proper apical localization of Btsz protein in *Drosophila* epithelial cells (Fig. 33).

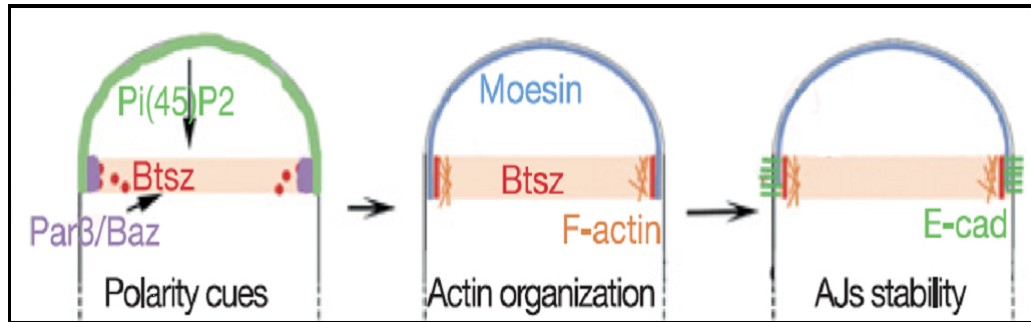


Figure 33. Model explaining the function of Btsz in the organization of adherens junctions. Upstream polarity cues (Par-3 and PtdIns(4,5)P2) define a domain in the apical junction region where Btsz protein localizes (red). Btsz and Moesin interaction organizes actin filaments, which in turn stabilizes E-cad. Image adapted from Pilot et al., 2006.

3.6.2 Functional characterization of *bitesize* in terminal tracheal branch development

Two *btsz* loss of function alleles, *btsz*^{K13-4} and *btsz*^{J5-2} generated by P element imprecise excision, have been described earlier. *btsz*^{J5-2} was derived from EP(3)3567 and contains a frameshift mutation that results in truncated Btsz0, Btsz2 and probably the absence of Btsz3. *btsz*^{K13-4} was derived from *l(3)10418* and introduces a deletion in the amino terminus of *btsz2* (residues 501–1,494). Although *btsz*^{J5-2} is a slightly stronger allele than *btsz*^{K13-4}, both mutants were reported to cause similar phenotypes (Serano, J. and Rubin, G., 2003). *btsz*^{J5-2}, which was initially reported as a homozygous viable allele was later found to be lethal, while *btsz*^{K13-4} does produce a few homozygous survivors (Pilot et al., 2006).

To study the functional requirement of *btsz* in terminal branch development, I have analyzed terminal branches in *btsz*^{K13-4} homozygous mutant larvae. *btsz*^{K13-4} homozygous third instar larvae were filleted and processed for immunostaining. Antibodies against *Drosophila* serum response factor (SRF, transcription factor expressed in terminal tracheal cells) and Dof (Downstream of FGF) were used to mark the nuclei and cytosol respectively. Results from the immuno-stainings showed that the terminal branching is severely compromised in *btsz*^{K13-4} mutant larvae. The

Results

terminal cell specification was normal since the SRF expressing cells were present and the number of terminal cells was comparable to wild type. But the terminal branches were either absent or their numbers were greatly reduced in the mutant larvae, as revealed by the anti-Dof labeling. Although most of the terminal cells were affected, the phenotype is not completely penetrant (Fig. 34). In *btsz*^{K13-4} mutants Btsz2 protein isoform is made, but the protein carries a deletion in the amino terminus between residues 501–1494, while the rest of the protein including the C-terminus is unaffected (Serano and Rubin, 2003). Pilot et al., had identified a Moesin binding domain in Btsz2 protein, in the amino terminus region between residues 581-863, which is absent in the Btsz2 mutant protein made in *btsz*^{K13-4} mutants. The abnormal terminal branching phenotype in the *btsz*^{K13-4} mutants, in which the Moesin binding domain is absent, could be a consequence of the failure of the Btsz2 mutant protein in regulating the function of Moesin in terminal branches. This argument also leads to the question whether Moesin is required for terminal branch development and do *moesin* mutants have defects similar to *btsz*^{K13-4} mutant larvae.

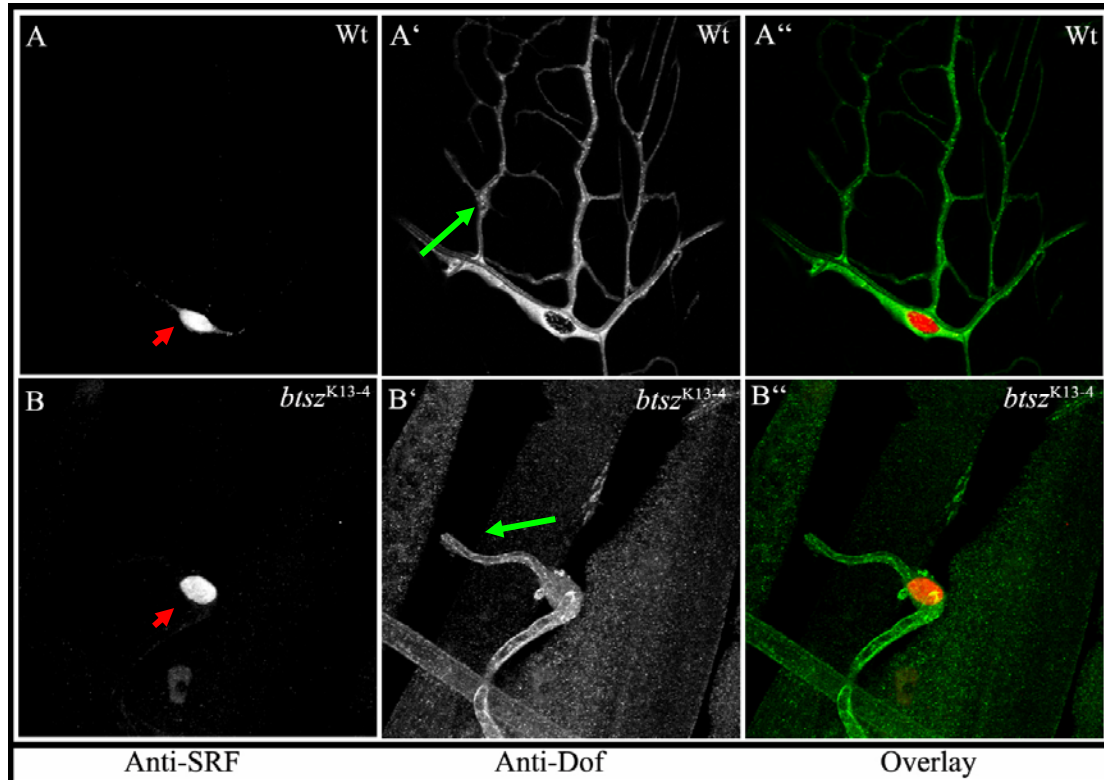


Figure 34. *btsz*^{K13-4} mutants show severe terminal branch defects. 3rd instar *btsz*^{K13-4} homozygous larvae were filleted, processed and immunostained with anti-SRF and anti-Dof. A, A' and A'' is wild type terminal cell. B, B' and B'' is a terminal cells from *btsz*^{K13-4} homozygous larvae. The nuclei of the terminal cells are marked with anti-SRF (A and B, red arrowhead) and the terminal branch are marked

Results

with anti-Dof (A' and B', green arrow). A'' and B'' are overlays of anti-SRF and anti-Dof labeling of the terminal cells A and B respectively.

The *btsz*^{K13-4} homozygous 3rd instar larvae had a substantially lower amount of fat cells than wild type larvae. The homozygous mutant larvae were almost transparent because of the lower amount of fat cells and the body size was also greatly reduced. These observations were interesting because a similar phenotype was seen in two other independent experiments. Tracheal specific expression of poly(A) binding protein as well as an activated form of Moesin (experiment is described in detail in a later chapter) also resulted in reduced number of terminal branches and a smaller body size, as in *btsz*^{K13-4} mutant larvae. Abnormal terminal branching or reduced number of terminal branches would result in inefficient oxygen supply to tissues, which in turn could reduce the general rate of metabolism and growth. These observations suggest that the nonautonomous growth defects of *btsz* mutants described in earlier reports is very likely an indirect effect of the reduced number of terminal branches and an inefficient oxygen supply.

3.6.3 Bitesize localizes at the apical membrane in terminal branches

An antibody against *Drosophila* Btsz protein has not been generated yet. To test the localization of the Btsz protein in terminal branches, I used available tagged *btsz2* constructs (*btsz2*-myc and *btsz2*-poly), which had previously been shown not to have any detectable defects when expressed in cells (Serano and Rubin, 2003). I expressed UAS-*btsz2*-poly (polyoma epitope tagged to *btsz2*) transgene together with UAS-GFP in tracheal cells and performed immunostainings on third instar larval fillets using an antibody against the polyoma epitope tag. The overexpressed and tagged form of Btsz2 localized or was enriched at the apical membrane around the lumen (Fig. 35). Localization of Btsz2-poly tagged protein at the apical membrane in terminal branches was consistent with the earlier published reports of Btsz2 localizing at the apical membrane in epithelial cells.

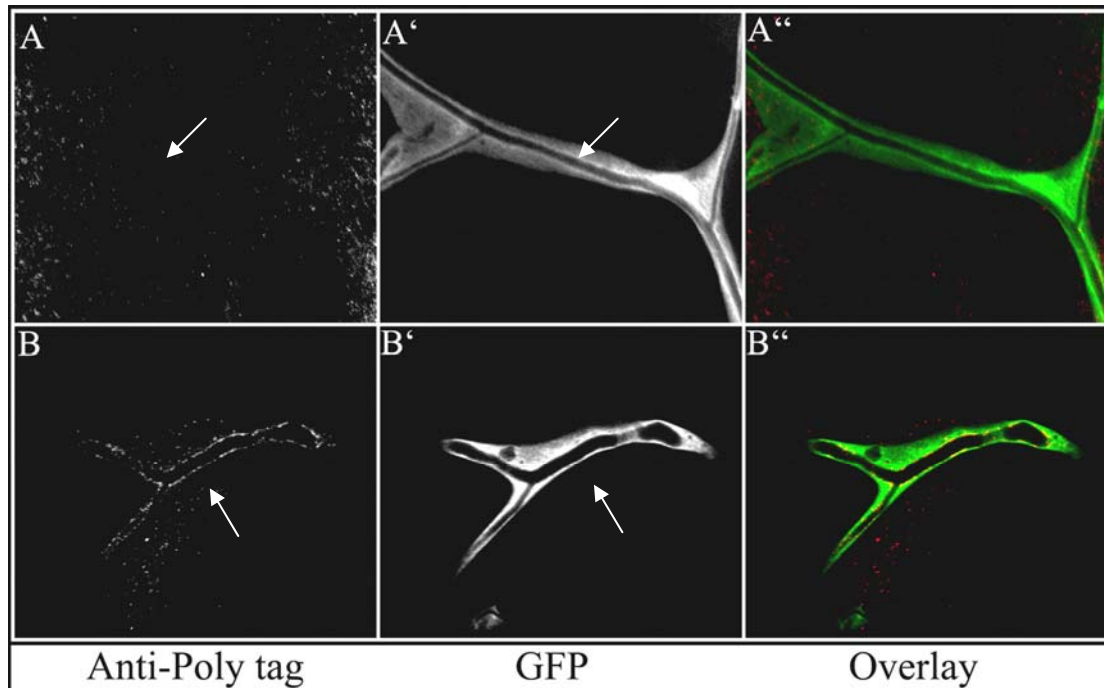


Figure 35. Over-expressed poly tagged form of Btsz2 protein localizes at the apical membrane facing the lumen. Btsz2-poly transgene was expressed in tracheal cells together with cytosolic GFP. A, A' and A'' show anti-poly tag immunostained wild type terminal branches. B, B' and B'' localization of Btsz2-Poly protein in terminal branches. A'' and B'' are overlays of anti-poly tag and GFP labeling. The white arrows mark the apical membrane facing the lumen in A, A', B and B'.

3.6.4 C-terminal C2 in Bitesize is required for its membrane localization

Synaptotagmin-like protein (SLP) family members are characterized by the presence of tandem carboxy-terminal C2 boxes, which have been implicated in the membrane association of these proteins. Btsz has two tandem carboxyl-terminal C2 domains. It was reported that the C2 domains of Btsz were necessary and sufficient for the localization of Btsz to the membrane (Pilot et al., 2006). A tagged form of Btsz2 lacking the C2 boxes (Btsz2- Δ C2-HA) when expressed in embryos, does not localize at the adherens junctions and was shown to be cytoplasmic. Conversely, a tagged form of the Btsz2 C2 domains (C2AB-HA) localized at the plasma membrane in embryos (Pilot et al., 2006).

After establishing the localization pattern of full length Btsz2 in the terminal branches, I looked at the requirement of C2 domains of Btsz2 for its localization at the apical membrane in the terminal branches. The UAS-*btsz2*- Δ C2-HA transgene (lacking the C2 domains) was expressed in tracheal cells marked with GFP and third instar larvae were processed and immunostained with an anti-HA antibody. The over-

Results

expressed *btsz2-ΔC2*-HA was found in the cytoplasm unlike the full length Btsz2 protein that tightly localizes at the apical membrane (Fig. 36).

A small portion of the overexpressed *btsz2-ΔC2*-HA did localize at the apical membrane (Fig. 37). It is possible that this is an overexpression artifact or could be a true localization event mediated by yet unidentified domain or domains in Btsz protein required for its membrane localization. Nevertheless, the predominant cytoplasmic localization of Btsz2 lacking C-terminal C2 domains suggests that Btsz2 protein localization at the apical membrane in terminal branches is dependent on the C2 domain.

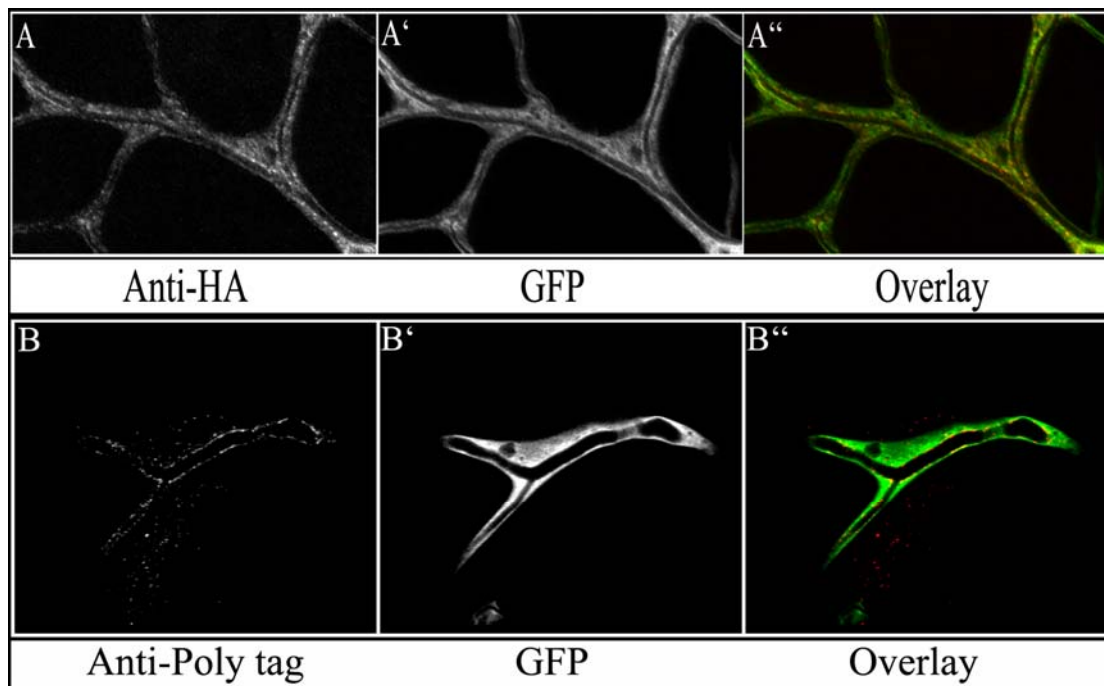


Figure 36. Cytoplasmic localization of Btsz2-ΔC2-HA protein. UAS-*btsz2-ΔC2*-HA was expressed in tracheal cells marked with GFP. 3rd instar fillets were immunostained with anti-HA antibody to visualize the localization of Btsz2-ΔC2-HA protein. A) Btsz2-ΔC2-HA. A') Cytosolic GFP. A'') Overlay of A and A''). B) Full length Btsz2-poly tagged protein. B') Cytosolic GFP. B'') Overlay of B and B'.

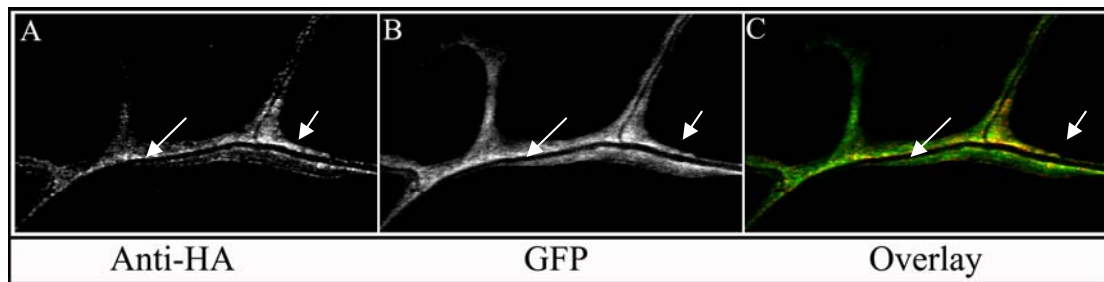


Figure 37. Localization of Btsz2- Δ C2-HA protein in terminal branches. A) Shows predominantly cytoplasmic distribution of Btsz2- Δ C2-HA and slight apical enrichment in some places (arrows). B) The branches marked with cytosolic GFP. C) Overlay of A and B.

3.6.5 Par3/Bazooka localization in terminal branches

The apical localization of Btsz in the epithelial cells was shown to be dependent on Par-3/Bazooka (Baz), which acts as polarized spatial cue (Pilot et al., 2006). In *baz* RNAi knockdown mutants, Btsz does not localize at the adherens junction and is cytoplasmic. It is not clear whether the Btsz mis-localization in Baz mutants is a direct or an indirect effect. *In vitro* biochemical experiments show that the C2 domains of Btsz interact with phosphatidylinositol mono and bisphosphate in a Ca^{2+} dependent manner. Further PtdIns(4,5)P2 is seen enriched in the apical junction region in embryonic epithelial cells (Pilot et al., 2006). Reports also show that Baz indirectly regulates PtdIns(4,5)P2 synthesis through its interaction with PTEN, which converts PtdIns(3,4,5)P3 into PtdIns(4,5)P2 (von Stein et al., 2005). Although it is not clear whether Baz interacts with Btsz directly, it is evident from earlier studies that Baz does act as an essential polarized spatial cue for Btsz localization (Pilot et al., 2006).

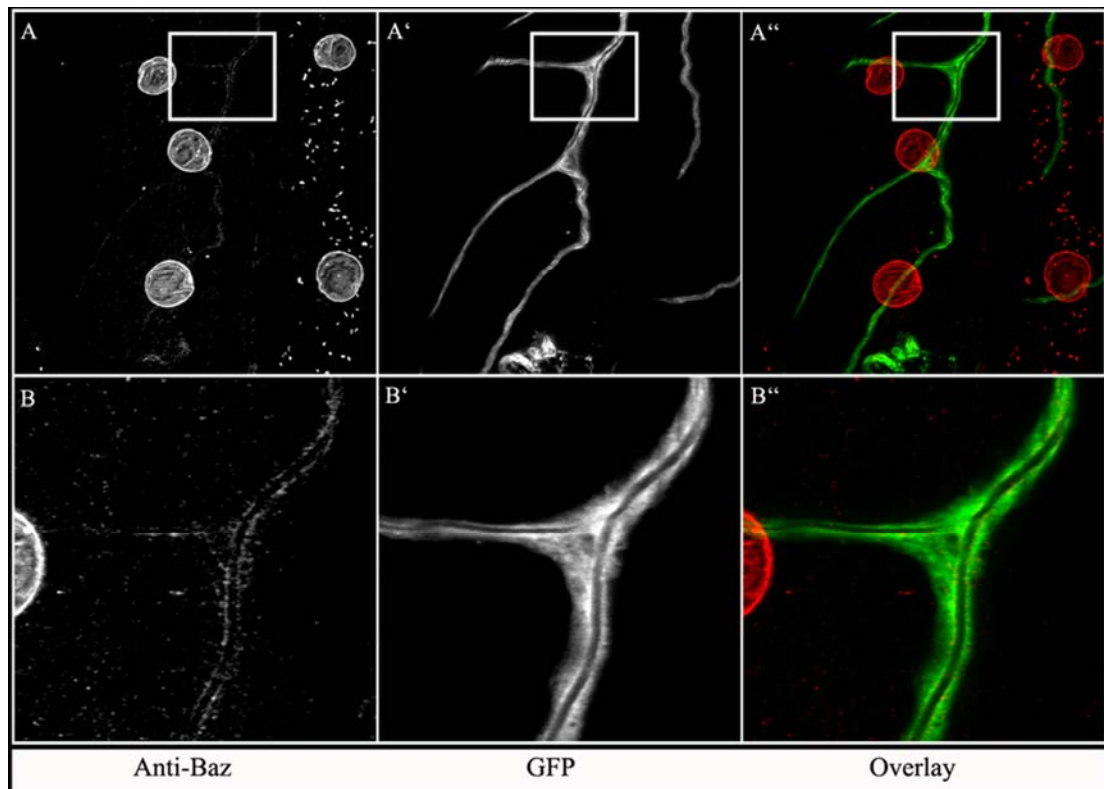


Figure 38. Bazooka localizes at the apical membrane in terminal branches. *btl-Gal*, UAS-GFP 3rd instar fillets were immunostained with anti-Baz antibody to visualize the localization of Baz. A shows apical localization of Baz in terminal branches, in A' the branches marked with cytosolic GFP are shown and A'' is the overlay of A and A'. The boxed area in A, A' and A'' are enlarged in B, B' and B'' respectively.

The apical localization of Btsz in epithelial cells being dependent on Baz raised the question whether the same mechanism regulates Btsz localization at the apical membrane surrounding the lumen in terminal branches. If so, Baz should also localize at the apical membrane in terminal branches, similar to Btsz2 localization. Immuno-stainings with anti-Baz antibody, on third instar *btl-Gal*, UAS-GFP larval fillets, revealed that Baz localizes at the apical membrane like Btsz2 (Fig. 38). This result suggests the possibility of Baz being the spatial cue for Btsz2 localization at the apical membrane in terminal branches. The analysis of Baz mutants is necessary to study the role of Baz as the spatial cue for Btsz2 localization in terminal branches.

3.6.6 Par6, aPKC and Crumbs localization in terminal branches

Par3/Bazooka acts in a complex along with Par6 and aPKC, which plays a critical role in establishment of apical-basal polarity in cells. The components of this complex display a mutually dependent apical localization and activation (Macara,

Results

2004). The Par6/aPKC/Baz complex regulates the apical-basal polarity together with the Crumbs–Stardust (Sdt)–Pals1-associated TJ protein (Patj) complex (Crumbs Complex) (Hurd et al., 2003). Crumbs, a transmembrane protein localized in the apical membrane, acts as the anchor with which Sdt and Patj interact (Bachmann et al., 2001; Hong et al., 2001). A current concept is that the Par6/aPKC/Baz core complex is a universal effector of polarity and that the Crumbs complex is a specific adaptor targeting this effector in epithelial polarity. Par6, aPKC and Crumbs are essential for the localization and function of Baz, which in turn acts as a spatial cue for Btsz2 localization. Hence, I looked at the distribution of Par6 and aPKC in terminal branches by immunostainings with specific antibodies and found apical localization of both Par6 and aPKC in the terminal branches (Fig. 39 and Fig. 40).

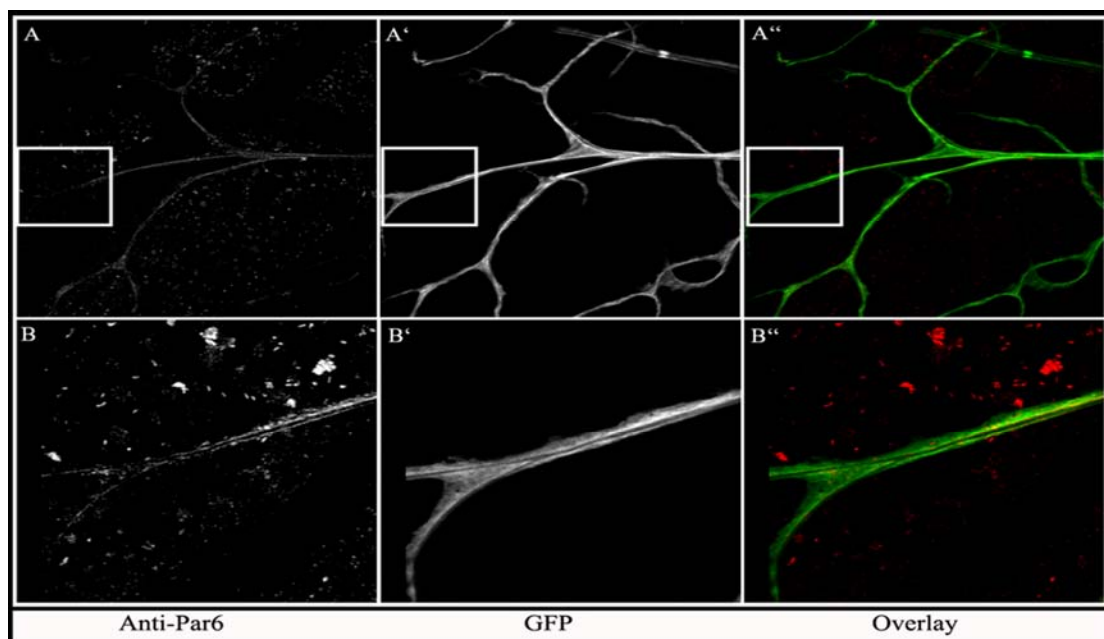


Figure 39. Par6 localizes at the apical membrane in terminal branches. *btl-Gal4*, UAS-GFP 3rd instar fillets were immunostained with anti-Par6 antibody to visualize the localization of Par6 protein. A shows apical localization Par6 in terminal branches. A' cytosolic GFP. A'' is an overlay of A and A'. The boxed area in A, A' and A'' are enlarged in B, B' and B'' respectively.

Results

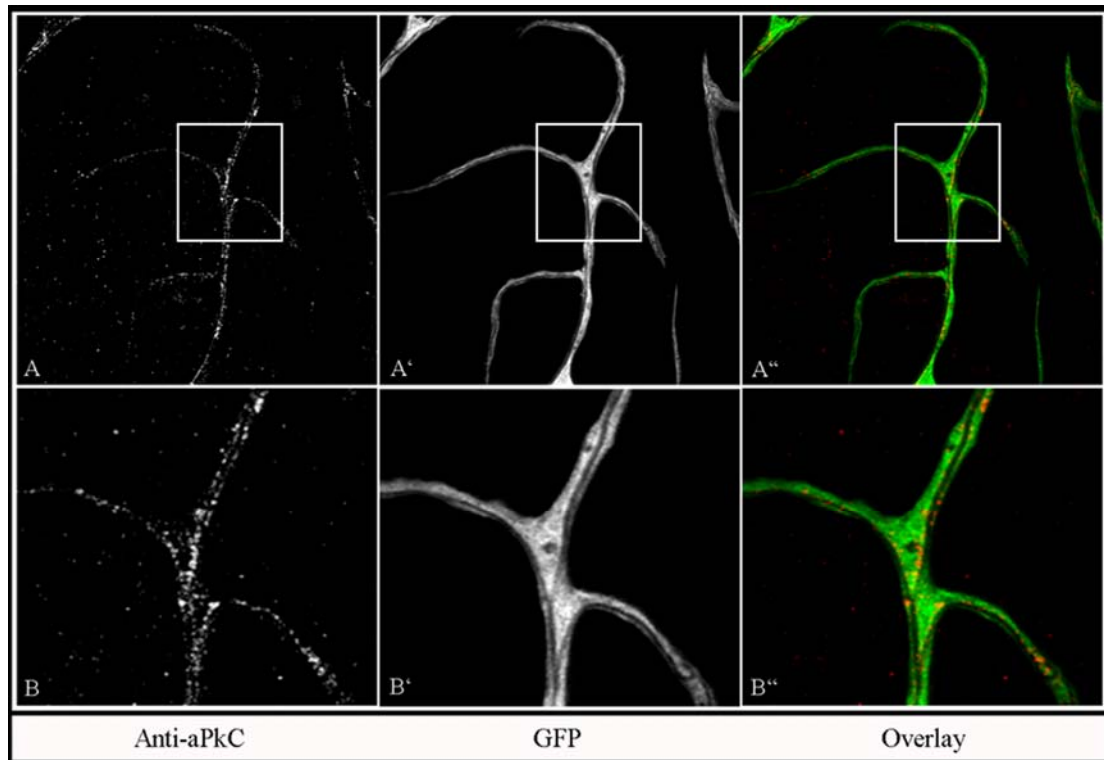


Figure 40. aPKC localizes at the apical membrane in terminal branches. *btl*-Gal4, UAS-GFP 3rd instar fillets were immunostained with anti-aPKC antibody to visualize the localization of aPKC protein. A shows apical localization of aPKC in terminal branches, in A' the branches marked with cytosolic GFP are shown and A'' is the overlay of A and A'. The boxed areas in A, A' and A'' are enlarged in B, B' and B'', respectively.

Due to the technical limitations in imaging Crumbs immunostained terminal branches, I adopted a different approach to visualize Crumbs localization in terminal branches. A Crumbs-GFP transgene (Pellikka et al., 2002) was expressed in tracheal cells together with UAS-DsRed and terminal branches in third instar fillets were analyzed. Crumbs-GFP localized at the apical membrane (Fig. 41) like Par6, aPKC and Baz. The Presence of Par6, aPKC, and Crumbs at the membrane surrounding the lumen does raise the possibility that these molecules that interact with and regulate Baz might also have a regulatory effect on Btsz localization. This assumption can be verified by analyzing mutants of Par6, aPKC and Crumbs, which if involved in Btsz localization, should show similar terminal branch defects to *btsz* mutants.

Further, Crumbs-GFP was also observed in vesicles at distal tips of terminal branches where either the lumen was not developed or was beginning to develop (Fig. 42). Localization of Crumbs-GFP in vesicles at distal regions in terminal branches was a very interesting observation. The *de novo* lumen formation in terminal branches

Results

is believed to be a consequence of vesicular fusion (Keister, 1948; Locke, 1966; Shafiq, 1963). It is a likely scenario that these Crumbs-GFP positive vesicles in the distal region of terminal branches fuse to form the lumen. Further, Crumbs through its interaction with the Par6/aPKC/Baz complex could confer apical identity to the membrane facing the lumen, which is an essential requirement for cuticle development in the lumen and consequent stabilization of the lumen.

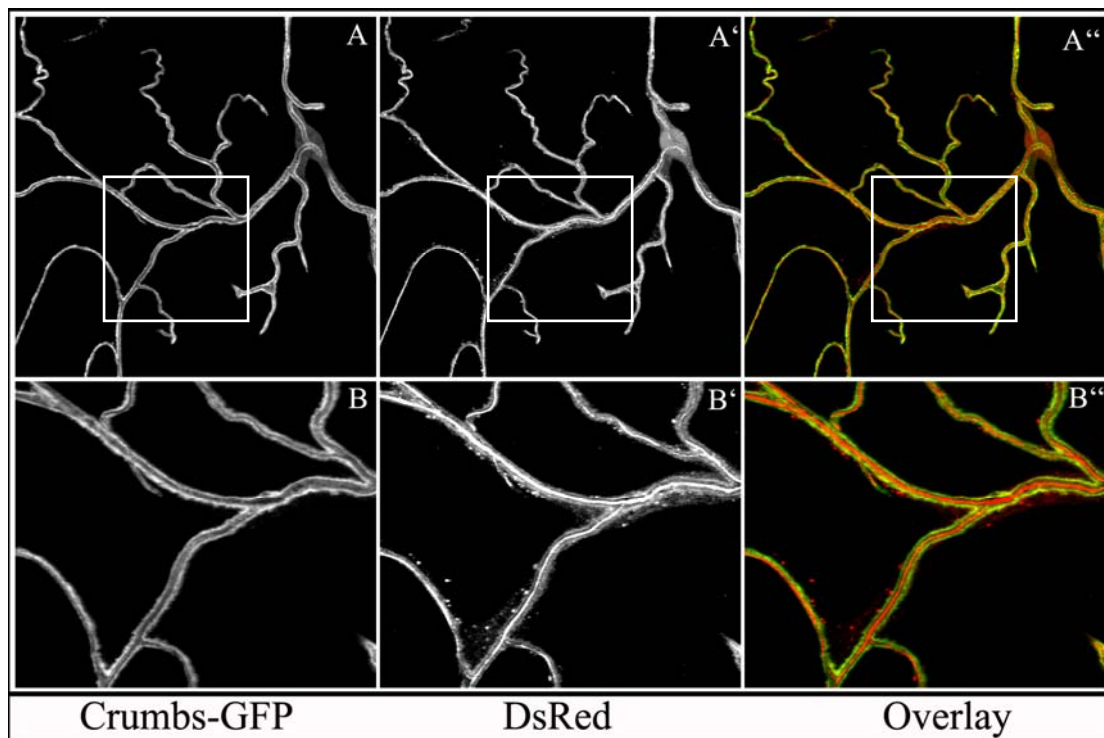
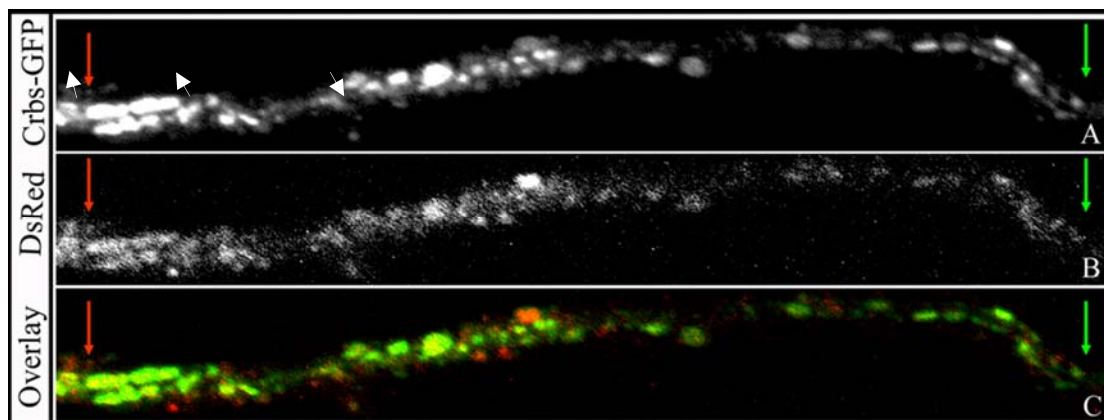


Figure 41. Crumbs-GFP localizes at the apical membrane in terminal branches. UAS-Crums-GFP was expressed in tracheal cells together with DsRed. A, Apical localization of Crumbs-GFP in terminal branches, A', branches marked with DsRed. A'', Overlay of A and A'. The boxed area in A, A' and A'' are enlarged in B, B' and B'', respectively.



Results

Figure 42. Crumbs-GFP localization in vesicles in terminal branches. The images show the distal most tip of a terminal branch where the lumen is beginning to develop. A, Crumbs-GFP localized in vesicles. B, Branch marked with DsRed. C, Overlay of A and B. The red and green arrows mark the proximal (to the nucleus) and distal ends of the branch, respectively.

3.6.7 Phosphorylated Moesin localizes at the apical membrane facing the lumen in terminal branches

In a yeast two hybrid screen, Btsz and Moesin were identified as interacting partners (Formstecher et al., 2005). Btsz and Moesin colocalize at the adherens junctions and Btsz mediated recruitment of Moesin is essential for the proper organization of the actin cytoskeleton at adherens junctions. A Moesin Binding Domain (MBD) in the Btsz2 protein was also identified in the amino terminus region between residues 581-863 (Pilot et al., 2006). The abnormal terminal branching phenotype in the *btsz*^{K13-4} mutant, which codes for the Btsz2 mutant protein lacking the Moesin binding domain leads to the question whether Moesin is required for terminal branch development.

If Moesin is required for terminal branch development and its function is dependent on Btsz, then localization of endogenous Moesin should correlate with Btsz2 localization in the terminal branches. To visualize activated endogenous Moesin in terminal branches, an antibody against phosphorylated mammalian Ezrin/Radixin/Moesin, which recognizes *Drosophila* phosphorylated Moesin, was used for immunostaining analysis (Polesello et al., 2002; Karagiosis and Ready, 2004). The results clearly showed that phosphorylated Moesin, like Btsz, localized at the apical membrane facing the lumen (Fig. 43). This result further strengthens the possibility of Btsz interacting with Moesin in a manner similar to what has been shown in adherens junctions.

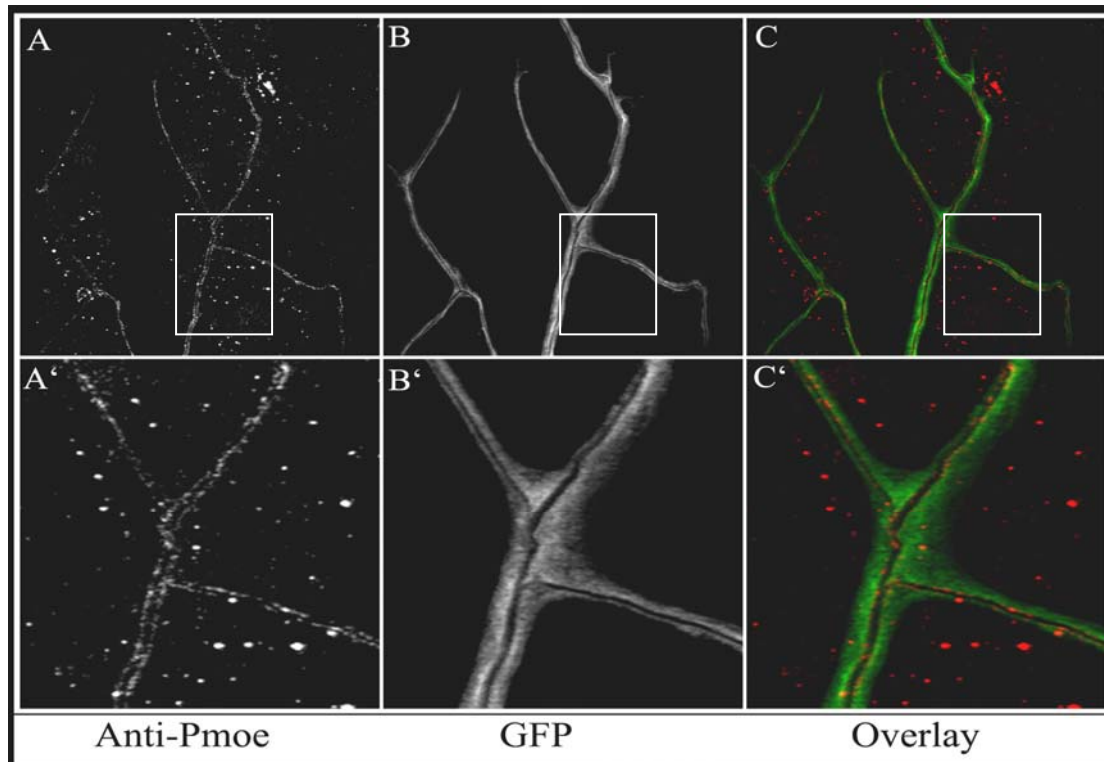


Figure 43. Phosphorylated Moesin localized at the apical membrane in terminal branches. 3rd instar *btl-Gal4*, UAS-GFP larval fillets were immunostained with anti-Phos-Moesin antibody. A and A' shows the localization of phosphorylated Moesin in terminal branches. In B and B' the terminal branches are marked with GFP. C and C' are overlays of A-A' and B-B', respectively. The boxed area in A, B and C are enlarged in A', B' and C', respectively

3.6.8 Function of Moesin in terminal branches

The distribution of phosphorylated Moesin in a pattern resembling the localization of Btsz2, raised the following questions: does Moesin regulate the development of the terminal branches and does it function together with Btsz. Moesin has pleiotropic functions and is involved in a number of morphogenetic processes, e.g., oocyte axis determination, organelle organization and biogenesis, actin cytoskeleton organization and biogenesis, compound eye photoreceptor development (Hughes and Fehon, 2007). Hence, most of the available *moesin* mutants are homozygous lethal and do not survive until larval stages. To study if *moesin* mutants exhibit terminal branch defects similar to the *btsz*^{K13-4} mutant, I performed RNAi knockdown experiments.

A *moesin* RNAi construct (UAS-*moe*-IR.327-775, Karagiosis and Ready, 2003) was expressed in tracheal cells together with cytosolic GFP and third instar

Results

larvae were analyzed for a terminal branch phenotype. *moesin* knockdown in tracheal cells did indeed result in an abnormal terminal branch phenotype. *moesin* mutant terminal cells had terminal branches with multiple convoluted lumens and the numbers of terminal branches were also greatly reduced (Fig. 44). The penetrance of the multi-lumen phenotype of *moesin* knockdown was not 100%.

Similar multi-lumen phenotypes in terminal branches have been reported previously. Mutant alleles of *rhea*^{79a}, *mys*^{XG43} and double mutant combinations of *mew*^{M6} and *ij*^{k27e} (the two α -integrin genes in *Drosophila*) all show multiple convoluted lumen in terminal branches (Fig. 45, Levi et al., 2006). The talin-integrin complexes, at the basal membrane, are required to anchor terminal branches to the underlying substratum and possibly through their association with the actin cytoskeleton, stabilize the lumen in terminal branches (Levi et al., 2006). The apical localization of Moesin and the multiple lumen phenotype in *moesin* mutant terminal cells raise an interesting prospect: Moesin, an actin organizer localized at the apical membrane, probably stabilizes the actin cytoskeleton, which at the basal membrane is stabilized by the talin-integrin complex. Further, one could visualize that this Moesin function is dependent on Btsz, since both localize at the apical membrane and Btsz has been implicated in the membrane localization and function of Moesin in epithelial cells.

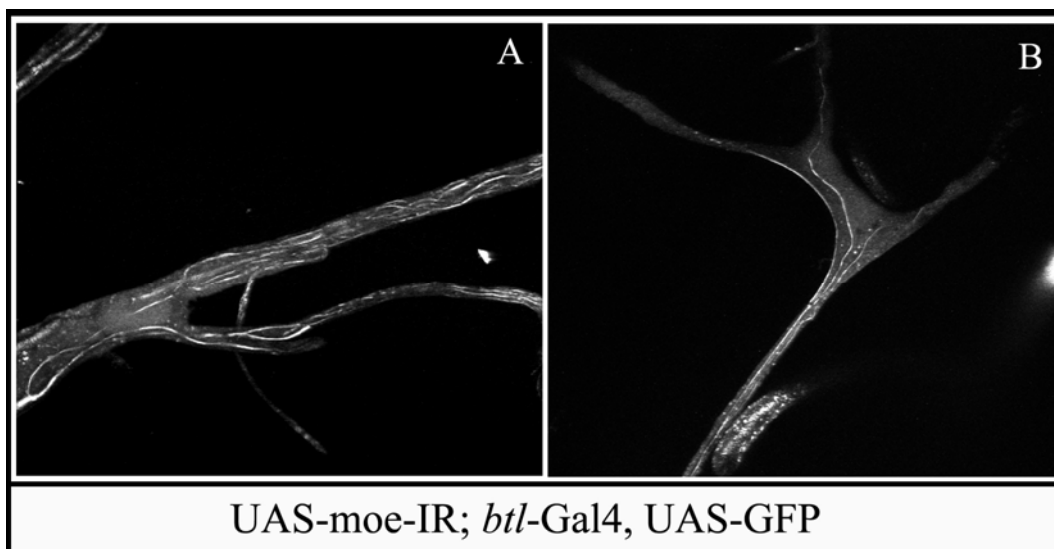


Figure 44. RNAi mediated knockdown of moesin results in a multi-lumen phenotype. UAS-moe-IR.327-775 (moesin RNAi transgene) was expressed in trachea marked with cytosolic GFP. A and B are two different terminal branches where moesin is depleted by RNAi mediated knockdown.

Results

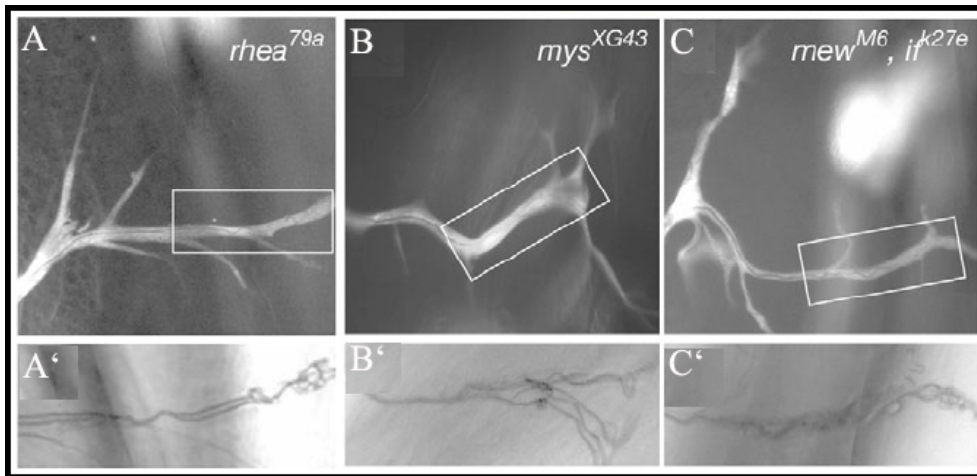


Figure 45. Multi-lumen phenotype in *Drosophila* talin and integrin mutants . A, B and C are images showing multi-lumen phenotypes in terminal branches of mutant alleles of *rhea*, β *mys* and *mew* and *if* (double mutants), respectively. A', B' and C' are enlargements of the boxed area in C, D and E, respectively. Images adapted from Levi et al., 2006

Studies have reported that a threonine residue (position 559) in the actin-binding tail of Moesin is phosphorylated concomitant with its activation and this threonine residue is conserved in all known ERM proteins. Confirming the critical role of this threonine residue, the analysis of a phosphomimetic Moesin variant (MoesinT559D) revealed that the positional activation of Moesin along with its membrane localization is tightly regulated. Ectopically expressed MoesinTD, although it localizes at the membrane, causes abnormal phenotypes related to disorganization of the actin cytoskeleton (Karagiosis and Ready, 2003).

When the phosphomimetic form of Moesin (MoesinTD) was expressed in the terminal tracheal cells, it resulted in severe terminal branching abnormalities. The number and length of terminal branches was reduced and the lumen was highly disorganized (Fig. 46). Endogenous Moesin is localized and activated concomitantly at the membrane and this process is tightly regulated. In wild type terminal branches phosphorylated Moesin localizes at the apical membrane around the lumen, which suggests that Moesin is activated at the apical membrane. The phosphomimetic MoesinTD expressed in terminal cells probably bypasses the tight regulatory process and causes abnormal phenotypes. Regulation of Moesin activation at the apical membrane is very likely essential for normal lumen patterning and terminal branch

Results

development. The factor responsible for localization of Moesin at the apical membrane in terminal branches is not known yet. Btsz could fulfill this role in terminal branches, like in epithelial cells.

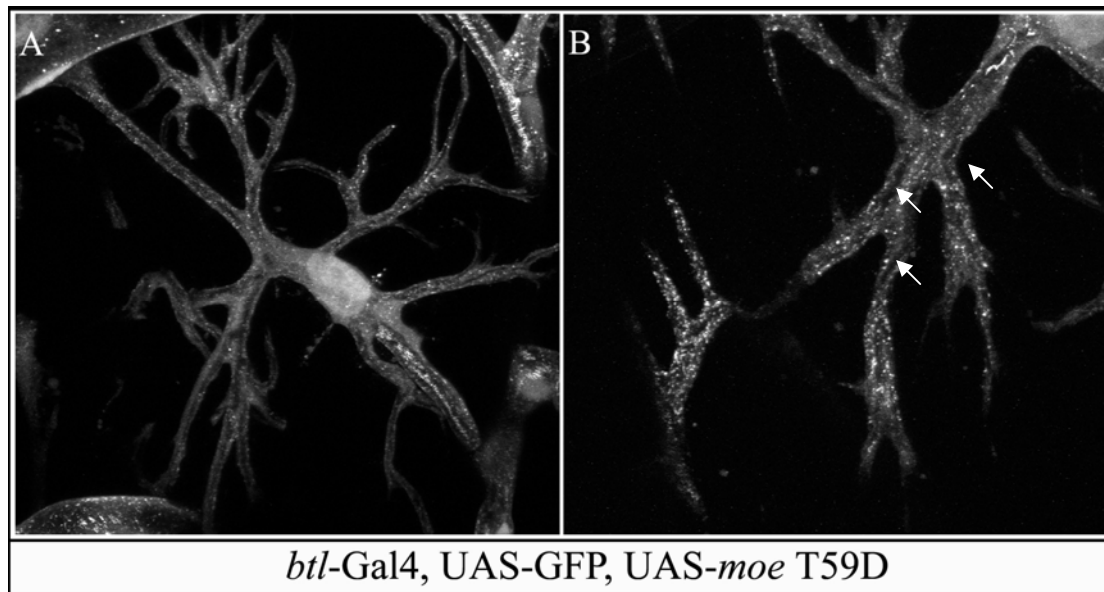


Figure 46. Expression of the phosphomimetic form of Moesin in tracheal cells results in severe terminal branch defects. MoesinTD expression in tracheal cells results in terminal cells with shorter and reduced number of terminal branches (image A) and the lumen is severely disorganized (image B arrows). Tracheal cells are marked with cytosolic GFP.

4. Discussion

1. Terminal branch patterning - a carefully orchestrated process

The *Drosophila* tracheal system has been extensively used to study the molecular and cellular basis of how epithelial cells organize into branched tubes. Although studies elucidating tracheal patterning and tube formation events during *Drosophila* embryonic development are abundant, the tracheal developmental events during the larval phase are relatively unexplored. Most of the terminal tracheal branch development, the final outpost of the tracheal system that supplies oxygen to target tissues, occurs during the larval phase. Except for a few details very little is known about the morphology, molecular and cellular mechanisms regulating terminal branch development in *Drosophila*. Morphological characterization of terminal branches in *Rhodnius prolixus* have illustrated that the terminal branch lumen has a diameter of 0.7 to 1 μm or less and it was described to be similar in other insects including *Drosophila* (Wigglesworth, 1954; Rizki and Rizki, 1979; Wigglesworth and Lee, 1982). While this description holds good, my studies characterizing the morphology of terminal branches show that there is a refined pattern of lumen diameters in terminal branches.

The lumen diameters vary in different branches and based on this I have categorized them into Type-A and Type-B branches. The lumen diameter in Type-A branches progressively decreases along the proximal-distal axis from the nucleus and it also substantially differs between Type-A and Type-B branches. In both instances the diameter decreases by approximately 40%. This diameter difference between branches of the same terminal cell indicates that a regulatory mechanism determining terminal branch lumen diameter must exist. An aspect that adds an interesting dimension to this process is the observations that the lumen in terminal branches appear to form as a consequence of vesicular fusion (Keister, 1948; Locke, 1966; Shafiq, 1963). My findings raise unsolved questions concerning the regulation of lumen diameter in terminal branches for future research: How does the terminal cell confer specific lumen sizes to different branches, what is the regulatory mechanism? Do differently sized vesicles fuse to form tubes with

Discussion

different diameters or is the diameter size regulated post vesicular fusion? If there is a regulatory mechanism, is it similar to the one that operates in primary and secondary branches?

2. Localized translation and developmental plasticity of terminal branches

Terminal branch development is regulated by oxygen physiology, is highly variable and is not stereotyped nor under fixed developmental control. In response to a hypoxic signal, the terminal cells have to develop branches efficiently and quickly to meet the oxygen demands of target tissues, with terminal branches often formed at a significant distance from the nucleus (Wigglesworth, 1954; Locke, 1958; Jarecki et al., 1999). The developmental plasticity exhibited by terminal branches imposes a number of unique demands with respect to development, growth and survival and raises the questions: What is the source of proteins required for the local morphological differentiation at sites far away from the cell body? Do specific RNAs localize in the terminal branches, away from the cell body? Does localized translation, an important mechanism regulating developmental plasticity in neurons (Gottlieb, 1990; Job and Eberwine, 2001; Martin, 2004), regulate terminal branch development?

An essential prerequisite for localized translation to occur in the terminal branches would be the presence of the translational and co-translational machinery; which includes ribosomes, polysomes, endoplasmic reticulum and the Golgi bodies and proteins involved in translational regulation. From the transmission electron microscopic and immuno-histochemical studies presented here it is evident that the components of translational and co-translational machinery are present in the terminal branches, away from the nucleus. These findings suggest that the conditions for translation to occur exist in terminal branches. Therefore the question of which RNAs localize in terminal branches and investigating the function of such localized RNAs is interesting.

*Discussion***3. The EP-MS2 technique - a novel method of screening for localized RNAs**

To investigate if specific RNAs localize in terminal branches, we have developed a new technique, the EP-MS2 technique. The rationale of this new strategy was to tag RNAs with GFP *in vivo* and to track the localization of such tagged RNAs in the terminal tracheal cells. This new technique can be used in genome wide genetic screens for asymmetrically localizing RNAs in different cell types in *Drosophila*.

By performing a pilot screen, I have addressed two important questions: does the technique work efficiently and can it be used in different cell types? The technique was tested in tracheal cells, oocytes and da2 neurons. From the three cell types candidate lines, with the targeted genes transcribing subcellularly localized RNA, were identified. However, none of the candidate lines showed an overlap between the three cell types. While a good degree of candidate overlap can be expected between tracheal cells and neurons the same is not expected between tracheal cells and oocytes. Such an assumption is based on the finding that most of the localizing RNAs identified in oocytes are involved in patterning and establishing polarity (Bullock and Ish-Horowicz, 2001; Ding et al., 1993; Deshler et al., 1997; Forrest and Gavis, 2003; St Johnston, 2005; Santos and Lehmann, 2004). In comparison localized RNAs identified in neurons encode proteins involved in cytoskeletal organization, plasma membrane synthesis and translational regulation (Moccia et al., 2003). Terminal branch localized RNAs described in this study is the first report of RNA localization in the tracheal cells. Hence, a bigger picture of different species of localized RNAs in the tracheal cells is still incomplete. Nevertheless, we do expect a good degree of candidate overlap between terminal tracheal cells and neurons based on the similarities these two cell types share in their development and morphology. A larger screen in tracheal cells and neurons would delineate the extent of overlap of subcellularly localized RNAs, between these cell types.

In light of past studies to identify localized RNAs we expected candidate genes encoding proteins involved in a range of biological activity including cytoskeletal organization, plasma membrane synthesis and molecules regulating translation. Our

Discussion

screen for localized RNAs in tracheal cells indeed has yielded candidates that are involved in cytoskeletal organization (Btsz) and membrane localized proteins (ATPalpha, Na pump α subunit).

A cDNA library prepared from isolated *Aplysia* sensory neuronal axons had yielded about 250 candidates, most of which were genes encoding cytoskeletal proteins and proteins that are components of the translational-co translational machinery (Giustetto et al. 2003; Martin et al. 1998; Moccia et al., 2003; Steward and Levy, 1982). A recent high-resolution fluorescent in situ hybridization study, where 3370 genes were analyzed during early *Drosophila* embryogenesis showed that 71% of the analyzed genes encode subcellularly localized mRNAs (Lecuyer et al., 2007). Compared to these studies the number of candidates in our screen, which was about 4%, was less. Nevertheless, the EP-MS2 technique enables us to perform tissue specific screens, which is a significant advantage. Candidates from different cell types will further our understanding of specific *cis-acting* RNA localization signals, the machinery regulating RNA localization in different cells and the biological relevance of RNA localization. Additional advantages of the EP-MS2 technique are that the genetic screen can be performed as an F1 screen, it combines the advantages of a conventional EP screen, including analysis of over-expression phenotypes, easy mapping of candidates and mutagenesis by P element excision.

There are a few potential problems that can be envisaged concerning this technique. One potential problem was the possibility of P element integration disrupting the endogenous localization signal of the targeted RNA. Moreover, P elements preferentially integrate upstream of genes near the transcriptional start, whereas RNA localization signals are generally found in the 3'UTR. Therefore, it is unlikely that this strategy disrupts localization signals. This is substantiated by the PCR mapping results which showed that EP-MS2 insertions in all the candidate genes were at the 5 prime region of the genes. Another issue of concern was whether tagging RNAs with the MS2 stem loop could cause a localization artifact. The technique of tagging RNAs with the

Discussion

MS2 stem loop and visualizing RNA localization has been tested in different systems (in yeast, mammalian cells and *Drosophila* tissues) and with different RNAs. So far there is no evidence suggesting any localization artifacts caused by MS2-binding site tags in RNA. The question whether an over-expression strategy could cause a localization artifact can be tested by RNA *in situ* hybridization, which would allow comparing and confirming the localization of endogenous RNA of the candidates with that of the MS2-GFP tagged version.

4. Candidate Characterization: *bitesize*, a determinant for lumen formation and stability in terminal branches?

Studies in *Sciara coprophilas*, *Calpodes ethlius* and *Drosophila melanogaster* suggest that the terminal branch lumen forms as result of vesicular fusions (Keister, 1948; Locke, 1966; Shafiq, 1963) and it is believed that the lumen in terminal branches of other insects including *Drosophila* forms by a similar mechanism (Wigglesworth and Lee, 1982). The vesicular fusion begins at the most distal regions of the developing terminal branches resulting in “elongate” vesicles. Such elongate vesicles then become continuous with the main tracheal lumen (Keister, 1948; Locke, 1966; Shafiq, 1963). This *de novo* lumen formation mechanism in terminal branches raises fascinating questions. Is vesicular fusion random or does it happen in a guided and orderly fashion? What mechanism guides the vesicular fusions? How are the tubular vesicles positioned, stabilized and connected to the lumen of the secondary branches? A number of possible mechanisms, including a role for the cell cytoskeleton, can be envisaged in the regulation of *de novo* lumen formation in terminal branches.

A recent study had speculated on a role for the actin cytoskeleton in lumen formation (Levi et al., 2006). Mutants of talin/integrin complex components have abnormal terminal branches and disorganized terminal branch lumen. The talin/integrin complex localizes in the basal membrane of the terminal branches and presumably mediates attachment of the branch to the surrounding tissues. Talin is a crucial mediator of the interaction between integrins and the actin cytoskeleton. Therefore, it was

Discussion

speculated that the lumen defect in the talin/integrin complex mutants is probably a consequence of actin destabilization at the basal membrane in terminal branches (Levi et al., 2006). Based on the model proposed by Levi et al., if the actin cytoskeleton does regulate lumen development, then there should also be an actin organizing and/or stabilizing complex at the apical membrane that surrounds the lumen in terminal branches. Such an actin organizing/stabilizing at the apical membrane in terminal branches is yet to be identified. We believe that in *btsz* we have identified a crucial factor of the actin organizing/stabilizing complex, at the apical membrane in terminal branches.

5. Abnormal terminal branches in *bitesize* mutant larvae

A recent study had shown that *Btsz*, together with Moesin, is required for actin organization at adherens junctions in *Drosophila* embryonic epithelial cells. Further, *Btsz* protein localization was shown to be dependent on Bazooka and PtdIns(4,5)P2 (Pilot et al., 2006).

I have shown that *btsz* is required for terminal branch development. In *btsz* mutant terminal branches are either absent or their numbers are reduced. This is not an effect of failed fate determination as shown by immuno-staining against the terminal tracheal cell specific SRF protein which is expressed properly in the mutant cells. The known function of *Btsz* in actin organization raised the argument whether the terminal branching defect in *btsz* mutants is a consequence of a disorganized actin cytoskeleton in terminal branches. Based on findings that *Btsz* together with Moesin organizes the actin cytoskeleton (Pilot et al., 2006), we speculated that *moesin* mutants should also have abnormal terminal branches. Indeed *moesin* RNAi knockdown mutants had abnormal terminal branches and showed a multi-lumen phenotype. This phenotype although abnormal was not as severe as *btsz*. There are two possible explanations for the differences in the strength of *btsz* and *moesin* mutant phenotypes. The weaker phenotype in *moesin* mutant could be explained by the efficiency of RNAi knockdown experiments, which has been found to yield milder effects, than the genetic loss of function of a gene, probably because of incomplete target knockdown. *Btsz* acts upstream of Moesin and is essential for recruiting and activating

Discussion

moesin at the apical membrane, but Btsz could also have other functions in the terminal branch development that is independent of Moesin. This could be an alternate explanation for the stronger phenotype in *btsz* mutants.

The multi-lumen phenotype in *moesin* RNAi mutants in itself was interesting since this phenotype was described as a possible consequence of destabilized actin cytoskeleton in terminal branches (Levi et al., 2006). Immuno-histochemical studies of the localization of Btsz and the phosphorylated active form of Moesin showed that both localize at the apical membrane surrounding the lumen. Localization of Btsz and Moesin at the apical membrane makes this complex an attractive partner for the basal membrane localized Talin/Integrin complex. Together these apical and basal membrane localized actin organizing complexes might stabilize the actin cytoskeleton in terminal branches.

Btsz localizes at the apical membrane surrounding the lumen in the terminal branches and this apical localization is dependent on the C2 domains. *Drosophila* Bazooka/Par3 acts as an upstream polarizing cue to localize Btsz protein in embryonic epithelial cells (Pilot et al., 2006). In the terminal branches Bazooka, like Btsz, localizes at the apical membrane. In addition, Par6, aPKC (essential for Bazooka localization and function) and Crumbs (which refines localization of the Baz/Par6/aPKC complex) also localize at the apical membrane facing the lumen. The apically localized Baz/Par6/aPKC complex and Crumbs suggest that the polarization cue essential for localizing Btsz in terminal branches is probably the same as that in embryonic epithelial cells. Baz/Par6/aPKC complex and Crumbs are core complexes that act as universal effectors of polarity and could regulate actin organization independent of Btsz. Hence, the Btsz dependent and independent functions of the Baz/Par6/aPKC complex and Crumbs in terminal branch development need to be further delineated.

Based on these results I propose a model (Fig. 47) wherein a Btsz/Moesin complex in the apical membrane acts as an anchor for organizing or stabilizing the actin

Discussion

cytoskeleton, which is connected to the Talin/Integrin complex localized in the basal membrane, which in turn is essential for proper lumen formation and terminal branch development.

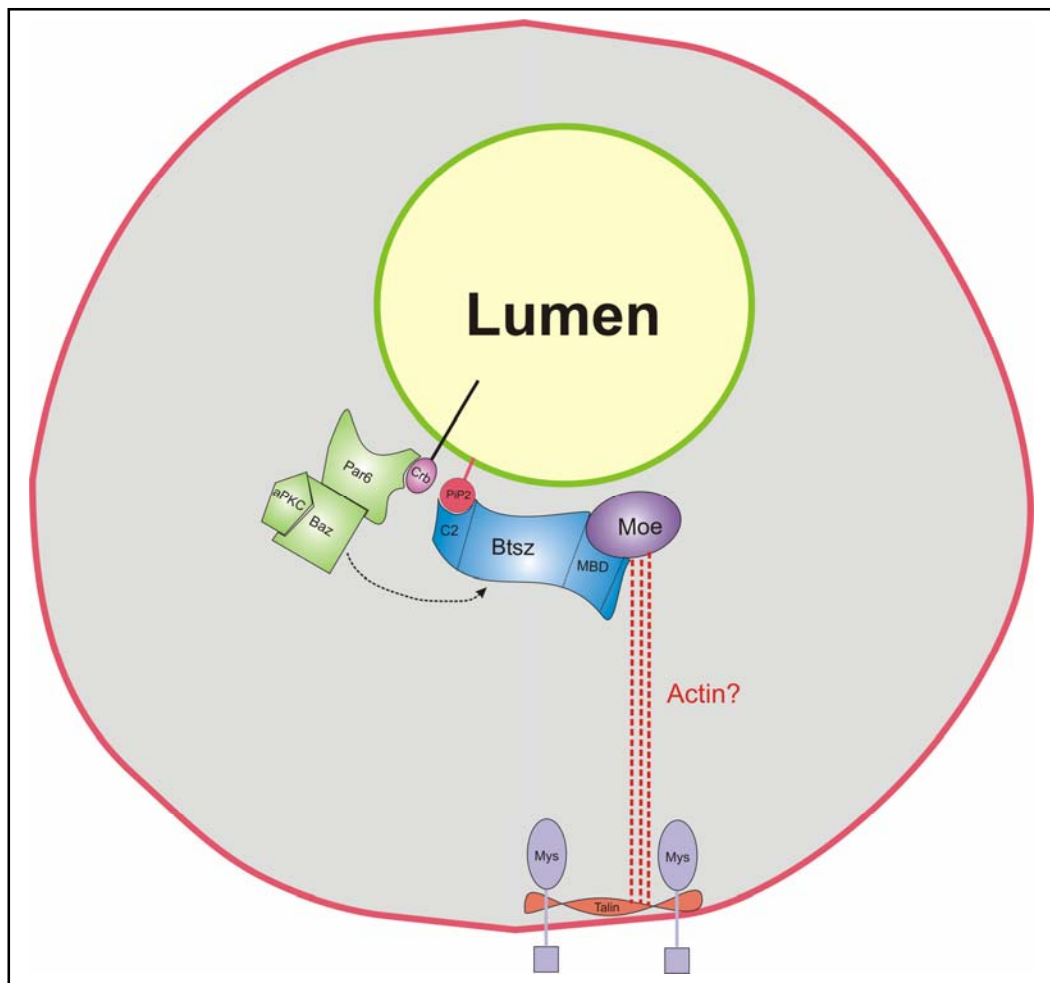


Figure 47. Model. Schematic of a cross section of a terminal branch. The apical membrane faces the lumen (green) and the basal membrane (red) faces outwards. Btsz, Moesin, Bazooka, Par6, aPKC and Crumbs localize at the apical membrane. Talin and β myospheroid localize at the basal membrane. The actin cytoskeleton is represented in red dotted lines.

However the absence of terminal branches in *btsz* mutants cannot be completely explained based on the proposed model and needs further explanation. Studies in *Sciara coprophila*, *Calpodes ethlius* and *Drosophila melanogaster* suggest a possible mechanism

Discussion

of cytoplasmic vesicular fusion resulting in lumen formation in the terminal branches (Keister, 1948; Locke, 1966; Shafiq, 1963). A similar process has been demonstrated in mammalian angiogenesis *in vitro* (Folkman and Haudenschild, 1980).

In my studies on Crumbs localization I found that Crumbs localizes at the apical membrane, but in addition to this I found Crumbs-labeled vesicles at the distal regions of developing terminal branches in which the lumen had not yet formed. Crumbs complex regulates localization of Bazooka, which in turn acts as a polarized localization cue for Btsz. Therefore, one could speculate on a second function for Btsz in terminal branch development. Consistent with the function of C2-domain containing proteins, Btsz could have a role in vesicular transport and fusion leading to lumen formation in terminal branches. The membrane anchored Btsz, like its mammalian homologue Granuphilin (Yi et al., 2002) could regulate vesicular fusion. Subsequent to its function in vesicular fusion Btsz together with Moesin could organize the actin cytoskeleton at the apical membrane. Figure 48 describes this additional role for Btsz in lumen formation in terminal branches.

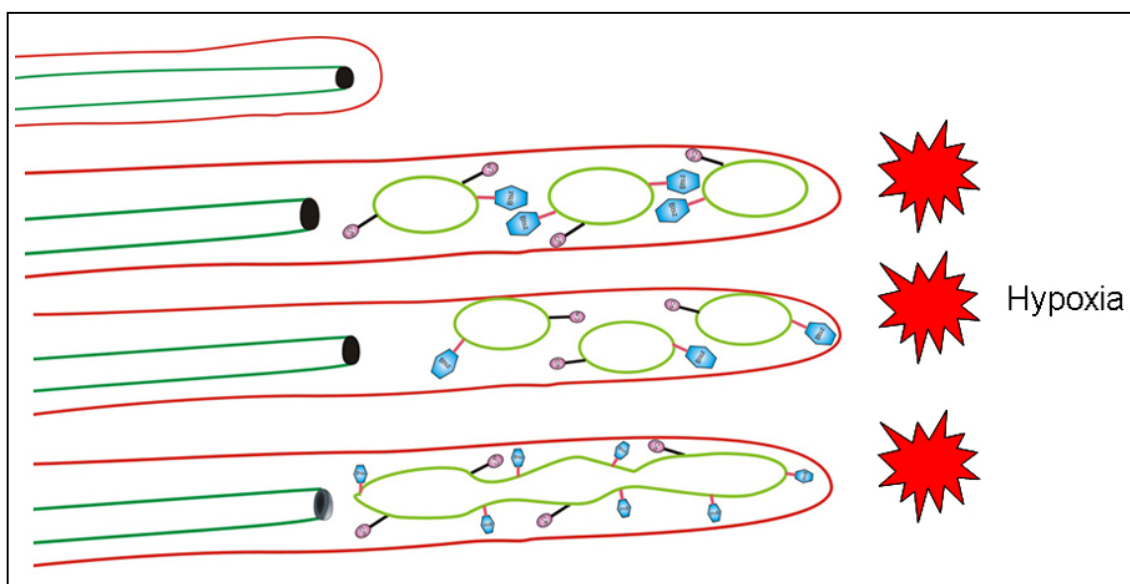


Figure 48. Model for vesicular fusion during terminal branch development. Crumbs containing vesicles (purple circles) are seen in developing regions of branches. These vesicles may also have Btsz (blue boxes) which could have a role in vesicular fusion.

5. Bibliography

Adryan, B., Decker, H. J., Papas, T. S. and Hsu, T. (2000). Tracheal development and the von Hippel-Lindau tumor suppressor homolog in *Drosophila*. *Oncogene* **19**, 2803-11.

Affolter, M., Bellusci, S., Itoh, N., Shilo, B., Thiery, J. P. and Werb, Z. (2003). Tube or not tube: remodeling epithelial tissues by branching morphogenesis. *Dev Cell* **4**, 11-8.

Affolter, M., Montagne, J., Walldorf, U., Groppe, J., Kloter, U., LaRosa, M. and Gehring, W. J. (1994). The *Drosophila* SRF homolog is expressed in a subset of tracheal cells and maps within a genomic region required for tracheal development. *Development* **120**, 743-53.

Affolter, M. and Shilo, B. Z. (2000). Genetic control of branching morphogenesis during *Drosophila* tracheal development. *Curr Opin Cell Biol* **12**, 731-5.

Anderson, P. and Kedersha, N. (2006). RNA granules. *J Cell Biol* **172**, 803-8.

Angerer, L. M. and Angerer, R. C. (1991). Localization of mRNAs by in situ hybridization. *Methods Cell Biol* **35**, 37-71.

Ashburner, M., (1989) *Drosophila – A laboratory handbook*. Cold Spring Harbor Laboratory Press.

Bachmann, A., Schneider, M., Thellenberg, E., Grawe, F. and Knust, E. (2001). *Drosophila* Stardust is a partner of Crumbs in the control of epithelial cell polarity. *Nature* **414**, 638-643.

Bibliography

- Bashirullah, A., Cooperstock, R. L. and Lipshitz, H. D.** (1998). RNA localization in development. *Annu Rev Biochem* **67**, 335-94.
- Beitel, G. J. and Krasnow, M. A.** (2000). Genetic control of epithelial tube size in the *Drosophila* tracheal system. *Development* **127**, 3271-82.
- Bertrand, E., Chartrand, P., Schaefer, M., Shenoy, S. M., Singer, R. H. and Long, R. M.** (1998). Localization of ASH1 mRNA particles in living yeast. *Mol Cell* **2**, 437-45.
- Black, M. M. and Lasek, R. J.** (1977). The presence of transfer RNA in the axoplasm of the squid giant axon. *Journal of Neurobiol* **8**:229–37
- Bloom, K. and Beach, D. L.** (1999). mRNA localization: motile RNA, asymmetric anchors. *Curr Opin Microbiol* **2**, 604-9.
- Bramham, C. R. and Wells, D. G.** (2007). Dendritic mRNA: transport, translation and function. *Nat Rev Neurosci* **8**, 776-89.
- Brand, A. H. and Perrimon, N.** (1993). Targeted gene expression as a means of altering cell fates and generating dominant phenotypes. *Development* **118**, 401-15.
- Bratu, D. P., Cha, B. J., Mhlanga, M. M., Kramer, F. R. and Tyagi, S.** (2003). Visualizing the distribution and transport of mRNAs in living cells. *Proc Natl Acad Sci U S A* **100**, 13308-13.
- Brittis, P. A., Lu, Q. and Flanagan, J. G.** (2002). Axonal protein synthesis provides a mechanism for localized regulation at an intermediate target. *Cell* **110**, 223-35.

Bibliography

Bullock, S. L. and Ish-Horowicz, D. (2001). Conserved signals and machinery for RNA transport in *Drosophila* oogenesis and embryogenesis. *Nature* **414**, 611-6.

Cabernard, C., Neumann, M. and Affolter, M. (2004). Cellular and molecular mechanisms involved in branching morphogenesis of the *Drosophila* tracheal system. *J Appl Physiol* **97**, 2347-53.

Carson, J. H., Kwon, S. and Barbarese, E. (1998). RNA trafficking in myelinating cells. *Curr Opin Neurobiol* **8**, 607-12.

Cha, B. J., Koppetsch, B. S. and Theurkauf, W, E. (2001). In vivo analysis of *Drosophila bicoid* mRNA localization reveals a novel microtubule-dependent axis specification pathway. *Cell* **106**:35–46.

Chang P., Torres J., Lewis R.A., Mowry K.L., Houlston E, King ML. (2004). Localization of RNAs to the mitochondrial cloud in *Xenopus oocytes* through entrapment and association with endoplasmic reticulum. *Mol Biol Cell* **15**, 4669–81.

Chernukhin, I. V., Seago, J.E. and Newbury SF. (2001). *Drosophila* 5'→3'-exoribonuclease Pacman. *Methods Enzymol.* **342**:293-302.

Czaplinski, K. and Mattaj, I. W. (2006). 40LoVe interacts with Vg1RBP/Vera and hnRNP I in binding the Vg1-localization element. *Rna* **12**, 213-22.

Czaplinski, K. and Singer, R. H. (2006). Pathways for mRNA localization in the cytoplasm. *Trends Biochem Sci* **31**, 687-93.

Davis, I. and Ish-Horowicz, D. (1991). Apical localization of pair-rule transcripts requires 3' sequences and limits protein diffusion in the *Drosophila* blastoderm embryo. *Cell* **67**, 927-40.

Bibliography

Deshler, J. O., Highett, M. I. and Schnapp, B. J. (1997). Localization of Xenopus Vg1 mRNA by Vera protein and the endoplasmic reticulum. *Science* **276**, 1128-31.

Ebner, A., Kiefer, F. N., Ribeiro, C., Petit, V., Nussbaumer, U. and Affolter, M. (2002). Tracheal development in *Drosophila melanogaster* as a model system for studying the development of a branched organ. *Gene* **287**, 55-66.

Farina, K. L. and Singer, R. H. (2002). The nuclear connection in RNA transport and localization. *Trends Cell Biol* **12**, 466-72.

Folkman, J and Haudenschlid, C., (1980). Angiogenesis in vitro. *Nature* 288: 551-556

Formstecher, E., Aresta, S., Collura, V., Hamburger, A., Meil, A., Trehin, A., Reverdy, C., Betin, V., Maire, S., Brun, C. et al. (2005). Protein interaction mapping: a *Drosophila* case study. *Genome Res* **15**, 376-84.

Fukuda, M. and Mikoshiba, K. (2001). Synaptotagmin-like protein 1-3: a novel family of C-terminal-type tandem C2 proteins. *Biochem Biophys Res Commun* **281**, 1226-33.

Fukuda, M., Saegusa, C. and Mikoshiba, K. (2001). Novel splicing isoforms of synaptotagmin-like proteins 2 and 3: identification of the Slp homology domain. *Biochem Biophys Res Commun* **283**, 513-9.

Fusco, D., Accornero, N., Lavoie, B., Shenoy, S. M., Blanchard, J. M., Singer, R. H. and Bertrand, E. (2003). Single mRNA molecules demonstrate probabilistic movement in living mammalian cells. *Curr Biol* **13**, 161-7.

Bibliography

Gao, F. B. (1998). Messenger RNAs in dendrites: localization, stability, and implications for neuronal function. *Bioessays* **20**, 70-8.

Ghabrial, A., Luschnig, S., Metzstein, M. M. and Krasnow, M. A. (2003). Branching morphogenesis of the *Drosophila* tracheal system. *Annu Rev Cell Dev Biol* **19**, 623-47.

Gottlieb, E. (1990). Messenger RNA transport and localization. *Curr Opin Cell Biol* **2**, 1080-6.

Gottlieb, E. (1992). The 3' untranslated region of localized maternal messages contains a conserved motif involved in mRNA localization. *Proc Natl Acad Sci U S A* **89**, 7164-8.

Giuditta, A., Metafora, S., Felsani, A. and Del Rio, A. (1977). Factors for protein synthesis in the axoplasm of squid giant axons. *Journal of Neurochemistry* **28**:1393-95

Guillemin, K., Groppe, J., Ducker, K., Treisman, R., Hafen, E., Affolter, M. and Krasnow, M. A. (1996). The pruned gene encodes the *Drosophila* serum response factor and regulates cytoplasmic outgrowth during terminal branching of the tracheal system. *Development* **122**, 1353-62.

Giustetto, M., Hegde, A. N., Si, K., Casadio, A. and Inokuchi, K. (2003). Axonal transport of eukaryotic translation elongation factor 1alpha mRNA couples transcription in the nucleus to long-term facilitation at the synapse. *Proc Natl Acad Sci U S A* **100**: 13680-85

Hamilton, R. S. and Davis, I. (2007). RNA localization signals: deciphering the message with bioinformatics. *Semin Cell Dev Biol* **18**, 178-85.

Bibliography

Hong, Y., Stronach, B., Perrimon, N., Jan, L. Y. and Jan, Y. N. (2001). *Drosophila* Stardust interacts with Crumbs to control polarity of epithelia but not neuroblasts. *Nature* **414**, 634-638.

Hughes, S.C. and Fehon, R.G., (2007). Understanding ERM proteins – the awesome power of genetics finally brought to bear. *Current Opinion in Cell Biology* **19**:51–56.

Hurd, T. W., Gao, L., Roh, M. H., Macara, I. G. and Margolis, B. (2003). Direct interaction of two polarity complexes implicated in epithelial tight junction assembly. *Nat. Cell. Biol.* **5**, 137-142.

Jansen, R. P. and Kiebler, M. (2005). Intracellular RNA sorting, transport and localization. *Nat Struct Mol Biol* **12**, 826-9.

Jarecki, J., Johnson, E. and Krasnow, M. A. (1999). Oxygen regulation of airway branching in *Drosophila* is mediated by branchless FGF. *Cell* **99**, 211-20.

Job, C. and Eberwine, J. (2001). Localization and translation of mRNA in dendrites and axons. *Nat Rev Neurosci* **2**, 889-98.

Johnstone, O. and Lasko, P. (2001). Translational regulation and RNA localization in *Drosophila* oocytes and embryos. *Annu Rev Genet* **35**, 365-406.

Kedersha, N., Stoecklin, G., Ayodele, M., Yacono, P., Lykke-Andersen, J., Fritzler, M. J., Scheuner, D., Kaufman, R. J., Golan, D. E. and Anderson, P. (2005). Stress granules and processing bodies are dynamically linked sites of mRNP remodeling. *J Cell Biol* **169**, 871-84.

Bibliography

King, M. L., Messitt, T. J. and Mowry, K. L. (2005). Putting RNAs in the right place at the right time: RNA localization in the frog oocyte. *Biol Cell* **97**, 19-33.

Kloc, M., Zearfoss, N. R. and Etkin, L. D. (2002). Mechanisms of subcellular mRNA localization. *Cell* **108**, 533-44.

Koenig, E. and Giuditta, A. (1999). Protein-synthesizing machinery in the axon compartment. *Neuroscience* **89**, 5-15.

Lavista-Llanos, S., Centanin, L., Irisarri, M., Russo, D. M., Gleadle, J. M., Bocca, S. N., Muzzopappa, M., Ratcliffe, P. J. and Wappner, P. (2002). Control of the hypoxic response in *Drosophila melanogaster* by the basic helix-loop-helix PAS protein similar. *Mol Cell Biol* **22**, 6842-53.

Lecuyer, E., Yoshida, H., Parthasarathy, N., Alm, C., Babak, T., Cerovina, T., Hughes, T. R., Tomancak, P. and Krause, H. M. (2007). Global analysis of mRNA localization reveals a prominent role in organizing cellular architecture and function. *Cell* **131**, 174-87.

Levi, B. P., Ghabrial, A. S. and Krasnow, M. A. (2006). *Drosophila* talin and integrin genes are required for maintenance of tracheal terminal branches and luminal organization. *Development* **133**, 2383-93.

Locke, M. (1958). The formation of tracheae and tracheoles in *Rhodnius prolixus*. *Quarterly Journal of Microscopical Science* **99**: 29-46

Lubarsky, B. and Krasnow, M. A. (2003). Tube morphogenesis: making and shaping biological tubes. *Cell* **112**, 19-28.

Bibliography

Macara, I. G. (2004). Parsing the polarity code. *Nat. Rev. Mol. Cell. Biol.* **5**, 220-231.

MacDougall, N., Clark, A., MacDougall, E. and Davis, I. (2003). *Drosophila gurken* (TGF α) mRNA localizes as particles that move within the oocyte in two dynein-dependent steps. *Dev Cell* **4**:307–19.

Mangus, D. A., Evans, M. C. and Jacobson, A. (2003). Poly(A)-binding proteins: multifunctional scaffolds for the post-transcriptional control of gene expression. *Genome Biol* **4**, 223.

Martin, K. C. (2004). Local protein synthesis during axon guidance and synaptic plasticity. *Curr Opin Neurobiol* **14**, 305-10.

Martin, R., Vaida, B., Bleher, R., Crispino, M. and Giuditta, A. (1998). Protein synthesizing units in presynaptic and postsynaptic domains of squid neurons. *Journal of Cell Science* **111**:3157–66

Metzger, R. J. and Krasnow, M. A. (1999). Genetic control of branching morphogenesis. *Science* **284**, 1635-9.

Mignone, F., Gissi, C., Liuni, S. and Pesole, G. (2002). Untranslated regions of mRNAs. *Genome Biol* **3**, REVIEWS0004.

Moccia, R., Chen, D., Lyles, V., Kapuya, E., Yaping E., Kalachikov, S., Spahn, C.M.T., Frank, J., Kandel, E.R., Barad, M. and Martin, K.C. (2003). An Unbiased cDNA Library prepared from isolated *Aplysia* sensory neuron processes is enriched for cytoskeletal and translational mRNAs. *The Journal of Neuroscience* **23**(28):9409 –9417

Bibliography

Montagne, J., Groppe, J., Guillemin, K., Krasnow, M. A., Gehring, W. J. and Affolter, M. (1996). The *Drosophila* Serum Response Factor gene is required for the formation of intervein tissue of the wing and is allelic to blistered. *Development* **122**, 2589-97.

Munro, S. and Freeman, M. (2000). The notch signalling regulator fringe acts in the Golgi apparatus and requires the glycosyltransferase signature motif DXD. *Curr Biol* **10**, 813-20.

Nagao, M., Ebert, B. L., Ratcliffe, P. J. and Pugh, C. W. (1996). *Drosophila* melanogaster SL2 cells contain a hypoxically inducible DNA binding complex which recognises mammalian HIF-binding sites. *FEBS Lett* **387**, 161-6.

Oshima, K., Takeda, M., Kuranaga, E., Ueda, R., Aigaki, T., Miura, M. and Hayashi, S. (2006). IKK epsilon regulates F actin assembly and interacts with *Drosophila* IAP1 in cellular morphogenesis. *Curr Biol* **16**, 1531-7.

Peabody, D. S. (1993). The RNA binding site of bacteriophage MS2 coat protein. *Embo J* **12**, 595-600.

Peabody, D. S. (1997). Role of the coat protein-RNA interaction in the life cycle of bacteriophage MS2. *Mol Gen Genet* **254**, 358-64.

Pelikka, M., Tanentzapf, G., Pinto, M., Smith, C., McGlade, C. J., Ready, D. F. and Tepass, U. (2002). Crumbs, the *Drosophila* homologue of human CRB1/RP12, is essential for photoreceptor morphogenesis. *Nature* **416**, 143-9.

Petit, V., Ribeiro, C., Ebner, A. and Affolter, M. (2002). Regulation of cell migration during tracheal development in *Drosophila melanogaster*. *Int J Dev Biol* **46**, 125-32.

Bibliography

Pilot, F., Philippe, J. M., Lemmers, C. and Lecuit, T. (2006). Spatial control of actin organization at adherens junctions by a synaptotagmin-like protein Btsz. *Nature* **442**, 580-4.

Ribeiro, C., Neumann, M. and Affolter, M. (2004). Genetic control of cell intercalation during tracheal morphogenesis in *Drosophila*. *Curr Biol* **14**, 2197-207.

Rorth, P. (1996). A modular misexpression screen in *Drosophila* detecting tissue-specific phenotypes. *Proc Natl Acad Sci U S A* **93**, 12418-22.

Samakovlis, C., Hacohen, N., Manning, G., Sutherland, D. C., Guillemin, K. and Krasnow, M. A. (1996). Development of the *Drosophila* tracheal system occurs by a series of morphologically distinct but genetically coupled branching events. *Development* **122**, 1395-407.

Samakovlis, C., Manning, G., Steneberg, P., Hacohen, N., Cantera, R. and Krasnow, M. A. (1996). Genetic control of epithelial tube fusion during *Drosophila* tracheal development. *Development* **122**, 3531-6.

Santos, A. C. and Lehmann, R. (2004). Germ cell specification and migration in *Drosophila* and beyond. *Curr Biol* **14**, R578-89.

Sato, M. and Kornberg, T. B. (2002). FGF is an essential mitogen and chemoattractant for the air sacs of the *Drosophila* tracheal system. *Dev Cell* **3**, 195-207.

Serano, J. and Rubin, G. M. (2003). The *Drosophila* synaptotagmin-like protein bitesize is required for growth and has mRNA localization sequences within its open reading frame. *Proc Natl Acad Sci U S A* **100**, 13368-73.

Bibliography

Simmonds, A. J., dosSantos, G., Livne-Bar, I. and Krause, H. M. (2001). Apical localization of wingless transcripts is required for wingless signaling. *Cell* **105**, 197-207.

Singer, R. H. (2003). RNA localization: visualization in real-time. *Curr Biol* **13**, R673-5.

Skaer, H. (1997). Morphogenesis: FGF branches out. *Curr Biol* **7**, R238-41.

St Johnston, D. (2005). Moving messages: the intracellular localization of mRNAs. *Nat Rev Mol Cell Biol* **6**, 363-75.

Steward, O. and Schuman, E. M. (2001). Protein synthesis at synaptic sites on dendrites. *Annu Rev Neurosci* **24**, 299-325.

Steward, O. and Levy, W. B. (1982). Preferential localization of polyribosomes under the base of dendritic spines in granule cells of the dentate gyrus. *Journal of Neuroscience* **2**:284-291.

Sutherland, D., Samakovlis, C. and Krasnow, M. A. (1996). branchless encodes a *Drosophila* FGF homolog that controls tracheal cell migration and the pattern of branching. *Cell* **87**, 1091-101.

Tekotte, H. and Davis, I. (2002). Intracellular mRNA localization: motors move messages. *Trends Genet* **18**, 636-42.

Treisman, R. (1994). Ternary complex factors: growth factor regulated transcriptional activators. *Curr Opin Genet Dev* **4**, 96-101.

Uv, A., Cantera, R. and Samakovlis, C. (2003). *Drosophila* tracheal morphogenesis: intricate cellular solutions to basic plumbing problems. *Trends Cell Biol* **13**, 301-9.

Bibliography

Vincent, S., Wilson, R., Coelho, C., Affolter, M. and Leptin, M. (1998). The *Drosophila* protein Dof is specifically required for FGF signaling. *Mol Cell* **2**, 515-25.

von Stein, W., Ramrath, A., Grimm, A., Muller-Borg, M. and Wodarz, A., (2005). Direct association of Bazooka/PAR-3 with the lipid phosphatase PTEN reveals a link between the PAR/aPKC complex and phosphoinositide signaling. *Development* **132**, 1675--1686

Wickens, M., Anderson, P. and Jackson, R. J. (1997). Life and death in the cytoplasm: messages from the 3' end. *Curr Opin Genet Dev* **7**, 220-32.

Wigglesworth, V. B. and Lee, W. M. (1982). The supply of oxygen to the flight muscles of insects: a theory of tracheole physiology. *Tissue Cell* **14**, 501-18.

Wilkie, G. S. and Davis, I. (2001). *Drosophila* wingless and pair-rule transcripts localize apically by dynein-mediated transport of RNA particles. *Cell* **105**, 209-19.

Ye, B., Petritsch, C., Clark, I. E., Gavis, E. R., Jan, L.Y., and Jan1, Y. N. (2004). *nanos* and *pumilio* Are Essential for Dendrite Morphogenesis in *Drosophila* Peripheral Neurons. *Current Biology* **14**: 314-321

Yi, Z., Yokota, H., Torii, S., Aoki, T., Hosaka, M., Zhao, S., Takata, K., Takeuchi, T. and Izumi, T. (2002). The Rab27a/granuphilin complex regulates the exocytosis of insulin-containing dense-core granules. *Mol Cell Biol* **22**, 1858-67.

Zelzer, E. and Shilo, B. Z. (2000). Cell fate choices in *Drosophila* tracheal morphogenesis. *Bioessays* **22**, 219-26.

6. Appendix

6.1 List of genes involved in tracheal morphogenesis

TABLE 1. Genes Regulating Tracheal Morphogenesis

Gene	Protein	Role in trachea	Tracheal phenotype
<i>tracheless (trh)</i>	bHLH-PAS transcription factor	Specification of tracheal identity	Tracheal placodes missing and uninvasinated
<i>dritter/ventral veinless (dfr/vvl)</i>	POU-homeo domain transcription factor	Specification of tracheal identity	Tracheal pits invaginate but fail to migrate
<i>dpp</i>	TGF β homologue, secreted protein	Specification of dorsal tracheal placode border, determination of dorsal and lateral branches	Dorsal extension of placode, absence of dorsal and lateral branches
<i>thickveins (tkv)</i>	TGF β type I receptor	Determination of dorsal and lateral branches	Absence of dorsal and lateral branches
<i>knirps (kni)</i>	Nuclear hormone receptor	Dorsal and lateral branch specification	Dorsal and lateral branch defects
<i>DER/EGFR</i>	EGF receptor tyrosine kinase	Specification of ventral tracheal placode border, determination of dorsal trunk and visceral branch	Ventral extension of placodes, dorsal trunk and visceral branch missing
<i>spitz (spi)</i>	TGF α homologue, EGFR ligand	Determination of dorsal trunk and visceral branch	Dorsal trunk and visceral branch missing
<i>rhomboid (rho)</i>	Multi transmembrane domain protein	Determination of dorsal trunk and visceral branch	Dorsal trunk and visceral branch missing
<i>Star (S)</i>	Type II transmembrane protein	Determination of dorsal trunk and visceral branch	Dorsal trunk and visceral branch missing
<i>spalt (sal)</i>	Zinc finger protein	Determination of dorsal trunk, repression of tracheal fates at embryonic termini	Dorsal trunk defective, extra tracheal pits
<i>breathless (btl)</i>	FGF receptor tyrosine kinase	Directed migration of tracheal cells	No tracheal cell migration
<i>branchless (bnl)</i>	FGF homologue, Btl ligand	Directed migration of tracheal cells	No tracheal cell migration
<i>dot/heartbroken/stumps</i>	Novel, contains two ankyrin repeats	Cytoplasmic relay of Btl signaling	No tracheal cell migration
<i>pruned/SRF/blistered</i>	MADS-box transcription factor	Determination of terminal cell fate	Terminal cells missing
<i>escargot (esg)</i>	Zinc finger protein	Determination of fusion cell fate	Fusion cells missing
<i>Notch (N)</i>	Transmembrane protein	Repression of fusion and terminal fates	Excess fusion and terminal cells
<i>Delta (Dl)</i>	Transmembrane protein, Notch ligand	Repression of fusion and terminal fates	Excess fusion and terminal cells
<i>pointed (pnt)</i>	ETS domain transcription factor	Induction of SRF and <i>sprouty</i> expression	Absence of terminal cells, defective migration
<i>sprouty (sty)</i>	Novel, contains cysteine-rich region	Inhibition of terminal cell fate	Excess terminal cells
<i>headcase (hdc)</i>	Novel	Inhibition of terminal cell fate	Excess terminal cells

Table.1 Describes a list of genes and there function in tracheal morphogenesis. Table adapted from Elazar Zelzer, E. and Shilo, B-Z., (2000)

6.2. Measurements from Type-A and Type-B branches: Data set 1 and data set 2.

Data set-1	Diameter in μm	Data set-2	Diameter in μm
A1	1.17	A1	0.74
A2	1.17	A2	0.74
A3	0.90	A3	0.64
A4	1.17	A4	0.74
A5	1.06	A5	0.74
B1	1.27	A6	0.64
B2	1.06	A7	0.74
B3	1.27	A8	0.74
B4	1.17	A9	0.74
B5	1.17	A10	0.64
C1	1.27	B1	0.53
C2	1.27	B2	0.64
C3	1.06	B3	0.74
C4	1.17	B4	0.74
C5	1.06	B5	0.74
D1	1.38	B6	0.64
D2	1.48	B7	0.64
D3	1.17	B8	0.64
D4	0.85	B9	0.74
D5	1.38	C1	0.64
E1	1.27	C2	0.74
E2	1.38	C3	0.53
E3	0.74	C4	0.74
E4	1.38	C5	0.74
E5	1.17	C6	0.74
Median	1.17	D1	0.85
Std.Dev	0.17	D2	0.74
		D3	0.74
		D4	0.64
		D5	0.74
		E1	0.74

Appendix

E2	0.64
E3	0.74
E4	0.64
E5	0.64
Median	0.74
Std.Dev	0.07

A-E represents five different terminal cells from which measurement were taken. Measurements taken from Type-A branch, 25 measurements from five cells, are included in data set 1. Measurements from Type-B branches, total of 35 measurements, are included in data set 2. The median and standard deviation of both the data sets are shown in red.

6.3 Measurement along the proximal-distal axis of Type-A branch:

Data set 3

	B1	B2	B3	B4	B5	B6
P1	1.17	1.06	1.17	1.272	1.378	1.378
P2	1.272	1.06	1.17	1.378	1.378	1.272
P3	1.17	1.17	1.06	1.047	1.272	1.272
P4	1.06	1.17	0.9	0.742	1.17	1.06
P5	1.047	1.06	0.9	-	0.742	1.06
P6	0.9	0.636	0.636	-	-	-
P7	0.742	-	-	-	-	-
Average	1.051571	1.026	0.972667	1.10975	1.188	1.2084
Stdev	0.180527	0.198514	0.204653	0.281342	0.263864	0.142214

B1-B6 represents 6 different Type-A branch and P1-P7 represents measurement taken from each Type-A branch. The median and standard deviation of both the data sets are shown in red.

6.4 Lumen and cell diameter measurements from the same positions in Type-A branches: Data set 4

Lumen diameter	Diameter in μm	Cell Diameter	Diameter in μm
P1	1.17	P1	2.757
P2	1.272	P2	3.393
P3	1.17	P3	3.817
P4	1.06	P4	4.241
P5	1.047	P5	4.772
P6	0.9	P6	3.935
P7	0.742	P7	2.757
P8	1.06	P8	3.287
P9	1.06	P9	2.332
P10	1.17	P10	2.651
P11	1.17	P11	4.347
P12	1.06	P12	3.499
P13	0.636	P13	2.226
P14	1.17	P14	5.514
P15	1.17	P15	2.863
P16	1.06	P16	3.075
P17	0.9	P17	2.226
P18	0.9	P18	5.09
P19	0.636	P19	3.605
P20	1.272	P20	4.772
P21	1.378	P21	7.529
P22	1.047	P22	3.817
P23	0.742	P23	4.453
P24	1.378	P24	3.287
P25	1.378	P25	3.817
P26	1.272	P26	4.135
P27	1.17	P27	3.711
P28	0.742	P28	3.923
P29	1.378	P29	4.665
P30	1.272	P30	3.181
P31	1.272	P31	5.726

Appendix

P32	1.06	P32	3.711
P33	1.06	P33	3.605
Median	1.06	Median	3.711
Std Dev	0.211754123	Std Deviation	1.105886818

Data set 4 includes lumen diameter and cell diameter measurements taken at same positions from six different branches. A total of 33 measurements of lumen diameter and cell diameter were taken. The median and standard deviation of both the data sets are shown in red.

*Abbreviations***Abbreviations**

Btsz	Bitesize
<i>moe</i>	<i>moesin</i>
Baz	Bazooka
Par6	<i>Drosophila</i> Par6
aPKC	atypical Protein Kinase C
Crbs	Crumbs
PtdIns(3,4,5)P2	phosphatidylinositol (4,5)-bisphosphate
β <i>mys</i>	β myospheroid
<i>mew</i>	<i>multiple edematous wings</i>
<i>if</i>	<i>inflated</i>
Dof	Downstream of FGF
<i>btl</i>	<i>breathless</i>
<i>CenG1A</i>	Centurian Gamma 1A
<i>HsP70Aa</i>	Heatshock protein
<i>Lola</i>	Longitudinal lacking
<i>Hr39</i>	Hormone receptor 39
UAS	<u>U</u> pstream <u>a</u> ctivating <u>s</u> equence
MBD	<u>M</u> oesin <u>b</u> inding <u>d</u> omain
SHD	<u>S</u> ynaptotagmin like protein family <u>H</u> omology <u>D</u> omain
SLP	<u>S</u> ynaptotagmin <u>l</u> ike <u>p</u> rotein family
Pac	Pacman
TEM	Transmission electron microscopy
ER	Endoplasmic reticulum
nt	nucleotide
BSA	Bovine Serum Albumen
dNTP	deoxy Nucleotide Tri Phosphate
PCR	Polymerase Chain Reaction

*Abstract***Abstract**

Asymmetrical localization of mRNAs and localized protein synthesis have an important role in establishing and maintaining polarity in cells such as neurons or the *Drosophila* oocyte and in the regulation of developmental plasticity. In *Drosophila* a subset of highly branched cells of the respiratory system exhibits both a high degree of polarity and developmental plasticity. These tracheal cells respond to the need for oxygen in the surrounding tissue by outgrowth of branches, often at sites very distant from the nucleus. The experiments presented here are based on the assumption that some of the proteins required at the site of outgrowth are synthesized locally rather than near the nucleus. I have demonstrated that the translational and co-translational machinery is present in the terminal branches, which indicates that the conditions for localized translation to occur exist in the terminal branches. Based on this knowledge I have developed a strategy for screening for mRNAs with asymmetric subcellular localization using a technique of tagging mRNAs with GFP *in vivo*. With this experimental setup I have performed a pilot screen in *Drosophila* tracheal cells and have identified 8 candidates exhibiting specific subcellular localization in terminal tracheal cells. Analysis of this experimental strategy shows that the technique is also suitable for other cells such as neurons and oocytes.

One of the candidates *bitesize* (*btsz*) was investigated to analyze its function in terminal branch development. In *btsz* mutants terminal branch are either absent or their numbers are reduced. Mutation in *moesin*, a *btsz* interacting partner, also shows an abnormal branching phenotype. Both *Btsz* and *Moesin* localize at the apical membrane, which surrounds the lumen of terminal branches. Taking into account that *btsz* together with *moesin* is required for organizing actin at adherens junctions in embryonic epithelial cells; I propose a model by which *Btsz/Moesin* regulates terminal branch development by acting as an anchor for the actin cytoskeleton on the plasma membrane surrounding the lumen in terminal branches.

*Zusammenfassung***Zusammenfassung**

Die asymmetrische mRNA-Lokalisierung und lokalisierte Proteinsynthese haben eine wichtige Funktion in der Etablierung und Aufrechterhaltung der Polarität in Zellen wie etwa Neuronen oder *Drosophila* Oozyten und in der Regulation der Entwicklungsplastizität. In *Drosophila* besitzt eine Subpopulation von hochverzweigten Zellen des Respirationssystems einen hohen Grad an Polarität und Entwicklungsplastizität. Diese Zellen des Tracheensystems reagieren auf den Sauerstoffbedarf des umliegenden Gewebes mit einem Auswachsen der Tracheenäste, oft an Stellen die sehr weit vom Zellkern entfernt sind. Den hier beschriebenen Experimenten liegt die Annahme zugrunde, dass einige der an der Stelle des Auswachsens benötigten Proteine vor Ort synthetisiert werden und nicht in der Nähe des Zellkerns. Ich konnte zeigen, dass die Translations- und Co-Translationsmaschinerie in den terminalen Tracheenästen vorhanden ist, was darauf hindeutet, dass die Bedingungen, damit eine lokalisierte Translation stattfindet, in den terminalen Tracheenästen bestehen. Davon ausgehend habe ich eine Strategie entwickelt um nach mRNAs mit asymmetrischer subzellulärer Lokalisierung zu suchen und habe dazu eine Technik verwendet, bei der *in vivo* mRNAs mit GFP markiert werden. Mit diesem experimentellem System habe ich einen *Pilotscreen* in *Drosophila* Tracheenzellen durchgeführt und konnte dabei 8 Kandidaten identifizieren, die eine spezifische subzelluläre Lokalisierung in den terminalen Tracheenzellen aufweisen. Eine Analyse dieses experimentellen Systems zeigt, dass die Technik auch für andere Zelltypen wie Neuronen oder Oozyten geeignet ist.

Eines der identifizierten Kandidatengene, *bitesize (btsz)*, wurde untersucht um seine Funktion bei der terminalen Tracheenastentwicklung zu analysieren. In *btsz*-Mutanten sind die terminalen Tracheenäste entweder nicht vorhanden oder in ihrer Anzahl verringert. Eine Mutation in *moesin*, einem Interaktionspartner von *btsz*, führt ebenfalls zu einem Phänotyp, der durch abnormales Auswachsen der Tracheenäste gekennzeichnet ist. Sowohl *Btsz* als auch *Moesin* lokalisieren an der apikalen Membran, die das Lumen der terminalen Äste umgibt. Unter Berücksichtigung, dass *btsz* zusammen mit *moesin* für die Aktin-Organisation an Adhärenzverbindungen in embryonalen

Zusammenfassung

Epithelzellen benötigt wird, schlage ich als Modell vor, dass Btsz/Moesin die terminale Tracheenastentwicklung reguliert, indem es als Ankerpunkt für das Aktin Cytoskelett an der das Lumen der Äste umgebenden Plasmamembran dient.

*Erklärung***Eidesstattliche Erklärung**

Ich versichere, daß ich die von mir vorgelegte Dissertation selbständig angefertigt, die benutzten Quellen und Hilfsmittel vollständig angegeben und die Stellen der Arbeit – einschliesslich Tabellen, Karten und Abbildungen –, die anderen Werken im Wortlaut oder dem Sinn nach entnommen sind, in jedem Einzelfall als Entlehnung kenntlich gemacht habe; daß diese Dissertation noch keiner anderen Fakultät oder Universität zur Prüfung vorgelegen hat; daß sie – abgesehen von unten angegebenen Teilpublikationen – noch nicht veröffentlicht worden ist sowie, daß ich eine solche Veröffentlichung vor Abschluss des Promotionsverfahrens nicht vornehmen werde. Die Bestimmung dieser Promotionsverordnung sind mir bekannt. Die von mir vorgelegte Dissertation ist von Prof. Dr. Maria Leptin betreut worden.

Keine Teilpublikationen

Köln

Februar 2008

Jayan Nandan Nair

*Lebenslauf***Lebenslauf**

Name: Jayan Nandan Nair

Geburtsdatum: 21.02.1977

Geburtsort: Muvattupuzha, Indien

Staatsangehoerigkeit: Indisch

1990-1992 Gymnasium (SSLC), Kerala, Indien

1992-1994 Abitur (Pre Degree), Kerala, Indien

1994-1997 Bachelor of Science (B.Sc), MG University, Kerala, Indien

1998-2000 (Diplom) Master of Science (M.Sc), Mysore University, Indien

2000-2003 Junior Research Fellow
National Center for Biological Sciences, (TIFR),
Bangalore, Indien

2003-2007 Doktorarbeit bei Prof. Dr. Maria Leptin am
Institute fuer genetik
Universität zu Köln
Titel: "A genetic screen for asymmetrically localized RNAs in
Drosophila tracheal cells".

Köln
Februar 2008

Unterschrift